

MEMBRANE INLET MASS SPECTROMETRY (MIMS):
A NOVEL APPROACH TO THE OCEANIC MEASUREMENT OF
DIMETHYLSULFIDE

by

NINA NEMCEK

BSc., University of British Columbia, 2003

A THESIS SUBMITTED IN PARTIAL FULFILLMENT OF THE
REQUIREMENTS FOR THE DEGREE OF

MASTER OF SCIENCE

in

FACULTY OF GRADUATE STUDIES

(Oceanography)

UNIVERSITY OF BRITISH COLUMBIA

March 2007

© Nina Nemcek, 2007

Abstract

A novel technique, membrane inlet mass spectrometry (MIMS), was used to measure dimethylsulfide gas (DMS) and algal dimethylsulfoniopropionate (DMSPp) concentrations in two different marine ecosystems of the NE Pacific. In oceanic waters along Line P, DMS levels had been observed to be unusually high, yet particulate DMSP levels had not been extensively measured. DMSPp concentrations during 3 consecutive spring cruises ranged from 0.2-63.2 nM (mean 21.5 nM, s.d. 15.0 nM) in the upper 50 m of the water column, and varied significantly with depth, across stations and between study years. DMSPp generally decreased with depth and distance from the coast. DMSPp concentrations at most stations in 2003 were 2 to 3-fold higher than in subsequent years, and were significantly correlated to the biomass of dinoflagellates ($r^2 = 0.46$) across the survey region. Although phytoplankton biomass (chlorophyll *a*) also declined in 2004-2005, DMSPp:chl ratios did as well, indicating a physiological or taxonomic change in the phytoplankton community.

Surface DMS concentrations were measured underway along with $p\text{CO}_2$, O_2/Ar , temperature, salinity and chlorophyll *a* in productive, coastal waters off British Columbia. All parameters exhibited large ranges, ($p\text{CO}_2$, 200-747 ppm; DMS, <1-28.7 nM; chl *a*, <0.1-33.2 $\mu\text{g L}^{-1}$), highlighting the dynamic nature of the region. A tight anti-correlation between $p\text{CO}_2$ and O_2/Ar was observed across the region ($r^2 = 0.90$), with the distributions of these gases strongly influenced by both biological (photosynthesis and respiration) and physical (upwelling) processes. In contrast, DMS levels which exhibited rapid, fine-scale fluctuations irresolvable with traditional methods, were unrelated to any single variable. A significant linear relationship was however observed between DMS and the chlorophyll to mixed layer depth ratio ($r^2 = 0.83$), although with a different scaling factor to that derived from open ocean data. Lower resolution

sampling in this region can introduce errors as large as 41% of the mean concentration for DMS, emphasizing the utility of MIMS in dynamic areas. In conclusion, MIMS proved to be a significant advance for DMS measurement, yet improvements need to be made for it to be a viable alternative to other methods for DMSP measurements.

Table of Contents

Abstract.....	ii
Table of Contents.....	iv
List of Tables.....	vi
List of Figures.....	vii
Acknowledgements.....	ix
Dedication.....	x
Co-Authorship Statement.....	xi
Chapter 1: Introduction.....	1
1.1 Dimethylsulfide: Sources, Sinks and Climate Links.....	1
1.2 The CLAW Hypothesis: 20 Years Later.....	4
1.3 Membrane Inlet Mass Spectrometry.....	6
1.4 Thesis Objectives.....	7
1.5 References.....	8
Chapter 2: Springtime Variability in Particulate DMSP Concentrations along Line P, NE Pacific Ocean.....	11
2.1 Introduction.....	11
2.2 Materials and Methods.....	13
2.3 Results.....	19
2.4 Discussions.....	24
2.5 References.....	45
Chapter 3: High-Resolution Measurements of DMS, CO ₂ , and O ₂ /Ar in Productive, Coastal Waters around Vancouver Island, Canada.....	49
3.1 Introduction.....	49
3.2 Materials and Methods.....	52
3.3 Results.....	58
3.4 Discussion.....	67
3.5 Conclusions.....	78

3.6 References.....	89
Chapter 4: Conclusions.....	93
4.1 Thesis Overview.....	93
4.2 Evaluation of MIMS for DMSP/DMS Measurements.....	94
4.3 Successes and Pitfalls.....	95
4.4 Future Directions.....	97
4.5 References.....	99

List of Tables

Table 2.1: Ancillary oceanographic data for all stations surveyed during 2003.....	33
Table 2.2: Coefficients of determination (r^2) from linear regressions between DMSPp levels and the absolute and relative carbon biomass of different phytoplankton groups for all stations during the 2003 survey.....	34
Table 2.3: The contribution of DMSPp to total phytoplankton cell carbon in 2003.....	35
Table 3.1: Absolute and relative asymptotic interpolation errors along the 6 major transects.....	79

List of Figures

Figure 2.1: Map of the NE Pacific showing the 5 major stations along Line P.....	36
Figure 2.2: Depth profiles of DMSPp measured at the 5 major stations along Line P during 3 consecutive spring cruises.....	37
Figure 2.3: Depth profiles of chlorophyll <i>a</i> measured at the 5 major stations along Line P during 3 consecutive spring cruises.....	38
Figure 2.4: Depth profiles of the DMSPp:chl ratio measured at the 5 major stations along Line P during 3 consecutive spring cruises.....	39
Figure 2.5: Contour plots illustrating spatial and interannual variability in springtime DMSPp and chlorophyll levels along Line P.....	40
Figure 2.6: Relationship between chlorophyll and DMSPp concentrations along Line P for the 3 year pooled dataset.....	41
Figure 2.7: The relative abundance of the different phytoplankton groups enumerated at (a) 10 m depth and (b) the chlorophyll max. at all stations surveyed in 2003.....	42
Figure 2.8: The contribution of the different phytoplankton groups to total carbon biomass at (a) 10 m depth and (b) the chlorophyll max. at all stations surveyed in 2003.....	43
Figure 2.9: 50 m depth integrated DMSPp:chl ratios plotted against the mixed layer nitrate concentration.....	44
Figure 3.1: Map of southwestern British Columbia, Canada showing the location of underway transects.....	80
Figure 3.2: Surface plots of (a) temperature (°C), (b) salinity (psu), (c) chlorophyll <i>a</i> ($\mu\text{g L}^{-1}$), (d) $p\text{CO}_2$ (ppm), (e) O_2/Ar (torr ratio), and (f) DMS (nM).....	81
Figure 3.3: Detailed south-north view of all variables measured along T5.....	82
Figure 3.4: Detailed view of all variables measured along T7.....	83
Figure 3.5: The correlation across all transects between (a) $p\text{CO}_2$ and O_2/Ar ($r^2 = 0.90$) with corresponding chl <i>a</i> concentrations overlaid (colourbar), and (b) chl <i>a</i> and O_2/Ar ($r^2 = 0.19$) with corresponding temperature overlaid (colourbar).....	84
Figure 3.6: The correlation across all transects between chl <i>a</i> and DMS ($r^2 = 0.06$).....	85

Figure 3.7: Results of the PCA showing the strong separation between $p\text{CO}_2$ and O_2/Ar in two-dimensional space and the clear partitioning between physical (T, S) and biological (chl *a*) variables.....86

Figure 3.8: Average DMS concentrations plotted against CHL/MLD ratios for the $\frac{1}{4}$ degree grids.....87

Figure 3.9: Autocorrelation functions for all parameters measured along transect 5 (a); Average DLS for all parameters for the entire survey (b).....88

Acknowledgements

This project would not have been possible without the tireless efforts of Mark Buckley and Robert Stannard at Hiden Analytical in the development and troubleshooting of the MIMS. My supervisor Philippe Tortell, Celine Gueguen and Chris Payne also helped tremendously over the years with method development and repairs on “Herbie”.

The author would like to acknowledge the Captain, crew, and science personnel of the *CCGS John P. Tully* for their assistance during the Line P and Queen Charlotte Sound surveys. The Natural Sciences and Engineering Research Council of Canada (NSERC) and the University of British Columbia funded this project in the form of an Undergraduate Student Research Award (2003), Postgraduate Scholarship and University Fellowship (2004-2006).

A sincere thank you goes to the following people for their assistance with the Line P dataset: T. Peterson for performing phytoplankton identification and enumeration in 2003, M. Robert for organizing the cruises and providing access to CTD and ancillary data, W. Richardson and J. Barwell-Clarke for nutrient analysis, L. Richier for chlorophyll analysis in 2005, and M. Arychuk and C.S. Wong for method intercomparisons and fruitful discussions on DMS/DMSP trends in the NE Pacific. A special thank you goes to Darren Tuele for DMSPp sample collection in 2005 and invaluable support at sea during all cruises.

I am grateful to Debby Ianson for allowing me to participate in her Queen Charlotte Sound cruise, for providing ancillary CTD, nutrient, thermosalinograph and $p\text{CO}_2$ equilibrators data, and for her guidance and motivation during the writing of Chapter 3. Dave Mackas kindly provided unpublished CTD data and Marlene Jeffries helped with Matlab figures. Finally, I must thank my labmates for their camaraderie and support, and my supervisor Philippe Tortell for conceiving the application of MIMS for DMS analysis and for sending me to sea.

Dedication

To DT for pushing me to finish and to my parents for never pushing me.

Co-Authorship Statement

I will be the primary author of the manuscript “Interannual variability in springtime particulate DMSP concentrations along a coastal to oceanic transect in the NE Pacific” which will be written based on Chapter 2. I performed the DMSPp sample analysis in all three years, integrated and analyzed the ancillary data, and will write the manuscript. Nutrient, chlorophyll and CTD data were provided by Marie Robert of the Institute of Ocean Sciences. The second author, Dr. Tawnya Peterson performed phytoplankton counts and provided cell dimensions in 2003 from which I calculated cell biovolumes and the biomass of specific algal groups. The third author, my supervisor Dr. Philippe Tortell introduced me to the MIMS, assisted with sample analysis during the cruise in 2003, and provided lab space and resources. He also provided guidance on the project and edited the manuscript.

I wrote the manuscript “A high-resolution survey of DMS, CO₂, and O₂/Ar distributions in productive coastal waters”, based on Chapter 3, which was submitted to *Global Biogeochemical Cycles*. I devised the sampling strategy, collected and processed DMSP and chlorophyll samples and operated the MIMS during the Queen Charlotte Sound survey in 2004. Post-cruise, I processed the MIMS, pCO₂ equilibrator, and thermosalinograph data, the latter two provided by my second author Dr. Debby Ianson of the Institute of Ocean Sciences. Dr. Ianson provided a berth on her research cruise as well as ancillary CTD and nutrient data. The third author Dr. Philippe Tortell performed the principal components analysis and calculated autocorrelation functions and interpolation errors for my underway dataset. All other interpretations and ideas in the discussion were my own, however both of my co-authors’ edits improved the final manuscript greatly.

I certify that the above statements about authorship are correct.

1. Introduction

1.1 Dimethylsulfide: Sources, Sinks and Climate Links

Microscopic algae dwelling in surface waters of the world's oceans have a profound influence on Earth's climate through the consumption and production of climatologically active gases. One such gas, dimethylsulfide (DMS), is formed in the oceans from the breakdown of dimethylsulfoniopropionate (DMSP), a compound produced in large quantities by many species of phytoplankton for a variety of metabolic functions (see Section 2.1). In 1972, James Lovelock observed that DMS was ubiquitous in marine surface waters and postulated that the flux of DMS from the oceans to the atmosphere was sufficiently large to account for the "missing" sulfur in global transport models [Lovelock *et al.*, 1972]. Over the past two decades, extensive oceanic DMS measurements have supported this hypothesis. Despite a global mean surface water concentration of < 3 nM [Kettle *et al.*, 1999], DMS is everywhere supersaturated in the ocean resulting in a steady flux of sulfur to the atmosphere. This flux represents the largest natural source of atmospheric sulfur constituting 20 % of total global emissions, but over 40 % of the atmospheric sulfur burden due to the relatively longer lifetimes of DMS-derived aerosols compared to anthropogenic ones [Chin and Jacob, 1996].

It was not until the late 1980's when Lovelock and colleagues introduced the CLAW hypothesis (an acronym for the authors' names), that interest in DMS and its potential climatic effects skyrocketed [Charlson *et al.*, 1987]. The CLAW hypothesis states that phytoplankton regulate their environment (and by consequence the Earth's climate) through the production of DMS which affects planetary albedo. As noted earlier by Shaw [1983], DMS vented from the oceans is quickly oxidized in the atmosphere to non-sea-salt sulfate (NSS-SO₄) and methanesulfonic acid (MSA), species that act as cloud condensation nuclei (CCN), or seed

crystals for cloud formation. *Charlson et al.* [1987] argued that the DMS-derived NSS-SO₄ aerosols are the main source of CCN over much of the Earth's surface. Thus, according to the CLAW hypothesis, high solar irradiance stimulates algal DMS production which leads to increased planetary cloud cover and a reduction in the amount of radiation reaching the planet's surface. This in turn has a feedback effect on the phytoplankton that initiated the process through changes in sea surface temperature and incident sunlight, thereby closing the loop. However, the sign of this feedback was unclear at the time, since many of the factors controlling DMS production and its dependence on species composition were unknown. A negative feedback on DMS production would imply a self-regulating climate system mitigated by the marine biota [*Charlson et al.*, 1987].

The CLAW hypothesis stimulated the intense research efforts directed at elucidating the intricacies of the DMS cycle that have been occurring over the past two decades. From these efforts we have greatly improved our understanding of the complex foodweb dynamics that drive the cycling of DMSP and its byproducts. All DMS originates from algal or particulate DMSP (DMSPp). DMSP production varies widely by species with dinoflagellates and prymnesiophytes generally being major producers, and diatoms minor ones [*Keller et al.*, 1989]. However, even within algal groups there is significant variability in cellular DMSP content [*Keller et al.*, 1989], and external factors such as nutrient availability can increase DMSP production in species generally considered to be low producers [*Sunda et al.*, 2002].

Zooplankton grazing [*Dacey and Wakeham*, 1986] and viral lysis [*Malin et al.*, 1998] of phytoplankton promote the release of DMSP into seawater where it is rapidly consumed by various components of the marine foodweb. Heterotrophic bacteria are the dominant sink for dissolved DMSP (DMSPd), although recent evidence suggests autotrophic cyanobacteria and

diatoms are also capable of DMSP uptake and assimilation [Vila-Costa *et al.*, 2006]. Bacteria possess two competing pathways for the metabolic breakdown of DMSP. The demethylation pathway converts DMSP to methanethiol which is quickly incorporated into protein and bacterial biomass, thus diverting sulfur away from DMS [Gonzales *et al.*, 1999]. In contrast, the cleavage pathway utilizes DMSP-lyase to convert DMSP to DMS and acrylate, although this is the fate of only 5-10 % of the DMSP metabolized in the water column [Kiene *et al.*, 2000]. Thus, the production of climatologically important DMS constitutes only a small fraction of the large flux of reduced sulfur in the surface ocean.

Some phytoplankton species also possess the DMSP-lyase enzyme which mixes with its substrate during grazing or viral lysis leading to high DMS production [Malin *et al.*, 1998]. It is thought that algae with DMSP-lyase activity use this enzyme as an activated chemical defence against predators, as microzooplankton grazers are deterred by acrylate [Wolfe *et al.*, 1997]. More recently it has been shown that acrylate may also deter viruses, since high DMSP-lyase containing strains of the prymnesiophyte *Emiliania huxleyii* appear to be immune to viral attack [Evans *et al.*, 2006]. In addition, phytoplankton may use DMSP-lyase to trigger a powerful antioxidant cascade, as DMS, acrylate, DMSO, and other byproducts of DMSP are powerful free radical scavengers [Sunda *et al.*, 2002].

There are three major sinks for DMS in marine surface waters, (1) bacterial consumption, (2) photolysis and (3) ventilation to the atmosphere. The relative importance of each depends on the depth interval considered and the biological, chemical and meteorological conditions [Kieber *et al.*, 1996]. Ventilation is generally considered a minor sink because it occurs only at the air-sea interface, but is the dominant loss process at high wind speeds. Photolysis converts DMS to non-volatile compounds including DMSO and occurs over the depth range to which UV light can

penetrate [Kieber *et al.*, 1996]. This depth depends on cloud cover, geographic location and the local optical properties of seawater, and can range from a few meters in coastal waters to >75 m in optically clear waters under high UV flux [i.e. Toole *et al.*, 2004]. In addition, photolysis rates are strongly influenced by the concentrations of photosensitizers such as chromophoric dissolved organic matter (CDOM) [Kieber *et al.*, 1996; Toole *et al.*, 2004]. Bacterial consumption of DMS is likely the dominant sink for DMS over most of the surface ocean because it occurs over the greatest depth interval and over the largest range of conditions [Kiene *et al.*, 1990; Kieber *et al.*, 1996]. However, under high UV light conditions, photolysis can exceed bioconsumption as the dominant loss process as bacteria in surface waters become photoinhibited [Toole *et al.*, 2004].

1.2 The CLAW Hypothesis: 20 Years Later

There is no doubt that biogenic sulfur aerosols have a large influence on global climate. They are the main source of CCN over much of the remote marine atmosphere, particularly in the Southern Hemisphere where there are few terrestrial sources. Moreover, a strong coherence has been observed between seasonality in DMS emissions and CCN numbers [Ayers and Gras, 1991], as well as cloudiness [Boers *et al.*, 1994], at least in the Southern Hemisphere. Ice core data from Vostok, Antarctica reveal concentrations of NSS-SO₄ and MSA (a byproduct exclusive to DMS) were significantly higher during glacial periods compared to interglacial ones, and were tightly anti-correlated to past temperature fluctuations [Legrand *et al.*, 1991]. Thus, marine biota influence climate via the oceanic sulfur cycle, in addition to the biological carbon pump. Modelling studies reveal that 2/3 of the present day cooling resulting from biological production in the oceans can be attributed to DMS emissions, with only a 1/3

contribution from CO₂ uptake [*Watson and Liss, 1998*]. More recent models estimate that reducing present day DMS emissions by half would result in a 1.6 °C increase in global mean sea surface temperatures [*Gunson et al., 2006*].

Although it is clear that DMS emissions have a cooling effect on global climate, it is still unclear what impact a changing climate will have on future DMS emissions. Impending changes in solar radiation, surface ocean stratification, nutrient supply, and wind speeds will all influence the competing pathways that lead to net DMS production, such that neither the magnitude nor the sign of this effect is certain at present. Increases in the extent and strength of surface ocean stratification and in incident solar radiation predicted under global warming scenarios could indeed lead to increased DMS production for a number of reasons. Firstly, stratified, nutrient-depleted waters tend to favour the growth of high DMSP producing taxa such as dinoflagellates and prymnesiophytes [*Margalef, 1978; Keller et al., 1989*]. Secondly, high incident UV radiation promotes elevated DMSP production in these and other species as a physiological response to photo-oxidative stress [*Sunda et al., 2002*]. Finally, strong UV photoinhibition of bacterial growth in a stratified water column results in less sulfur assimilation into biomass and a higher proportion of DMSP converted to DMS [*Simo and Pedros-Alio, 1999*]. Most recent studies predict dramatic latitudinal variability in modelled DMS fluxes under global warming, with small to moderate increases in net global DMS emissions [*Bopp et al., 2003; Gabric et al., 2004*]. These predictions do support the self-regulating negative feedback CLAW hypothesis, although only weakly and with large uncertainty. An improved mechanistic understanding of the complex web that is the oceanic DMS cycle is urgently needed to reduce this uncertainty.

1.3 Membrane Inlet Mass Spectrometry

Traditionally, oceanic measurements of DMS and related sulfur compounds have been performed by purge and trap gas chromatography (PTGC). In this method, discrete seawater samples are sparged with an inert gas to transfer the volatile sulfur analyte into a concentrating cryogenic trap. The trap is subsequently heated to release the analyte into a gas chromatographic column that separates the various sulphur compounds for measurement by either a chemiluminescent or photometric detector. Although this method offers excellent sensitivity (as a result of the cryogenic trapping step), it is labour intensive, and time-consuming. Furthermore, it is limited to the analysis of discrete samples, and thus offers poor spatial resolution capabilities. In contrast, the application of membrane inlet mass spectrometry (MIMS) to the measurement of DMS in seawater circumvents many of these shortcomings.

MIMS is not a new method; it was first introduced in the early 1960s [*Hoch and Kok, 1963*] and is quickly gaining acceptance as an alternative to gas chromatography for the rapid analysis of volatile organic compounds in air and water samples [*Ketola et al., 1996*]. MIMS offers the advantages of shorter analysis time and a much larger linear dynamic range over PTGC methods, with comparable detection limits [*Ketola et al., 1996*]. Our adaptation of this technique uses a gas-permeable dimethylsilicone membrane as the interface between a seawater sample and the vacuum of the mass spectrometer. The sensitivity of the system is directly proportional to the surface area of the membrane exposed to the sample. Any gases dissolved in the aqueous sample diffuse through the membrane into the vacuum chamber, where they are ionized by electron impact and separated in a quadrupole filter based on their mass-to-charge (m/z) ratios. Major gases (CO_2 , O_2 , Ar, N_2) are detected by a Faraday cup and trace gases such as DMS by a secondary electron multiplier (SEM). The system can be used with a membrane inlet

probe for discrete applications or connected directly to a ship's seawater intake system for continuous, underway monitoring of dissolved gas concentrations. By employing the single ion monitoring (SIM) mode of the mass spectrometer software, and cycling through their respective m/z ratios, multiple gases can be monitored in real-time, pseudo-simultaneously with very little effort. Thus the main advantages of the MIMS system over PTGC for the analysis of DMS are its (1) significantly higher spatial resolution capabilities and (2) rapid, semi-automated analysis capabilities. One of the main contributions of this thesis is the development, troubleshooting and field-testing of a sea-going MIMS system.

1.4 Thesis Objectives

The foremost objective of this work was to determine whether MIMS could be successfully applied to the measurement of trace DMS and DMSP concentrations in seawater. Once this initial goal had been achieved, the research objectives were (1) to measure particulate DMSP concentrations in the NE Pacific along Line P where such measurements did not previously exist, (2) to examine the spatial and interannual variability in particulate DMSP levels along Line P in the context of phytoplankton species composition and nutrient levels, (3) to use the high-resolution underway capabilities of the MIMS to identify fine-scale structure in DMS concentrations in dynamic and productive waters of coastal B.C. and finally, (4) to use these high-resolution DMS data in conjunction with underway ancillary parameters to examine the factors driving the observed DMS distributions. As a result of the complex cycling of DMS in seawater and its dependence on a myriad of biological, meteorological, physical and chemical factors, it was hypothesized that DMS distributions would be unrelated to any single variable and would best be simulated by algorithms incorporating multiple components.

1.5 References

- Ayers, G.P. and J.L. Gras (1991), Seasonal relationship between cloud condensation nuclei and aerosol methanesulphonate in marine air, *Nature*, 353, 834-835.
- Boers, R., G.P. Ayers and J.L. Gras (1994), Coherence between seasonal variation in satellite-derived cloud optical depth and boundary-layer CCN concentrations at a mid-latitude Southern Hemisphere station, *Tellus, Ser B*, 46, 123-131.
- Bopp, L., O. Aumont, S. Belviso and P. Monfray (2003), Potential impact of climate change on marine dimethyl sulphide emissions, *Tellus, Ser B*, 55(1), 11-22.
- Charlson, R.J., J.E. Lovelock, M.O. Andreae, and S.G. Warren (1987), Oceanic phytoplankton, atmospheric sulfur, cloud albedo and climate, *Nature*, 326, 655-661.
- Chin, M., and D.J. Jacob, (1996) Anthropogenic and natural contributions to tropospheric sulphate: a global model analysis, *J. Geophys. Res.*, 101, 18,691-18,699.
- Dacey, J.W.H., and S.G. Wakeham (1986), Oceanic dimethylsulfide: Production during zooplankton grazing on phytoplankton, *Science*, 233(4770), 1314-1316.
- Evans, C, G. Malin, W.H. Wilson, and P.S. Liss (2006), Infectious titers of *Emiliana huxleyi* virus 86 are reduced by exposure to millimolar dimethyl sulphide and acrylic acid, *Limnol. Oceanogr.* 51(5), 2468-2471.
- Gabric, A.J., R. Simo, R.A. Cropp, A.C. Hirst and J. Dachs (2004), Modeling estimates of the global emission of dimethylsulfide under enhanced greenhouse gas conditions, *Global Biogeochem. Cycles*, 18, GB2014, doi:10.1029/2003GB002183.
- Gonzalez, J. M., R. P. Kiene and M.A. Moran (1999), Transformation of sulfur compounds by an abundant lineage of marine bacteria in the alpha-subclass of the class Proteobacteria, *App. Environ. Microbiol.* 65(9), 3810-3819.
- Gunson, J.R., S.A. Spall, T.R. Anderson, A. Jones, I.J. Totterdell, and M.J. Woodage (2006), Climate sensitivity to ocean dimethylsulphide emissions, *Geophys. Res. Lett.*, 33, L07701, doi:10.1029/2005GL024982.
- Hoch, G. and B. Kok (1963), A mass spectrometer inlet system for sampling gases dissolved in liquid phases, *Arch. Biochem. Biophys.*, 101, 160-170.
- Keller, M.D., W.K. Bellows, and R.R.L. Guillard (1989), Dimethyl sulfide production in marine phytoplankton, in *Biogenic sulfur in the environment*, edited by E.S. Saltzman and W.J. Cooper, p. 167-180, American Chemical Society, Washington, D.C.

- Ketola, R.A., V.T. Virkki, M. Ojala, V. Komppa and T. Kotiaho (1996), Comparison of different methods for the determination of volatile organic compounds in water samples, *Talanta*, 44, 373-382.
- Kettle, A.J. et al. (1999), A global database of sea surface dimethylsulfide (DMS) measurements and a procedure to predict sea surface DMS as a function of latitude, longitude and month, *Global Biogeochem. Cycles*, 13, 399-444.
- Kieber, D.J., J. Jiao, R.P. Kiene, and T.S. Bates (1996), Impact of dimethylsulfide photochemistry on methyl sulfur cycling in the equatorial Pacific Ocean, *J. Geophys. Res.*, 101(C2), 3715-3722.
- Kiene, R.P., and T.S. Bates (1990), Biological removal of dimethyl sulfide from sea water, *Nature*, 345, 702-705.
- Kiene, R.P., L.J. Linn, and J.A. Bruton (2000), New and important roles for DMSP in marine microbial communities, *J. Sea Res.* 43, 209-224.
- Legrand, M., C. Feniet-Saigne, E.S. Saltzman, C. Germain, N.I. Barkov and V.N. Petrov (1991), Ice-core record of oceanic emissions of dimethylsulphide during the last climate cycle, *Nature*, 350, 144-146.
- Lovelock, J.E., R.J. Maggs and R.A. Rasmussen (1972), Atmospheric sulphur and the natural sulphur cycle, *Nature*, 237, 452-453.
- Malin, G., W.H. Wilson, P.S. Liss and G. Bratbak (1998), Elevated production of dimethylsulfide resulting from viral infection of cultures of *Phaeocystis pouchetii*, *Limnol. Oceanogr.* 43, 1389-1393.
- Margalef, R. (1978), Life-forms of phytoplankton as survival alternatives in an unstable environment, *Oceanol. Acta*, 1, 493-509.
- Shaw, G.E. (1983), Bio-controlled thermostasis involving the sulfur cycle, *Clim. Change*, 5, 297-303.
- Simo, R., and C. Pedros-Alio (1999), Role of vertical mixing in controlling the oceanic production of dimethyl sulphide, *Nature* 402, 396-399.
- Sunda, W., D.J. Kieber, R.P. Kiene, and S. Huntsman (2002), An antioxidant function for DMSP and DMS in marine algae, *Nature*, 418, 317-320.
- Toole, D.A., D.J. Kieber, R.P. Kiene, E.M. White, J. Bisgrove, D.A. del Valle, and D. Slezak (2004), High dimethylsulfide photolysis rates in nitrate-rich Antarctic waters, *Geophys. Res. Lett.*, 31, L11307, doi:10.1029/2004GL019863.

- Vila-Costa, M., R. Simo, H. Harada, J.M. Gasol, D. Slezak and R.P. Kiene (2006), Dimethylsulfoniopropionate uptake by marine phytoplankton, *Science*, 314, 652-654.
- Watson, A.J. and P.S. Liss (1998), Marine biological controls on climate via the carbon and sulfur geochemical cycles, *Phil. Trans. Roy. Soc. Lon. Ser. B-Biol. Sci* 353, (1365), 41-51.
- Wolfe, G.V., M. Steinke, and G.O. Kirst (1997), Grazing-activated chemical defense in a unicellular marine alga, *Nature*, 387, 894-897.

2. Springtime Variability in Particulate DMSP Concentrations along Line P, NE Pacific Ocean¹

2.1 Introduction

For the past two decades, intense research efforts have focused on dimethylsulfide (DMS), a volatile degradation product of the algal metabolite dimethylsulfoniopropionate (DMSP). This research has been largely motivated by the proposal that DMS may be involved in global climate regulation through its ability to stimulate cloud formation and thereby affect planetary albedo [Charlson *et al.*, 1987]. In contrast, interest in its precursor, DMSP has mainly been in the realm of algal cell physiology, with efforts directed largely at illuminating the cellular function of this compound [Malin and Kirst, 1997; Stefels and van Leeuwe, 1998; Stefels, 2000]. Algal DMSP production is species specific, with prymnesiophytes and dinoflagellates being the main producers [Keller *et al.*, 1989]. In some species within these classes, this molecule can constitute a significant fraction of the cellular sulfur and carbon quotas [Matrai and Keller, 1994]. Yet despite the high intracellular concentrations of DMSP found in many species, no clear consensus has been reached on its exact physiological role. DMSP is likely a multifaceted molecule that has been suggested to function as an osmoregulant, a cryoprotectant [as reviewed by Malin and Kirst, 1997], an overflow mechanism for excess cell energy [Stefels, 2000], and an antioxidant [Sunda *et al.*, 2002]. The enzymatic breakdown of DMSP into DMS and acrylic acid catalyzed by algal DMSP-lyase has also been suggested to function as a grazing deterrent [Wolfe *et al.*, 1997] and most recently as an anti-viral defense mechanism [Evans *et al.*, 2006].

¹A version of this chapter will be submitted as Nemcek, N., T.D. Peterson, and P.D. Tortell. Interannual variability in springtime particulate DMSP concentrations along a coastal to oceanic transect in the NE Pacific. *Limnol. Oceanogr.*

In recent years, investigations into the cycling of DMSP by the microbial food web have revealed that this compound is important not only to the phytoplankton species that produce it, but also to other components of marine food webs [as reviewed by *Kiene et al.*, 2000]. DMSP and its degradation products (DMS, DMSO) constitute the largest pool of reduced organic sulfur in the oceans, and as such have been shown to be important growth substrates for many species of marine bacteria [*Kiene et al.*, 2000]. In fact, despite being present at a million-fold lower concentration than sulfate, DMSP represents an energetically favourable form of sulfur and is the preferred substrate for heterotrophic bacteria [*Kiene et al.*, 2000]. Thus, in addition to its physiological role in phytoplankton, DMSP is emerging as an integral component of the biogeochemical sulfur cycle and may play an important role in the marine ecosystem. As more progress is made towards elucidating the dynamics of oceanic DMSP cycling, the ecological and biogeochemical roles of this compound may turn out to be as significant as the climatological role of DMS.

In an attempt to understand the cycling of DMS/DMSP and the factors that regulate their production, researchers have sought to correlate concentrations of these compounds with various biological [*Leck et al.*, 1990; *Scarratt et al.*, 2002; *Riseman and DiTullio*, 2004], chemical [*Turner et al.*, 1988; *Leck et al.*, 1990; *Curran et al.*, 1998; *Riseman and DiTullio*, 2004] and physical [*Belviso et al.*, 1993; *Simo and Pedros-Alio*, 1999] variables with varying success. For example, DMSP concentrations in the field tend to correlate better with the presence of specific algal groups such as dinoflagellates or prymnesiophytes as opposed to bulk chlorophyll levels [*Scarratt et al.*, 2002; *Riseman and DiTullio*, 2004]. In addition, DMSP accumulations in natural communities have been shown to coincide with high concentrations of photoprotective pigments, suggesting a role of light in DMSP production [*Belviso et al.*, 1993; *Riseman and DiTullio*,

2004]. More recently, iron availability has been suggested as an additional factor influencing phytoplankton DMSP production as this compound may alleviate the oxidative stress associated with iron limitation [Sunda *et al.*, 2002]. As a result, algal DMSP concentrations in iron-limited regions are expected to be relatively higher than in other areas.

Numerous measurements of particulate DMSP (DMSPp) have been made in iron-limited, high nitrate, low chlorophyll (HNLC) waters of both the Southern Ocean [Meyerdierks *et al.*, 1997; Curran *et al.*, 1998] and the equatorial Pacific [Hatton *et al.*, 1998; Riseman and DiTullio, 2004]. In both regions, the data indicate that DMSPp:chl ratios are indeed higher in iron-limited vs. iron-replete areas [Curran *et al.*, 1998; Riseman and DiTullio, 2004]. By comparison, almost no DMSPp data exist for the NE Pacific, the third major iron-limited HNLC region. In fact, from the large quantity of recently compiled DMS/DMSP measurements that have been made throughout the world's oceans, it is evident that DMSPp data from the NE Pacific are conspicuously absent [Kettle *et al.*, 1999]. We present the first extensive dataset of particulate DMSP measurements obtained from waters of the NE Pacific, spanning both coastal and oceanic regimes. These measurements are further unique as they represent the first application of membrane inlet mass spectrometry (MIMS) for discrete DMSP measurements. The distribution of DMSPp is examined in the context of phytoplankton community composition and nutrient concentrations, in an attempt to elucidate the biogeochemical regulators of DMSP production in the NE Pacific.

2.2 Materials and Methods

Study area- The data presented herein were obtained during three consecutive spring cruises along Line P in the eastern subarctic Pacific Ocean onboard the *CCGS John P. Tully*. Sampling

was conducted between May 27-June 15, 2003, June 1-18, 2004 and June 1-18, 2005 at the 5 major stations along Line P, which connects Ocean Station Papa (OSP or P26) to the southern British Columbia coast (Fig. 2.1). The Line P dataset represents one of the longest running oceanographic time series and much is now known about the seasonal dynamics of phytoplankton biomass and production in this region [Harrison, 2002]. Stations P4, P12 are considered “coastal” stations and are typically characterized by a diatom-dominated spring bloom that declines with the onset of macronutrient limitation [Boyd and Harrison, 1999]. Station P16 is in the transition zone and stations P20 and P26 fall within the HNLC boundary, where surface nitrate concentrations remain high year-round [Whitney *et al.*, 1998]. At these stations, phytoplankton growth is limited by iron availability, and there is little seasonality in both biomass and primary production [Boyd and Harrison, 1999]. At all stations in this study, we assume that high macronutrient concentrations in surface waters are indicative of iron limitation [Whitney *et al.*, 1998].

DMSPp measurements- Particulate DMSP concentrations were measured at 5-8 depths in the top 50 m of the water column during each of the three cruises with slight modifications in the methodology from year to year. In all cases, seawater was collected in 10 L Niskin bottles deployed on a rosette sampler equipped with a Seabird 911+ CTD. Samples were drawn from Niskin bottles into rinsed 250 ml polypropylene bottles and immediately filtered. In 2003, duplicate 250 ml aliquots of seawater were collected at each depth and filtered under low vacuum (< 5 in. Hg) onto 25 mm GF/F filters (nominal pore size 0.7 μm). The filters were then transferred to 25 ml Alltech glass vials equipped with gas tight ‘mini-nerf’ closures. A 2 ml aliquot of methanol was added to each vial and the filters were allowed to extract at -20° C for

several hours before 25 ml of 1 N NaOH was added to the vials. Sealed vials were left at room temperature overnight prior to analysis to ensure complete stoichiometric hydrolysis of DMSP to DMS [Dacey and Blough, 1987]. Headspace in the vials was minimal, providing negligible losses of DMS into the gaseous phase owing to the high solubility of this gas ($K_H = 0.48 \text{ mol L}^{-1} \text{ atm}^{-1}$) [De Bruyn *et al.*, 1995]. Samples were analyzed onboard ship the following day by MIMS as described below.

In 2004 and 2005, a single 250 ml sample was collected at each depth and gravity filtered onto a 47 mm GF/F filter. The filters were placed into 5 ml cryovials with 3 ml of methanol. The vials were stored at -20°C until analyzed in the laboratory within 2-6 months. DMSP stored in this manner is known to be stable for extended periods of time (J. Dacey, pers. comm.). Prior to analysis, 2 ml aliquots of the DMSPp extract in methanol were transferred into 14 ml glass serum vials, topped with 12 ml of 1N NaOH and sealed with Teflon-faced butyl liners (Wheaton) and aluminium crimp seals. The vials were vortexed and allowed to react overnight at room temperature under minimal headspace.

In all three years, DMSPp analysis was performed 12-24 hours after base hydrolysis by measuring the DMS concentration in the liquid phase using MIMS with a membrane inlet probe supplied by the manufacturer (Hiden Analytical, UK). The probe consists of a 1/16" stainless steel capillary tube fitted with a 0.005" thick dimethylsilicone sleeve that is ideally suited for analyzing small-volume, discrete samples. Although this probe has relatively low sensitivity due to the small surface area of the membrane, the reduced sensitivity was not a factor as DMSPp samples were concentrated by filtration, and the resultant DMS concentrations in the sample vials ranged from ~50-500 nM.

During analysis, the vials were uncapped and the membrane probe was inserted directly into the liquid sample. The sample was stirred to ensure a constant flow across the membrane. DMS was measured by single ion monitoring of the m/z 62 peak using the residual gas analysis (RGA) mode of the mass spectrometer control software (MASsoft, Hiden Analytical). Experiments with blank solutions (2 ml methanol + 25 ml 1N NaOH) showed that no other ions were detected at m/z 62. The mass spectrometer was run with an ion source emission current of 1000 μ A in 2003 which was reduced to 250 μ A in subsequent years following optimization of the quadrupole mass filter to a lower mass range. DMS was measured using a secondary electron multiplier (SEM) set to a voltage of 950 V with detector dwell and settle times of 300 ms.

For each sample measurement, the signal intensity was allowed to stabilize and was then monitored for 2-5 minutes before subsequent samples were introduced. The signal dropped instantaneously following removal of the probe from the samples, indicating no memory effects on the membrane. Although the vials were uncapped, the signal for individual samples was stable for the entire duration of analysis time, indicating minimal loss of DMS to the atmosphere. As a further test, some samples were left stirring, uncapped, with the probe in place for up to 30 minutes with no significant decline in the DMS signal (data not shown). The data stream from the MIMS was exported to a spreadsheet and the mean m/z 62 signal intensity for each sample was determined by averaging over a two-minute interval during the stable signal plateau. In all three years, a calibration curve was generated for each set of samples using fresh DMSP standards consisting of known aliquots of sterile DMSP solution (Research Plus Inc.) prepared in methanol and 1N NaOH. Standards were prepared at the same time, in the same vials, and in the same volumes of methanol and sodium hydroxide as the samples to prevent matrix effects on the

membrane, to ensure equivalent hydrolysis times, and to compensate for any small losses of DMS to the headspace.

Ancillary oceanographic measurements- Samples for chlorophyll *a* (chl *a*) analysis were drawn from the same Niskin bottles as the DMSPp samples and concentrations were determined using a fluorometric method following filtration of seawater samples onto 25 mm GF/F filters and extraction of pigments in 90% acetone for 24 hours [Parsons *et al.*, 1984]. Seawater nutrient concentrations were determined using a ship-board auto-analyzer while temperature and salinity data used to calculate potential density (σ_T) were obtained from the CTD. The lower boundary of the mixed layer was defined as the depth at which the value of σ_T changed by 0.02 from that of the surface.

In 2003, ^{14}C primary productivity and calcification rate measurements were made at the chlorophyll *a* maximum at each station. For these determinations, 200 ml of seawater were collected into acid-washed polycarbonate bottles and spiked with 20-50 μCi H^{14}CO_3 (50 mCi mmol^{-1}). Bottles were incubated in an onboard Plexiglass flow-through incubator at 30 % surface irradiance and *in situ* temperature for 24 hours. Following incubation, samples were harvested onto 25 mm GF/F filters, carefully rinsed with 0.2 μm filtered seawater to wash away unfixed H^{14}CO_3 , and immediately frozen in scintillation vials at -20°C . Upon return to the laboratory, filters were acidified with 1 ml 50 % phosphoric acid, capped, and placed on a shaker table overnight. Inorganic calcite collected on the GF/F was liberated as CO_2 by this acid treatment. This CO_2 was trapped in phenethylamine (base)-soaked filters (13 mm GF/D) stuck to the caps of the vials, while organic carbon was left behind on the primary GF/F. The base-soaked filters were placed in fresh vials and capped, and both sets of vials (comprising the inorganic and

organic ^{14}C fraction) were counted on a scintillation counter after the addition of 10 ml of scintillation cocktail (Scintisafe, Fisher Scientific). Four bottle replicates were run at each station and both productivity and calcification measurements were corrected for ^{14}C uptake in dark bottles.

In 2003, samples for phytoplankton enumeration and taxonomy were collected from two depths at each station into 250 ml glass amber bottles and fixed with hexamethylene-tetramine-buffered formalin to a final concentration of 0.4 %. Identification and counts were performed on 40 or 100 ml subsamples using inverted microscopy with Utermohl settling chambers following a 24-hour settling period. Cell volumes for individual phytoplankton taxa were estimated using cell dimensions and basic geometric formulas (spheres, prolate spheres, cylinders, etc.). Cell carbon quotas were determined from volume estimates using the formulas of *Montagnes et al.* [1994] for flagellates:

$$C = 0.109 * V^{0.991} \quad (1)$$

and *Strathmann* [1967] for diatoms:

$$\log C = -0.314 + 0.712 * \log V \quad (2)$$

where C is carbon content per cell in pg, and V is cell volume in μm^3 .

2.3 Results

Application of MIMS to DMSPp analysis- MIMS proved to be an effective new tool for measuring particulate DMSP concentrations in seawater. Since DMSPp was measured directly from the liquid phase, analysis time was greatly reduced compared to that typical of purge and trap gas chromatography (PTGC), which requires sample sparging. In 2003 when MIMS was first field-tested, individual DMSP samples took an average of 5 minutes to analyze, allowing a complete depth profile with standards to be run in duplicate in under 2 hours. Although the method was simple and rapid, it produced high quality data. The calibration curves were linear over a 40-fold concentration range, and sample replication was good (mean s.d. of duplicates = 9.5 %). As a result, only single samples were collected at each depth in subsequent years. In 2004, a switch to a thinner membrane yielded faster response times, reducing the analysis time for each sample to 2 minutes.

The reduction in sensitivity (compared to the large membrane cuvette) resulting from the smaller surface area of the membrane inlet probe did not hinder our ability to accurately measure DMSPp concentrations in any samples. Although detection limits were not explicitly determined, 15 nM samples were easily measurable relative to blanks. Taking into account sample concentration by filtration, yielded a detection limit of <1 nM *in situ* DMSPp. This was well below the majority of concentrations encountered during the surveys. Due to the small size of the membrane probe, it is possible to significantly reduce the volume of the sample vials used (i.e. from 14 ml to 3 ml), which would reduce the volume of the initial seawater sample required and minimize potential filtration artefacts [as in *Kiene and Slezak, 2006*].

Variability in DMSPp concentration - Particulate DMSP concentrations in the upper 50 m of the water column along Line P showed considerable variability with depth, across stations, and between study years (Fig. 2.2). Due to inclement weather, samples were not collected at P16 in 2005. DMSPp levels ranged from a low of 0.2 nM at 50 m depth at P4 in 2004 to a high of 63.2 nM at 10 m depth at P12 in 2003, with an overall mean concentration for the 3 year survey of 21.5 nM ($n = 94$, $s.d. = 15.0$ nM). In general, the coastal stations (P4, P12) had higher maximum DMSPp concentrations than the offshore stations (P16-P26), in conjunction with higher levels of chlorophyll *a* (Figs. 2.2, 2.3). The one notable exception was P12 in 2005 when both the DMSPp and chlorophyll concentrations were uniformly low. Chlorophyll levels along Line P were usually less than $1 \mu\text{g L}^{-1}$, except for at P4 in 2004, where a prominent subsurface chlorophyll maximum of $2.2 \mu\text{g L}^{-1}$ was encountered (Fig. 2.3).

Both the DMSPp and chlorophyll *a* depth profiles at P4 and P12 were characterized by subsurface maxima and more vertical variability than found offshore (Figs. 2.2, 2.3). At these stations, the DMSPp maximum occurred near the base of the rather shallow mixed layer (<20 m), while the chlorophyll *a* maximum generally occurred just below this depth. In contrast, stations P16-P26 had deeper mixed layers (30-40 m) and relatively uniform depth profiles with very little vertical structure in either DMSPp or chlorophyll *a* concentrations in the upper 50 m of the water column (Figs. 2.2, 2.3). The progressive loss of vertical structure in the profiles moving offshore from P4 to P26 coincided with the progressive deepening of the mixed layer and likely also to a deepening of the euphotic zone due to decreased phytoplankton biomass (as estimated by chlorophyll *a*).

Variability in DMSPp concentrations along Line P between survey years was high (Fig. 2.2). This variability was most pronounced at P4 and P12, and appeared to be driven at least in

part by high variability in chlorophyll *a* levels (Fig. 2.3). The lone exception was station P20 which had relatively constant DMSPp and chlorophyll *a* concentrations in all three years. In general, DMSPp concentrations across the survey region were highest in 2003 and decreased significantly in the following years by in many cases more than 50 % (Fig. 2.2). The mean DMSPp concentrations across all stations in 2004 (14.6 nM) and 2005 (16.6 nM) were less than half the mean concentration in 2003 (33.6 nM). Although this decrease in DMSPp levels appeared to occur in conjunction with a decrease in chlorophyll *a* concentrations (Fig. 2.3), DMSPp:chl ratios also dropped in subsequent years, indicating that the decline in DMSPp levels was due to more than just a drop in overall phytoplankton biomass (Fig. 2.4). DMSPp:chl ratios along Line P ranged from 0.67 nmol μg^{-1} at 50 m at P4 in 2004 to 103 nmol μg^{-1} at 20 m at P26 in 2003 (Fig. 2.4). The mean ratio across all stations in 2003 (61.1 nmol μg^{-1}) was almost twice the mean ratio observed in 2004 (33.6 nmol μg^{-1}) and 2005 (37.0 nmol μg^{-1}). Contour plots illustrating the interannual and spatial variability of both DMSPp and chlorophyll *a* along Line P are presented in Figure 2.5.

DMSPp in relation to other variables- While DMSPp concentrations varied to some extent with total phytoplankton biomass, other factors including the physiological status and species composition of the phytoplankton community also likely affected the observed distributions. Along Line P, the depth profiles of DMSPp generally resembled those of chlorophyll at individual stations, but overall there was only a weak linear correlation between the two variables for the 3-year pooled dataset ($r^2 = 0.20$, $n = 94$, $p < 0.0001$; Fig. 2.6). Two significant outliers characterized by high chlorophyll concentrations confounded this relationship (P4, 20 and 25 m depth in 2004). With these outliers removed the positive linear correlation between

DMSPp and chlorophyll *a* was significantly strengthened ($r^2 = 0.45$, $n = 92$, $p < 0.0001$), although a good deal of scatter remained.

To examine other factors potentially influencing DMSPp variability, ancillary measurements including primary productivity and calcification rates, as well as detailed phytoplankton species counts were made during the 2003 survey. For interannual comparison purposes, only DMSPp data collected at the 5 major time-series stations along Line P are presented, however, measurements were also obtained at additional surrounding stations each year. In 2003, DMSPp concentrations and supporting parameters were also measured at stations A3, A4, and A6 (see Fig. 2.1 for station locations) and are included in the following analyses to increase the sample size (Table 2.1).

Detailed phytoplankton community composition data were collected at 10 m depth in the mixed layer and at the chlorophyll maximum at all stations during 2003. Various small, unidentified flagellates were numerically dominant at the more coastal stations (P4, P12, P16, A6; Fig. 2.7). Although these flagellates were still abundant offshore (P20, P26, A3, A4), small diatoms and prymnesiophytes increased in abundance at these oceanic stations (Fig. 2.7). DMSPp concentrations were not linearly correlated to the abundance of any phytoplankton group. However, when phytoplankton abundance was converted to carbon biomass using the appropriate conversion factors (see methods), the relative contribution of each group to the total community changed dramatically (Fig. 2.8). Despite contributing less than 10 % to total cell abundance, dinoflagellates dominated carbon biomass at P4 and P12, and made a significant contribution at the other stations (Fig. 2.8). A significant, positive relationship was observed between DMSPp concentrations and the relative carbon biomass of dinoflagellates across the survey region ($r^2 = 0.46$, $n = 16$, $p < 0.05$, Table 2.2). Small, pennate diatoms also contributed

significantly to carbon biomass at most stations particularly at the chlorophyll max. at stations P20, A4 and A6 (Fig. 2.8b). However, diatom biomass was lowest at P4, P12 and A3, the 3 stations with the highest DMSPp concentrations resulting in a significant inverse relationship between diatom biomass and DMSPp levels across all stations ($r^2 = 0.33$, $n = 16$, $p < 0.05$, Table 2.2). Given the estimates of phytoplankton carbon biomass, the percent cell carbon as DMSP in each sample was calculated using a C:S ratio of 5:1 for DMSP (Table 2.3).

Primary productivity rates measured at the chlorophyll *a* maximum in 2003 were ~3 times higher at P4 than at any other station and thus appeared to be unrelated to DMSPp levels (Table 2.1). In contrast, calcification rates expressed as a percentage of primary productivity rates were highest in offshore HNLC waters (P20, P26, A3 and A4; Table 2.1), in accordance with an increased proportion of prymnesiophytes (Figs. 2.7b, 2.8b). There was a significant linear relationship between relative calcification rates and the relative carbon biomass of prymnesiophytes (of which coccolithophores are a prominent subgroup) across the survey region ($r^2 = 0.69$, $n = 8$, $p = 0.01$, data not shown). However, neither absolute nor relative calcification rates were correlated to DMSPp or DMSPp:chl levels.

The effect of variable nutrient concentrations on the cross-transect and inter-cruise variability in DMSPp levels was examined. Depth integrated DMSPp:chl ratios are plotted against the mixed layer nitrate concentration at each station in Figure 2.9. Although there was some indication that higher DMSPp:chl ratios were associated with high nitrate, low iron waters in 2003, this trend did not hold in subsequent years (Fig. 2.9). Furthermore, variability in DMSPp:chl ratios between study years appeared unrelated to surface nitrate levels.

2.4 Discussion

The stations of the NE Pacific connected by Line P boast one of the longest and most comprehensive open ocean time series, and much oceanographic data has been collected here over the past 50 years, particularly at Ocean Station Papa (P26) [see review *Harrison, 2002*]. Despite all the information amassed on the dynamics of phytoplankton productivity and biomass [*Booth et al., 1993; Boyd and Harrison, 1999*], there have been virtually no DMSP measurements made in this region [see *Kettle et al., 1999*]. Prior to the recent publication of DMSPp measurements obtained during the SERIES iron-fertilization experiment conducted near Station Papa [*Levasseur et al., 2006*], the only DMSP data for the entire NE Pacific consisted of a single depth profile taken off the coast of Washington state [*Bates et al., 1994*]. This is surprising given the numerous measurements of surface water DMS concentrations [*Watanabe et al., 1995; Aranami et al., 2001; Wong et al., 2005*] that have been made in the area. A recently published 6-year time series of DMS concentrations along Line P [*Wong et al., 2005*] confirms earlier observations that this region hosts some of the highest spring/summer DMS levels in the world [*Kettle et al., 1999*], and may thus be an important source of this gas to the atmosphere. Since the production of DMS ultimately depends on the algal production of DMSP, measurements of this pool constitute the first step towards understanding the factors leading to elevated DMS levels in the NE Pacific. The data presented herein comprise the first extensive set of DMSPp measurements made in this region. These data reveal that concentrations of DMSPp exhibit significant inter-cruise and spatial variability, both with depth and across the survey area.

Spatial Variability in DMSPp levels- High spatial variability in DMSPp levels was observed in each survey year with a 2-3 fold range in maximum concentrations along Line P. In general,

DMSPp concentrations decreased offshore, though DMSPp:chl ratios showed no consistent trend between coastal and HNLC waters. At stations P4 and P12 where prominent depth maxima in both chlorophyll *a* and DMSPp were observed (Figs. 2.2, 2.3), DMSPp maxima were always shallower than chlorophyll *a* maxima. This is a commonly reported phenomenon [Turner *et al.*, 1988; Belviso *et al.*, 1993; Dacey *et al.*, 1998], and is likely due to the opposing effects of nutrients and light on the synthesis of chlorophyll and DMSP. In surface waters, conditions that promote oxidative stress such as high light [Sunda *et al.*, 2002; Slezak and Herndl, 2003] and low nutrients [Bucciarelli and Sunda, 2003] may promote increased algal production of DMSP. In contrast, deeper in the water column phytoplankton photoacclimate in response to higher nutrient and low light conditions by increasing their intracellular chlorophyll *a* concentrations [Falkowski and LaRoche, 1991]. Although it has been suggested that depth differences in DMSPp and chlorophyll *a* maxima may simply reflect changes in species composition with depth, [Dacey *et al.*, 1998], we did not observe any dramatic shifts in phytoplankton community composition between surface and deep waters (Figs. 2.7, 2.8). In fact, the biomass of prominent DMSP-producers such as dinoflagellates [Keller *et al.*, 1999], was higher at the chlorophyll max. than at 10 m depth in the mixed layer suggesting a physiological driver for the depth structure of DMSPp levels (Fig. 2.8).

DMSP in relation to other variables- Consistent with the results of many previous studies [Belviso *et al.*, 1993; Townsend and Keller, 1996; Dacey *et al.*, 1998], only a weak correlation between particulate DMSP and chlorophyll *a* concentrations was observed over the 3-year survey period along Line P (Fig. 2.6). Since significant DMSP production is confined to a few classes of phytoplankton [Keller *et al.*, 1989], DMSPp concentrations should be more strongly

correlated to the presence of certain taxonomic groups than to bulk chlorophyll concentrations, as has been observed previously [Scarratt *et al.*, 2002]. In 2003, only a weak linear correlation was observed between DMSPP levels and bulk chlorophyll at the 8 stations surveyed ($r^2 = 0.32$, $n = 46$, $p < 0.001$). Instead, DMSPP was more strongly correlated to the relative carbon biomass of dinoflagellates ($r^2 = 0.46$, $n = 16$, $p < 0.05$, Table 2.2), a group known for high DMSP quotas [Keller *et al.*, 1989]. Interestingly, DMSPP concentrations also showed a significant, inverse relationship to the relative carbon biomass of diatoms ($r^2 = 0.33$, $n = 16$, $p < 0.05$, Table 2.2), which generally produce little DMSP [Keller *et al.*, 1989]. In contrast, there was no linear correlation between DMSPP concentrations and the biomass of prymnesiophytes (Table 2.2), another group of prominent DMSP-producers, despite the fact that this group increased in abundance in HNLC waters in conjunction with elevated DMSPP:chl ratios and higher relative calcification rates (Table 2.1). This is not entirely surprising as in addition to taxonomic effects, DMSP production is influenced by physicochemical factors including nutrient availability [Stefels and van Leeuwe, 1998; Sunda *et al.*, 2002; Bucciarelli and Sunda, 2003] and both visible [Belviso *et al.*, 1993; Stefels and van Leeuwe, 1998] and UV light [Slezak and Herndl, 2003]. These factors vary widely in the marine environment and may obfuscate attempts to link the algal DMSP pool with any specific phytoplankton group.

Contribution of DMSP to carbon biomass- Based on measured DMSPP concentrations and the estimates of carbon biomass determined from phytoplankton cell counts, the relative contribution of DMSP to total autotrophic cell carbon was determined for each sample in 2003 (Table 2.3). Apart from at stations P4 and P12, the estimates of percent cell carbon as DMSP in this study were much higher (mean $20.3 \pm 15\%$) than those reported in previous field studies (1-10%),

despite the fact that the corresponding DMSP:chl ratios fell within the range of those in the literature [see review by *Kiene et al.*, 2000; *Simo et al.*, 2002]. Although many of these previous studies did not estimate carbon biomass directly and simply assumed a C:chl ratio of 50 g g^{-1} [i.e. *Simo et al.*, 2002], it is possible that some of the C:chl ratios calculated herein are underestimates (i.e. 6.5 g g^{-1} at 10 m P16, Table 2.3).

Carbon-to-chlorophyll ratios can range from 20-160 g g^{-1} and vary with depth, latitude, season [*Taylor et al.*, 1997], and proximity to the coast [*Chang et al.*, 2003]. With only a few exceptions (P4, P12), C:chl ratios in this study were all less than 30 g g^{-1} , values more typical of nutrient-replete, light-limited deep waters [*Taylor et al.*, 1997], rather than iron-limited surface waters. The C:chl ratio estimated for the iron-limited station P26 ($20\text{-}30 \text{ g g}^{-1}$) is about half the 50 g g^{-1} spring/summer average determined previously for this station [*Booth et al.*, 1993]. Stations P16 and A6 where the lowest C:chl ratios were measured were dominated by small unidentifiable flagellates (Fig. 2.7), whose exact numbers, dimensions and thus carbon content were prone to larger errors. In addition, preserved cells have a tendency to shrink, leading to reduced volume estimates and hence underestimated carbon quotas. Furthermore with the microscopic method used, it was not possible to enumerate cyanobacteria such as *Synechococcus* spp. which are known to be abundant at the oceanic stations along Line P [*Booth et al.*, 1993], and likely made a significant contribution to total autotrophic carbon biomass. This uncertainty in the biomass estimates may also have confounded attempts to relate DMSP levels to the carbon biomass of individual phytoplankton groups across the survey region. Applying a constant C:chl ratio of 50 g g^{-1} to all stations yields a percent contribution of DMSP to cell carbon of 2.5-18.8 % (mean 8.4 %), more in line with other oceanic field studies [*Kiene et al.*, 2000; *Simo et al.*, 2002].

Inter-cruise Variability in DMSPp along Line P- Variability in springtime DMSPp

concentrations along Line P between survey years was high, and was most pronounced at the coastal stations P4 and P12 (Figs. 2.2, 2.5). Stations P16 and P20 showed much less variability in DMSPp levels, while at P26 a dramatic (>3-fold) decline in DMSPp levels occurred after 2003, with concentrations remaining relatively constant in the following two years (Figs. 2.2, 2.5). Across the survey region, DMSPp concentrations (and DMSPp:chl ratios) were generally highest in 2003. The surveys in all 3 years occurred during almost the same three-week period, however, the timing of the spring bloom at the coastal stations may have differed leading to the high variability in both DMSPp (Fig. 2.2) and chlorophyll *a* levels (Fig. 2.3) observed at P4 and P12. As a result of the relatively shallow winter mixed layer, tight coupling between autotrophs and grazers, and persistent iron-limitation, stations P20-P26 exhibit much less seasonality in phytoplankton biomass [Boyd and Harrison, 1999], such that the timing of the cruises would have less impact on the observed variability.

Due to a lack of knowledge of the seasonal variability in DMSPp concentrations in this region, it is difficult to speculate whether the inter-cruise differences represent true inter-annual variability or different phases of the seasonal cycle. Methodological differences in DMSPp analysis also exist between study years, as samples were analyzed at sea in 2003, and several months after sample collection in 2004 and 2005. However, this is likely not a significant factor in determining inter-cruise variability, since samples were always measured relative to fresh standards and DMSPp is known to be stable in methanol for months (J. Dacey, pers. comm.). Differences in sea surface temperature greater than 2 °C were observed between study years at P26, and these along with changes in nutrient supply and chlorophyll biomass support the changes in DMSPp levels, arguing against a methodological cause of variability.

The differences in DMSPp:chl ratios at individual stations between study years (Fig. 2.4), coupled with the weak overall correlation between DMSPp and chlorophyll *a* (Fig. 2.6) point to a taxonomic or physiological driver of DMSPp variability. In 2003, DMSP-rich dinoflagellates made a significant contribution to total autotrophic carbon at all stations (Fig. 2.8). Although phytoplankton community composition data were not collected in subsequent years, it is possible that a decline in dinoflagellates could account for the drop in DMSPp levels and DMSPp:chl ratios after 2003. Dramatic shifts in the biomass of dinoflagellates and prymnesiophytes (up to 2 orders of magnitude) have been shown to occur in consecutive years at P26 [Wong *et al.*, 2006].

Nutrient conditions can also influence DMSPp variability. Since DMSP and its byproducts have been shown to function as powerful antioxidants [Sunda *et al.*, 2002], algal DMSP production is expected to increase under oxidative stressors such as iron-limitation. In 2003, there was some evidence to this effect as DMSPp:chl ratios at individual stations increased in conjunction with higher surface nitrate levels, an indicator of iron-limitation in this region (Fig. 2.9). Evidence for a positive relationship between DMSPp:chl ratios and nitrate concentrations also comes from HNLC waters of the Southern Ocean [Curran *et al.*, 1998; Jones *et al.*, 1998]. In this latter study, the highest DMSPp concentrations coincided with low chlorophyll levels and high nitrate waters [Curran *et al.*, 1998; Jones *et al.*, 1988]. The authors did not directly relate this observation to iron concentrations, but iron availability is known to limit phytoplankton growth in these waters [Curran *et al.*, 1998]. Perhaps the strongest field evidence for the effect of iron on DMSP production comes from the iron-limited waters of the equatorial Pacific where DMSPp:chl ratios were 2-6 higher in iron depleted offshore waters than in iron-rich coastal waters [Riseman and DiTullio, 2004].

The positive trend observed between DMSPp:chl ratios and nitrate levels in 2003 did not occur in subsequent years (Fig. 2.9). In 2004, a large decline in the DMSPp:chl inventory occurred at station P26 despite a relatively constant nitrate concentration. Interestingly in 2005, the spring surface nitrate concentration at P26 plummeted to about half the usual 14 μM value. In all 3 years, the previous winter's surface nitrate concentration at P26 was a constant $\sim 14 \mu\text{M}$, indicating that significant nitrate drawdown had occurred at this station in 2005, possibly as a result of an iron injection. Although both chlorophyll (Fig. 2.3) and DMSPp levels (Fig. 2.2) showed a slight increase over 2004 levels in conjunction with this drawdown, DMSPp:chl ratios remained largely unchanged from the previous year (Figs. 2.4, 2.9).

Without taxonomic data for 2004 and 2005 it is difficult to determine whether the interannual variability in DMSP levels along Line P was due to changes in phytoplankton community composition or physiology. Even with this data it is difficult to tease apart these two factors in the field since changes in nutrient concentrations tend to be linked to floristic shifts in the phytoplankton community. This was the case in the equatorial Pacific where an increase in DMSPp:chl ratios under iron-limitation was also associated with a shift from diatoms to cryptophytes and prymnesiophytes [Riseman and DiTullio, 2004]. Small cells such as flagellates that are prominent DMSP-producers [Keller *et al.*, 1989] tend to dominate when nutrient concentrations are low. Whether this floristic shift occurs precisely because these cells have a competitive advantage under low nutrient conditions not only because of their greater surface area to volume ratio, but also because of their DMSP production capabilities, has yet to be shown.

DMSPp variability in relation to DMS concentrations- The original impetus for this work was to determine if the unusually high spring/summer DMS levels characteristic of the HNLC region around Station Papa [Kettle *et al.*, 1999; Wong *et al.*, 2005] were associated with high DMSPp concentrations. DMS levels up to 25 nM have been reported during the spring/summer months at stations along Line P [Wong *et al.*, 2005]. These values are exceptional for open ocean areas where DMS rarely exceeds 5 nM [Kettle *et al.*, 1999], and are more typical of productive, coastal regions. Despite the unusually high DMS levels at Station Papa, the DMSPp pool had previously not been measured in this region. Given that DMSPp is the ultimate source of all DMS, its measurement provides important insight into the factors driving high DMS concentrations.

Unfortunately, DMS concentrations were uncharacteristically low in June during our 3-year survey period, as determined by MIMS in 2003 [Tortell, 2005] and independently by PTGC (C.S. Wong, unpublished data). At the oceanic stations beyond P12, DMS concentrations were less than 5 nM in all three years (C.S. Wong, unpublished data). This trend is consistent with the general decline in spring and summer DMS levels that occurred along Line P following the 1998-1999 transition from an El Nino to a La Nina event [Wong *et al.*, 2005]. The >10-fold decrease in DMS levels at P26 between 1998 and 1999 occurred in conjunction with a dramatic drop in the biomass of dinoflagellates and prymnesiophytes [Wong *et al.*, 2006], and thus presumably, DMSPp. The Wong *et al.* [2005] time series only presents data to 2001; interestingly, during the SERIES iron fertilization experiment conducted near Station Papa in July of 2002, DMS levels were once again high at >15 nM in the control waters outside the iron-enriched patch [Levasseur *et al.*, 2006]. Perhaps more significantly, corresponding DMSPp concentrations were between 98-130 nM and prymnesiophytes were very abundant [Levasseur *et al.*, 2006]. As noted by Levasseur *et al.* [2006], both the DMS and DMSPp concentrations

measured prior to SERIES were 2-6 times higher than those measured at the onset of previous iron fertilization experiments in HNLC waters of the equatorial Pacific and Southern Ocean. Moreover, DMS and DMSPp levels in July 2002 were at least 2-3 fold higher than any measured at the oceanic stations during the June 2003-2005 surveys. Thus, the high DMS levels observed previously in the NE Pacific HNLC region appear to occur in conjunction with high DMSPp concentrations. In the absence of sufficient evidence linking DMSPp variability to variations in nutrient supply during the present study, we conclude that changes in DMSPp concentrations are likely due to taxonomic shifts in the phytoplankton community, and drive the variability in DMS levels observed in recent years in this HNLC region.

Table 2.1: Ancillary oceanographic data for all stations surveyed during 2003. Mixed layer depth (MLD) is defined as a change in sigma-t (density) of 0.02 from that of the surface. Primary productivity (PP) and calcification rates (Calc.) were determined at the chl *a* max. at each station. DMSPP:chl ratios are 50 m depth integrated values.

STATION	MLD (m)	average ML [NO ₃ ⁻] (μM)	PP (μg C L ⁻¹ d ⁻¹)	Calc. (μg C L ⁻¹ d ⁻¹)	Calc./PP (%)	DMSPP:chl (μmol mg ⁻¹ m ⁻²)
P4	10	0.1	31.8	0.42	1.33	58.4 ± 3.8
P12	25	3.3	11.6	0.29	2.48	62.9 ± 1.5
P16	40	6.1	7.3	0.01	0.16	55.4 ± 1.7
P20	40	8.0	8.3	0.35	4.25	56.8 ± 1.1
P26	35	13.9	9.3	0.57	6.15	79.2 ± 2.4
A3	<10	15.4	9.5	0.26	2.69	118.2 ± 1.6
A4	<10	9.9	7.5	0.31	4.12	81.8 ± 1.8
A6	<10	3.0	10.5	0.12	1.16	49.5 ± 0.9

Table 2.2: Coefficients of determination (r^2) from linear regressions between DMSPp levels and the absolute and relative carbon biomass of different phytoplankton groups for all stations during the 2003 survey; $n = 16$, * denotes statistically significant relationships with $p < 0.05$, † denotes inverse relationship.

Group	DMSPp vs. C L⁻¹	DMSPp vs. % C contribution
misc. flagellates	0.13	0.016
Prymnesiophytes	4.1×10^{-6}	9.3×10^{-3}
Dinoflagellates	0.33*	0.46*
Prasinophytes	0.070	0.044
Diatoms	8.0×10^{-3}	0.33*†
Cryptophytes	0.12	0.048

Table 2.3: The contribution of DMSPP to total phytoplankton cell carbon in 2003. Phytoplankton biovolume was determined from microscopic cell counts and the appropriate geometric formulas at two depths at each station. Biovolume was converted to carbon biomass using the formulas of *Strathmann* [1967] for diatoms and *Montagnes et al.* [1994] for flagellates.

Station	depth (m)	chl <i>a</i> ($\mu\text{g L}^{-1}$)	C biomass ($\mu\text{g L}^{-1}$)	DMSPP (nM)	C:chl ratio ($\mu\text{g } \mu\text{g}^{-1}$)	DMSPP:chl ($\text{nmol } \mu\text{g}^{-1}$)	% cell C as DMSP
P4	10	0.66	65.8	60.3	99.1	90.8	5.5
	20	0.90	88.5	59.7	98.5	66.4	4.0
P12	10	0.76	21.3	63.2	27.9	63.2	7.9
	30	0.96	22.6	56.8	23.6	56.8	6.2
P16	10	0.44	2.8	26.6	6.53	60.5	55.6
	40	0.62	10.8	29.2	17.5	47.5	16.3
P20	10	0.38	9.8	22.6	26.2	60.1	13.8
	50	0.43	31.2	21.2	72.1	48.9	4.1
P26	10	0.42	12.6	37.3	30.1	88.8	17.7
	50	0.58	14.9	27.0	20.5	46.5	13.6
A3	10	0.39	8.2	59.1	21.1	152	43.1
	25	0.51	11.3	56.7	22.1	111	30.2
A4	10	0.37	7.9	37.0	21.5	101	28.1
	40	0.44	5.8	12.5	13.3	28.7	12.9
A6	10	0.59	7.1	40.2	12.0	68.0	34.0
	25	0.62	6.3	33.5	10.1	54.0	32.1

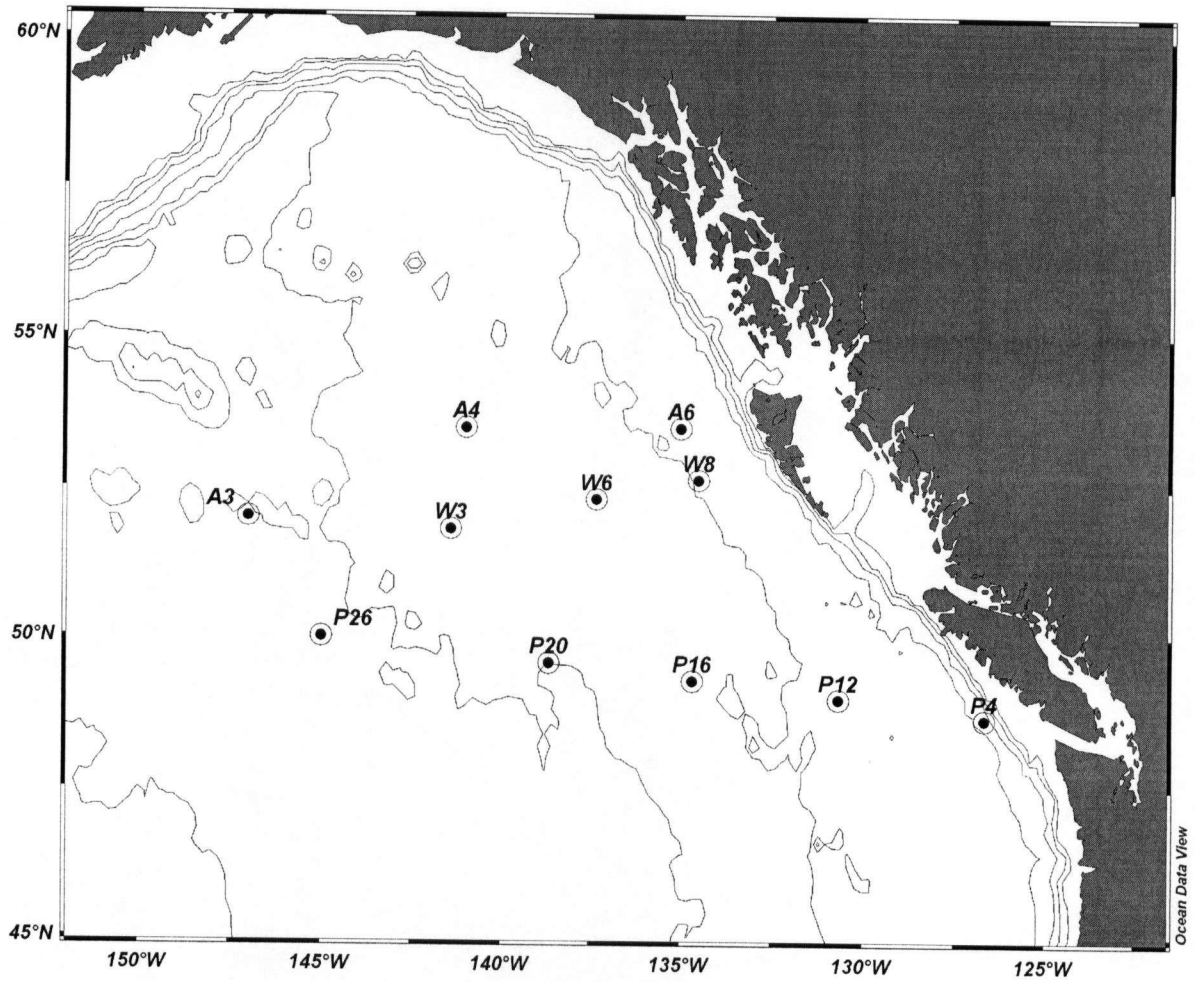


Figure 2.1: Map of the NE Pacific showing the 5 major stations along Line P. Also shown are supplemental stations where measurements were made in different years (A3, A4, A6 in 2003; W3, W6, W8 in 2005).

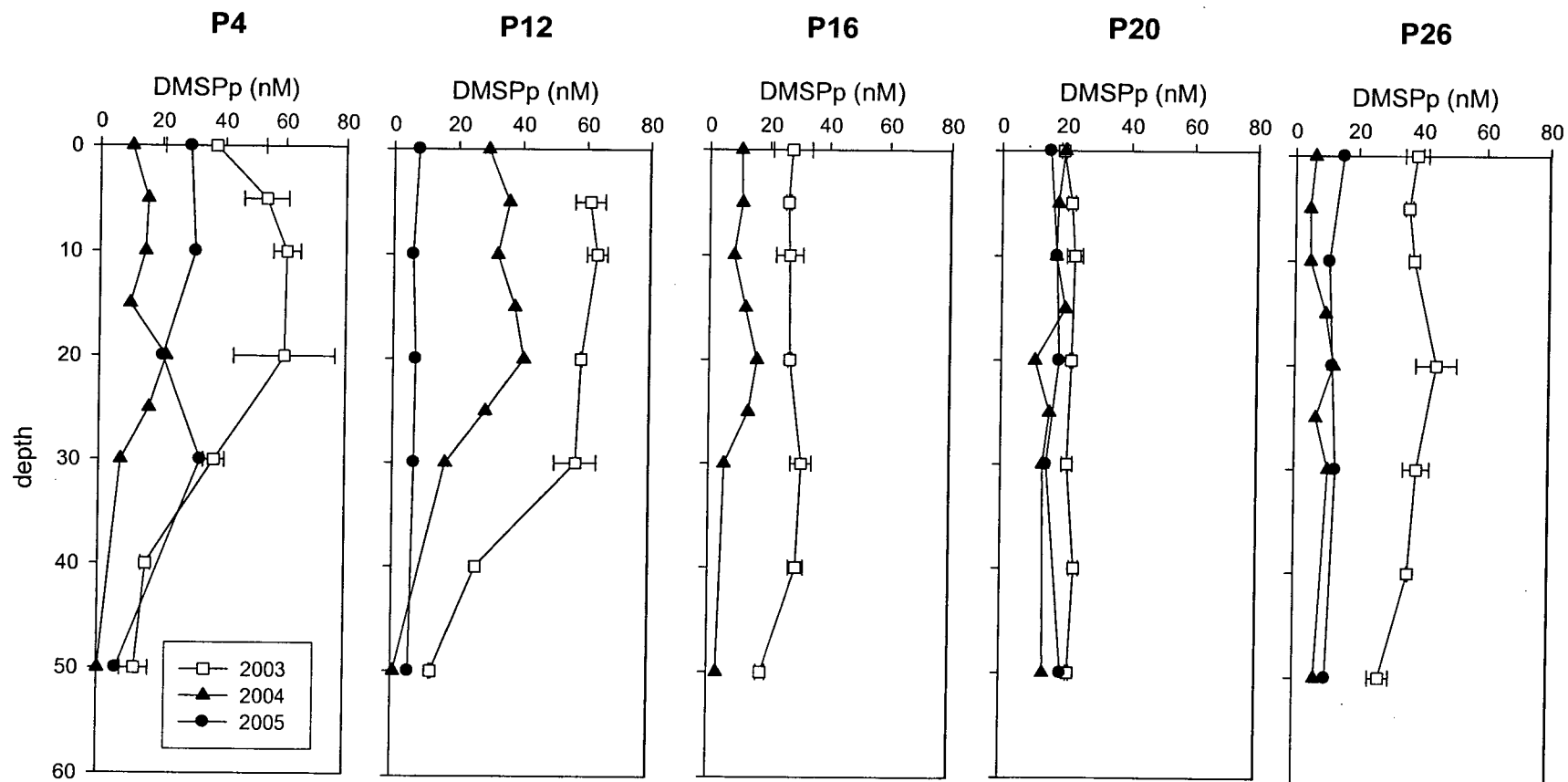


Figure 2.2: Depth profiles of DMSPp measured at the 5 major stations along Line P during 3 consecutive spring cruises. Error bars in 2003 represent standard deviations of duplicate samples.

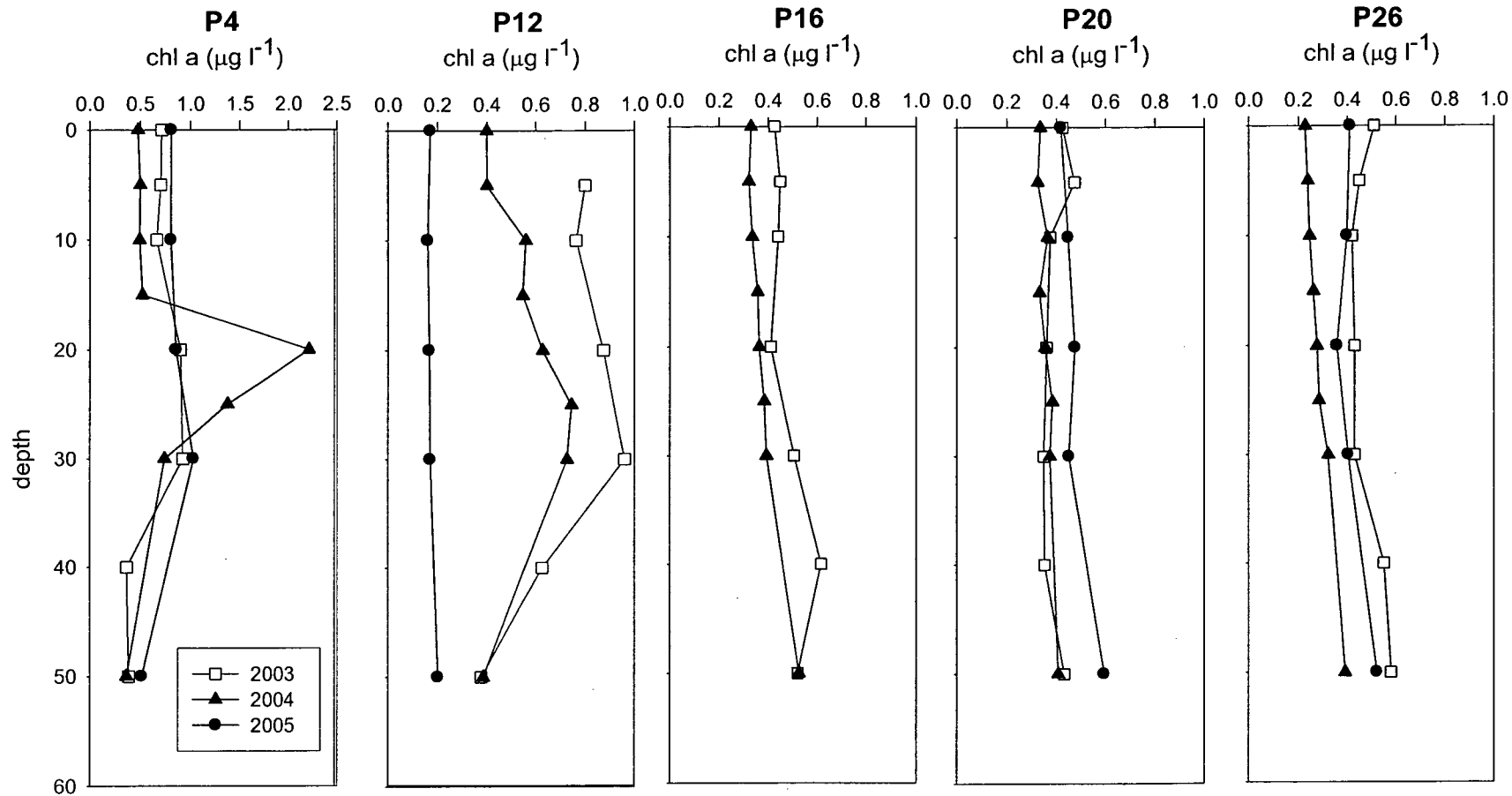


Figure 2.3: Depth profiles of chlorophyll *a* measured at the 5 major stations along Line P during 3 consecutive spring cruises. Note the different scale for station P4.

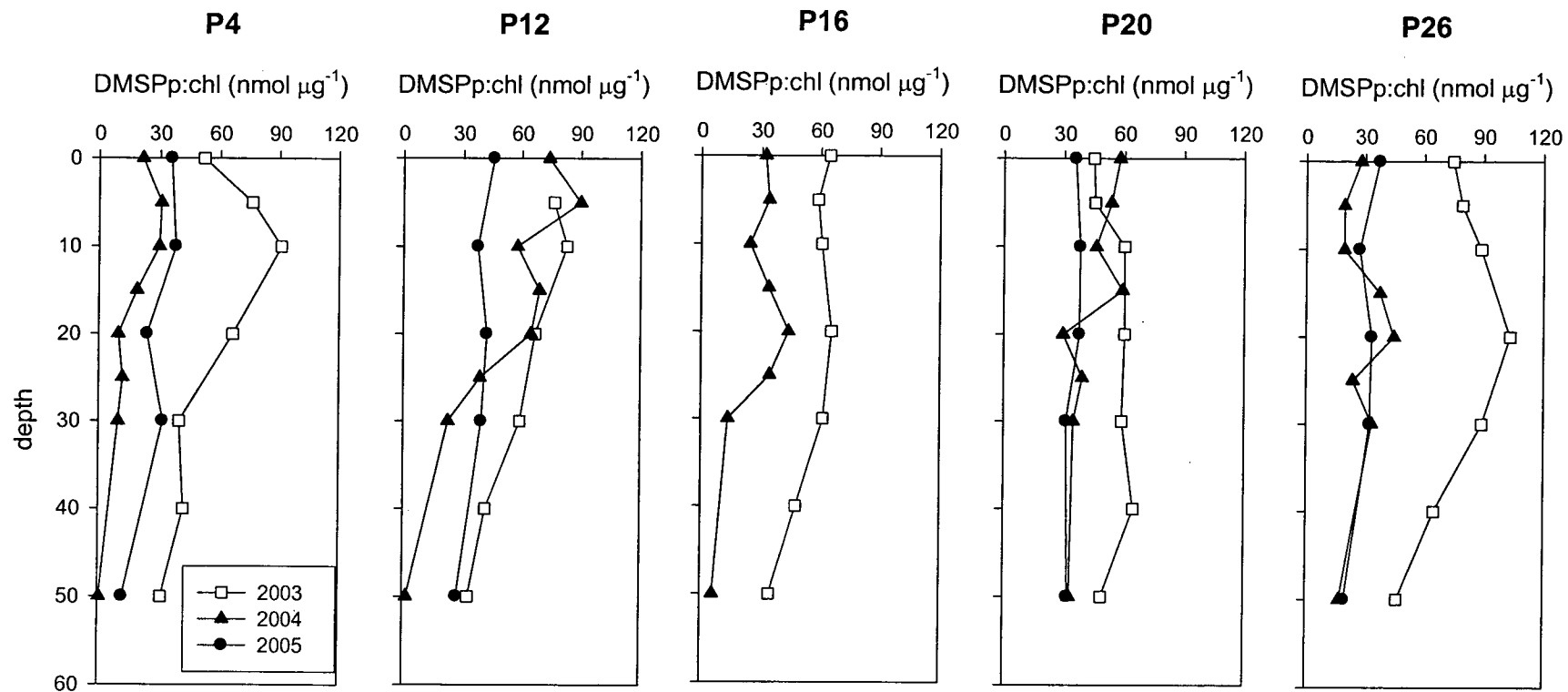


Figure 2.4: Depth profiles of the DMSPp:chl ratio measured at the 5 major stations along Line P during 3 consecutive spring cruises. Note that the ratios were generally highest in 2003.

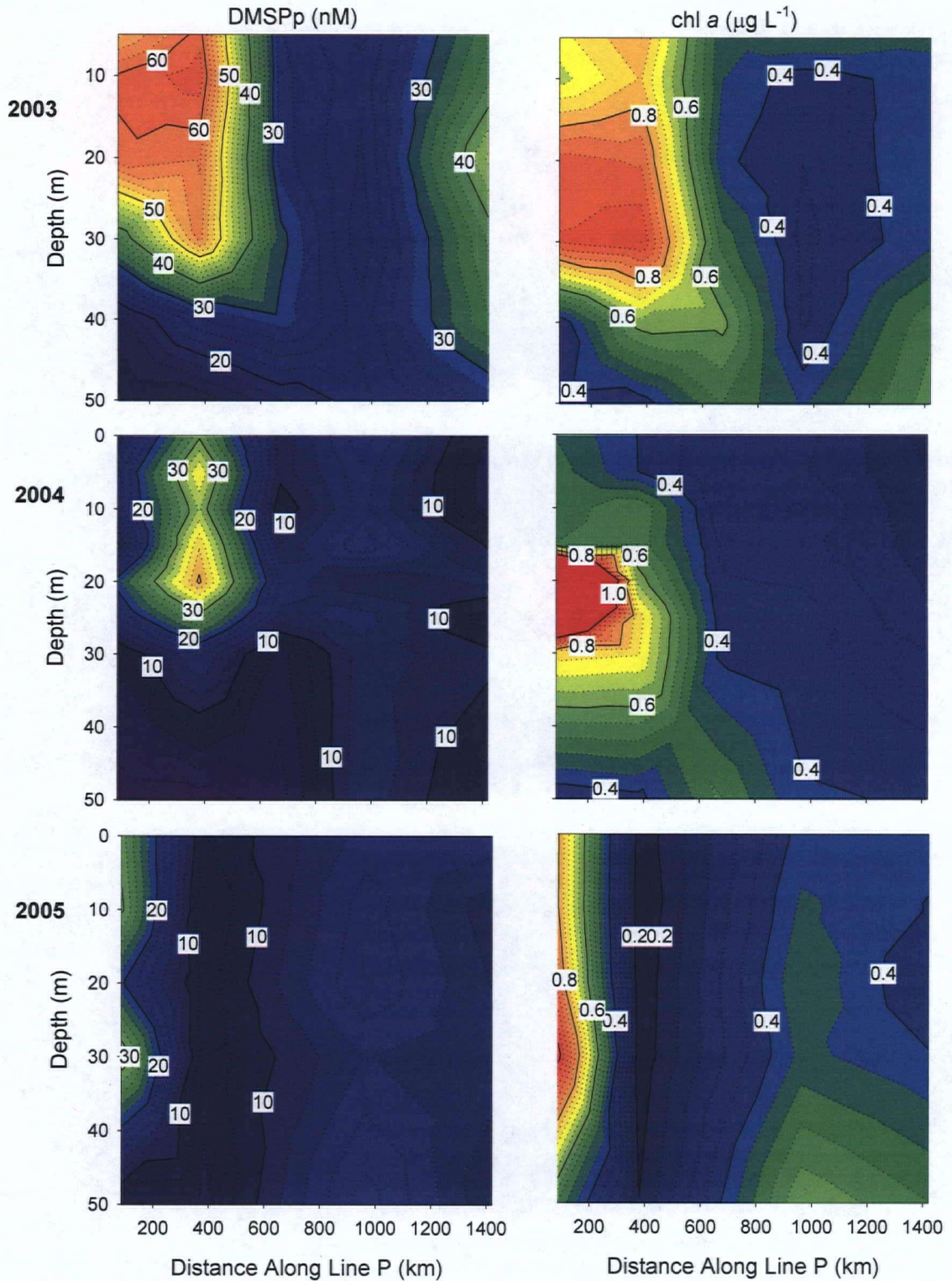


Figure 2.5: Contour plots illustrating spatial and interannual variability in springtime DMSPP and chlorophyll levels along Line P.

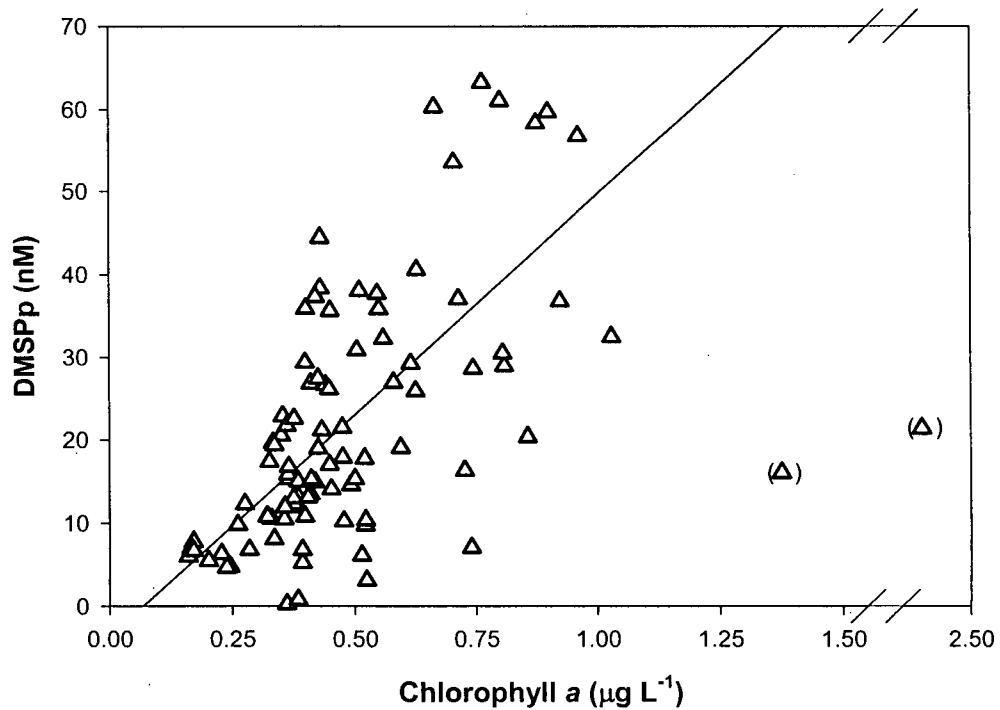


Figure 2.6: Relationship between chlorophyll and DMSPP concentrations along Line P for the 3 year pooled dataset ($r^2 = 0.20$, $n = 94$, $p < 0.0001$). Linear regression shown is with the two outliers in brackets excluded ($r^2 = 0.45$, $n = 92$, $p < 0.0001$).

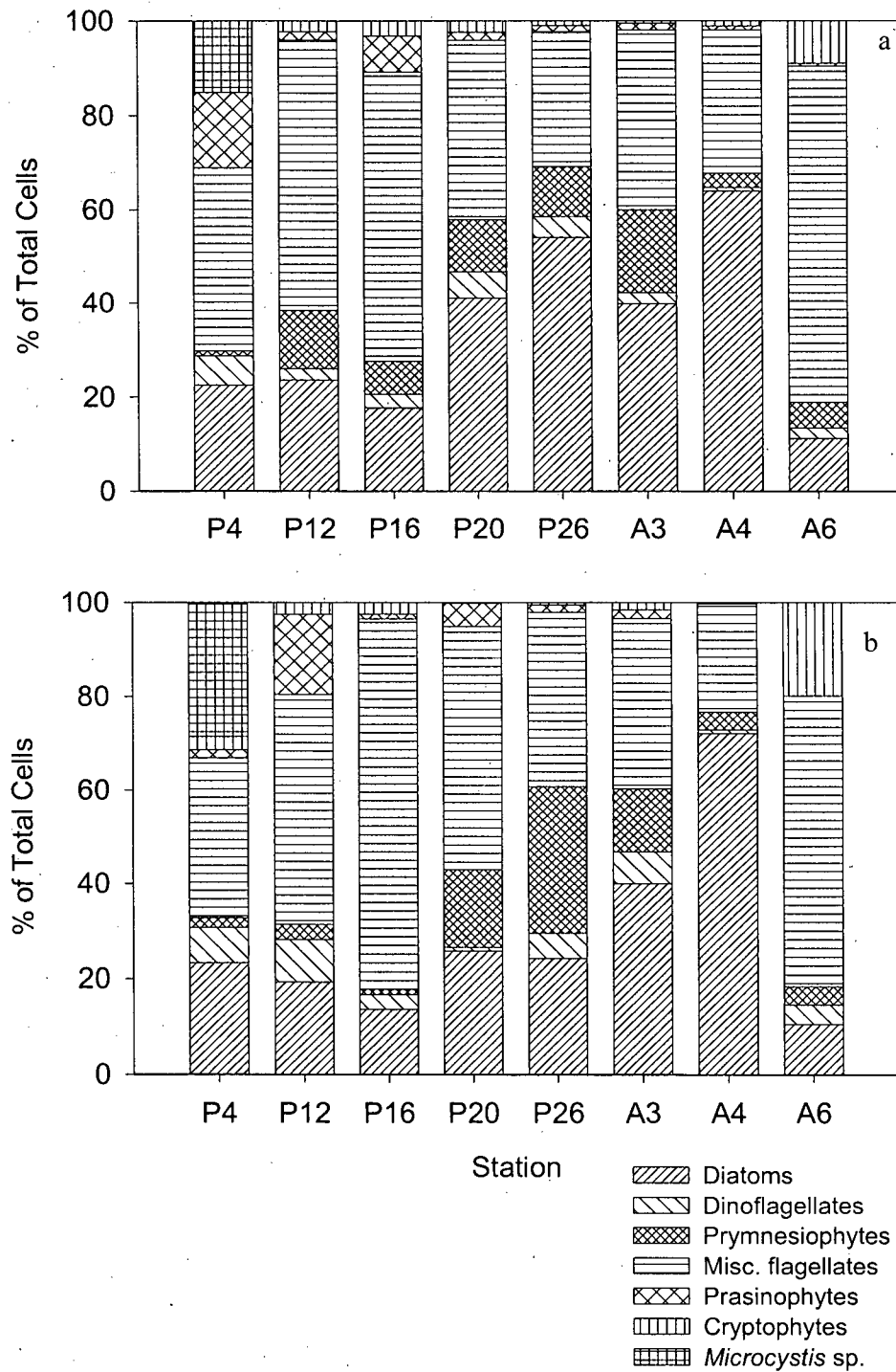


Figure 2.7: The relative abundance (percent of total cells) of the different phytoplankton groups enumerated at (a) 10 m depth and (b) the chlorophyll max. at all stations surveyed in 2003. See Table 2.3 for depths of chlorophyll max.

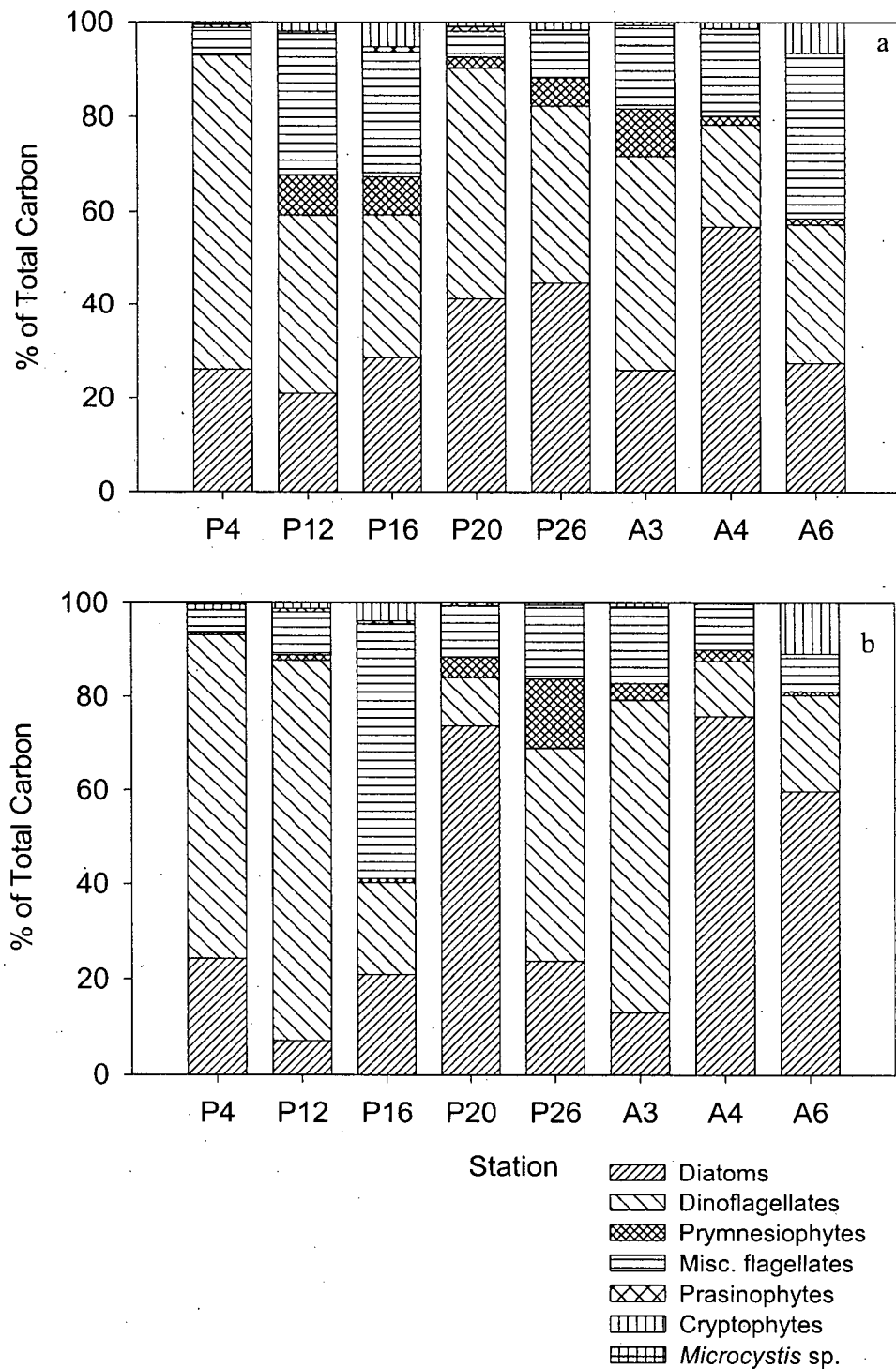


Figure 2.8: The contribution of the different phytoplankton groups to total carbon biomass at (a) 10 m depth and (b) the chlorophyll max. at all stations surveyed in 2003. See Table 2.3 for depths of chlorophyll max.

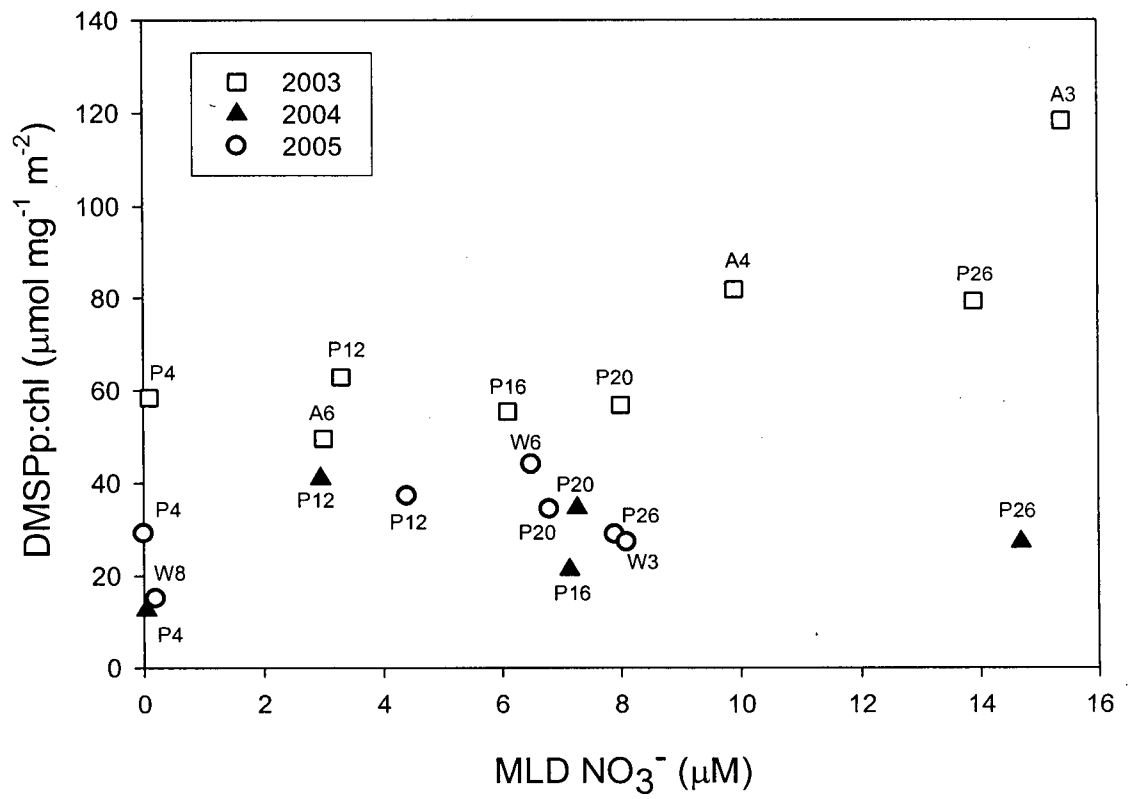


Figure 2.9: 50 m depth integrated DMSPp:chl ratios plotted against the mixed layer nitrate concentration. In 2003, stations A3, A4 and A6 are included; in 2005, stations W3, W6 and W8 are included (see Fig. 2.1 for locations). Note that in 2003, elevated DMSPp:chl ratios were found in high nitrate waters, but not in subsequent years.

2.5 References:

- Aranami, K., S. Watanabe, S. Tsunogai, M. Hayashi, K. Furuya, and T. Nagata (2001), Biogeochemical variation in dimethylsulfide, phytoplankton pigments and heterotrophic bacterial production in the Subarctic North Pacific during summer, *J. Oceanogr.* 57, 315-322.
- Bates, T.S., R.P. Kiene, G.V. Wolfe, P.A. Matrai, F.P. Chavez, K.R. Buck, B.W. Blomquist, and R.L. Cuhel (1994), The cycling of sulfur in surface seawater of the northeast Pacific, *J. Geophys. Res.* 99, 7835-7843.
- Belviso, S., P. Buat-Menard, J-P. Putaud, B.C. Nguyen, H. Claustre, and J. Neveux (1993), Size distribution of dimethylsulfoniopropionate (DMSP) in areas of the tropical northeastern Atlantic Ocean and the Mediterranean Sea, *Mar. Chem.* 44, 55-71.
- Booth, B.C., J. Lewin, and J. R. Postel (1993), Temporal variation in the structure of autotrophic and heterotrophic communities in the subarctic Pacific, *Prog. Oceanogr.* 32, 57-99.
- Boyd, P., and P.J. Harrison (1999), Phytoplankton dynamics in the NE subarctic Pacific, *Deep-Sea Res. II.* 46, 2405-2432.
- Bucciarelli, E., and W.G. Sunda (2003), Influence of CO₂, nitrate, phosphate, and silicate limitation on intracellular dimethylsulfoniopropionate in batch cultures of the coastal diatom *Thalassiosira pseudonana*, *Limnol. Oceanogr.* 48, 2256-2265.
- Chang, J., F. Shiah, G. Gong, and K.P. Chiang (2003), Cross-shelf variation in carbon-to-chlorophyll *a* ratios in the East China Sea, summer 1998, *Deep Sea Res. II.* 50, 1237-1247.
- Charlson, R.J., J.E. Lovelock, M.O. Andreae, and S.G. Warren (1987), Oceanic phytoplankton, atmospheric sulfur, cloud albedo and climate, *Nature*, 326, 655-661.
- Curran, M.A.J., G.B. Jones, and H. Burton (1998), Spatial distribution of dimethylsulfide and dimethylsulfoniopropionate in the Australasian sector of the Southern Ocean, *J. Geophys. Res.* 103, 16677-16689.
- Dacey, J.W.H., and N.V. Blough (1987), Hydroxide decomposition of DMSP to form DMS, *Geophys. Res. Lett.* 14, 1246-1249.
- Dacey, J.W.H., F.A. Howse, A.F. Michaels, and S.G. Wakeham (1998), Temporal variability of dimethylsulfide and dimethylsulfoniopropionate in the Sargasso Sea, *Deep-Sea Res. I* 45, 2085-2104.

- De Bruyn, W.J., E. Swartz, J.H. Hu, J.A. Shorter, P. Davidovits, D.R. Worsnop, M.S. Zahniser, and C.E. Kolb (1995), Henry's law solubilities and Setchenow coefficients for biogenic reduced sulfur species obtained from gas-liquid uptake measurements, *J. Geophys. Res.* 100, 7245-7251.
- Evans, C, G. Malin, W.H. Wilson, and P.S. Liss (2006), Infectious titers of *Emiliana huxleyi* virus 86 are reduced by exposure to millimolar dimethyl sulphide and acrylic acid, *Limnol. Oceanogr.* 51(5), 2468-2471.
- Falkowski, P.G. and J. LaRoche (1991), Acclimation to spectral irradiance in algae, *J. Phycol.*, 27, 8-14.
- Harrison, P.J. (2002), Station Papa time series: insights into ecosystem dynamics, *J. Oceanogr.* 58, 259-264.
- Hatton, A.D., S.M. Turner, G. Malin, and P.S. Liss (1998), Dimethylsulphoxide and other biogenic sulphur compounds in the Galapagos Plume, *Deep-Sea Res. II* 45, 1043-1053.
- Jones, G.B., M.A.J. Curran, H.B. Swan, R.M. Greene, F.B. Griffiths, and L.A. Clementson, (1998), Influence of different water masses and biological activity on dimethylsulfide and dimethylsulfoniopropionate in the subantarctic zone of the Southern Ocean during ACE 1, *J. Geophys. Res.* 103 (D13), 16691-16701.
- Keller, M.D., W.K. Bellows, and R.R.L. Guillard (1989), Dimethyl sulfide production in marine phytoplankton, in *Biogenic sulfur in the environment*, edited by E.S. Saltzman and W.J. Cooper, p. 167-180, American Chemical Society, Washington, D.C.
- Kettle, A.J. et al. (1999), A global database of sea surface dimethylsulfide (DMS) measurements and a procedure to predict sea surface DMS as a function of latitude, longitude and month, *Global Biogeochem. Cycles*, 13, 399-444.
- Kiene, R.P., L.J. Linn, and J.A. Bruton (2000), New and important roles for DMSP in marine microbial communities, *J. Sea Res.* 43, 209-224.
- Kiene, R.P., and D. Slezak (2006), Low dissolved DMSP concentrations in seawater revealed by small-volume gravity filtration and dialysis sampling, *Limnol. Oceanogr.: Methods*, 4, 80-95.
- Leck, C., U. Larsson, L.E. Bagander, S. Johansson, and S. Hajdu (1990), Dimethyl sulfide in the Baltic Sea: annual variability in relation to biological activity, *J. Geophys. Res.* 95, 3353-3363.

- Levasseur, M., M.G. Scarratt, S. Michaud, A. Merzouk, C.S. Wong, M. Arychuk, W. Richardson, R.B. Rivkin, M. Hale, E. Wong, A. Marchetti, and H. Kiyosawa (2006), DMSP and DMS dynamics during a mesoscale iron fertilization experiment in the Northeast Pacific- Part I: temporal and vertical distributions, *Deep-Sea Res. II*, 53, 2353-2369.
- Malin, G., and G.O. Kirst (1997), Algal production of dimethyl sulfide and its atmospheric role, *J. Phycol.* 33, 889-896.
- Matrai, P.A., and M.D. Keller (1994), Total organic sulfur and dimethylsulfoniopropionate in marine phytoplankton: intracellular variations, *Mar. Biol.* 119, 61-68.
- Meyerdierks, D., B. Bolt, and G.O. Kirst (1997), Spatial and vertical distribution of dimethylsulfoniopropionate (DMSP) during spring in the Atlantic sector of the Southern Ocean, *Deep-Sea Res. II* 44, 283-297.
- Montagnes, D.J.S, J.A. Berges, P.J. Harrison, and F.J.R. Taylor, (1994), Estimating carbon, nitrogen, protein and chlorophyll-a from volume in marine phytoplankton, *Limnol. Oceanogr.* 39 (5), 1044-1060.
- Parsons, T. R., Y. Maita, and C.M. Lalli (1984), *A manual of chemical and biological methods for seawater analysis*, Pergamon Press, New York, N.Y.
- Riseman, S.F. and G.R. DiTullio (2004), Particulate dimethylsulfoniopropionate and dimethylsulfoxide in relation to iron availability and algal community structure in the Peru Upwelling System, *Can. J. Fish. Aquat. Sci.* 61 (5), 721-735.
- Scarratt, M.G., M. Levasseur, S. Michaud, G. Cantin, M. Gosselin, and S.J. de Mora (2002), Influence of phytoplankton taxonomic profile on the distribution of dimethylsulfide and dimethylsulfoniopropionate in the northwest Atlantic, *Mar. Ecol. Prog. Ser.* 244, 49-61.
- Slezak, D. and G. J. Herndl (2003), Effects of ultraviolet and visible radiation on the cellular concentrations of dimethylsulfoniopropionate (DMSP) in *Emiliana huxleyii* (Strain L), *Mar. Ecol. Prog. Ser.* 246, 61-71.
- Stefels, J. and M.A. van Leeuwe (1998), Effects of iron and light stress on the biochemical composition of Antarctic Phaeocystis spp. (Prymnesiophyceae). I. Intracellular DMSP concentrations, *J. Phycol.* 34, 486-495.
- Stefels, J. (2000), Physiological aspects of the production and conversion of DMSP in marine algae and higher plants, *J. Sea Res.* 43, 183-197.
- Simo, R., and C. Pedros-Alio (1999), Role of vertical mixing in controlling the oceanic production of dimethyl sulphide, *Nature* 402, 396-399.

- Simo, R., S.D. Archer, C. Pedros-Alio, L. Gilpin, and C.E. Stelfox-Widdicombe (2002), Coupled dynamics of dimethylsulfoniopropionate and dimethylsulfide cycling and the microbial food web in surface waters of the North Atlantic, *Limnol. Oceanogr.*, 47, 53-61.
- Strathmann, R.R. (1967), Estimating the organic carbon content of phytoplankton from cell volume or plasma volume, *Limnol. Oceanogr.*, 12, 411-418.
- Sunda, W., D.J. Kieber, R.P. Kiene, and S. Huntsman (2002), An antioxidant function for DMSP and DMS in marine algae, *Nature*, 418, 317-320.
- Taylor, A.H., R.J. Geider, and F.J.H. Gilbert (1997), Seasonal and latitudinal dependencies of phytoplankton carbon-to-chlorophyll *a* ratios: Results of a modelling study, *Mar. Ecol. Prog. Ser.* 152, 51-66.
- Tortell, P.D. (2005), Dissolved gas measurements in oceanic waters made by membrane inlet mass spectrometry, *Limnol. Oceanogr. Methods*, 3, 24-37.
- Townsend, D.W., and M.D. Keller (1996), Dimethylsulfide (DMS) and dimethylsulfoniopropionate (DMSP) in relation to phytoplankton in the Gulf of Maine, *Mar. Ecol. Prog. Ser.* 137, 229-241.
- Turner, S.M., G. Malin, P.S. Liss, D.S. Harbour, and P.M. Holligan (1988), The seasonal variation of dimethylsulfide and dimethylsulfoniopropionate concentrations in nearshore waters, *Limnol. Oceanogr.* 33, 364-375.
- Watanabe, S., H. Yamamoto, and S. Tsunogai (1995), Dimethyl sulfide widely varying in surface water of the eastern North Pacific, *Mar. Chem.* 51, 253-259.
- Whitney, F.A., C.S. Wong, and P.W. Boyd (1998), Interannual variability in nitrate supply to surface waters of the Northeast Pacific Ocean, *Mar. Ecol. Prog. Ser.* 170, 15-23.
- Wolfe, G.V., M. Steinke, and G.O. Kirst (1997), Grazing-activated chemical defense in a unicellular marine alga, *Nature*, 387, 894-897.
- Wong, C.S., S.E. Wong, W.A. Richardson, G.E. Smith, M.D. Arychuck, and J.S. Page (2005), Temporal and spatial distribution of dimethylsulfide in the subarctic northeast Pacific Ocean: a high-nutrient-low chlorophyll region, *Tellus* 57B, 317-331.
- Wong, C.S., S.E. Wong, A. Pena, and M. Levasseur (2006), Climatic effect on DMS producers in the NE sub-Arctic Pacific: ENSO on the upper ocean, *Tellus* 58B, 319-326.

3. High-Resolution Measurements of DMS, CO₂ and O₂/Ar in Productive Coastal Waters around Vancouver Island, Canada²

3.1 Introduction

Rising concern about global climate change, driven mainly by high anthropogenic CO₂ emissions [Denman *et al.*, 1996], has led to increased efforts to quantify the ocean's role as a source or sink of climatologically-active gases. These include greenhouse gases such as CO₂ that lead to a rise in global temperatures, as well as gases such as dimethylsulfide (DMS), which can potentially cool Earth's climate through the formation of cloud condensation nuclei that promote cloud formation and scatter incoming radiation [Charlson *et al.*, 1987]. Decades of oceanographic gas surveys have culminated in the synthesis of thousands of measurements of pCO₂ and DMS into monthly global climatologies for both gases [Takahashi *et al.*, 2002 and Kettle *et al.*, 1999, respectively]. Although the number of measurements continues to steadily increase, data from continental shelf waters remain sparse. As a result, these regions suffer from low spatial and temporal resolution and are thus poorly represented in global gas climatologies [Takahashi *et al.*, 2002; Kettle *et al.*, 1999]. This is a significant limitation since coastal regions, despite their small areal extent, play a disproportionately large role in air-sea gas exchange due to their high productivity and dynamic physics. Coastal waters are particularly large sources of trace biogenic gases such as DMS. Neglecting to include these areas in global climatologies may thus impart significant errors on DMS flux estimates. Moreover, because DMS has a short atmospheric lifetime [Chin and Jacob, 1996], it is especially important to identify its local sources, particularly in coastal areas where biogenic sulfur sources affect the relative importance of anthropogenic ones [Jones *et al.*, 2001].

²A version of this chapter has been submitted for publication.

Nemcek, N., D. Ianson, and P.D. Tortell. A high-resolution survey of DMS, CO₂, and O₂/Ar distributions in productive coastal waters. *Global Biogeochem. Cycles*

Compounding the problem of low measurement resolution is our poor understanding of the underlying processes driving the observed gas distributions. For CO₂, the relative importance of the solubility pump versus the biological pump in oceanic carbon cycling needs to be evaluated [Volk and Hoffert, 1985]. Although biological processes such as photosynthesis, respiration and calcification are believed to dominate the seasonal variations in pCO₂ over most of the surface ocean [Takahashi et al., 2002], at high latitudes temperature changes likely play a larger role in driving air-sea CO₂ fluxes [Murata and Takizawa, 2003]. In our study region, strong biological CO₂ drawdown occurs in summer while out-gassing dominates in winter, yet net annual CO₂ fluxes are still poorly constrained [Janson and Allen, 2002].

The DMS cycle is more complex than that of CO₂ and we are still far from a mechanistic understanding of the factors driving DMS production [see Simo, 2004, and references therein]. Although it is clear that DMS originates from the algal metabolite dimethylsulfoniopropionate (DMSP), there are species-specific differences in DMSP production [Keller et al., 1989], which in turn are affected by the nutrient status of the cells [Sunda et al., 2002; Bucciarelli and Sunda, 2003]. Moreover, the process by which DMSP is released from cells and converted to volatile DMS involves the entire plankton community (from viruses to grazers) [Simo, 2001], which itself is profoundly affected by the physicochemical environment [Simo and Pedros-Alio, 1999]. As a result, attempts to relate DMS levels to total chlorophyll, phytoplankton species composition, or even DMSP concentrations have proven largely unsuccessful [Leck et al., 1990; Kettle et al., 1999]. Recent efforts have focussed on finding empirical relationships between DMS levels and combinations of relevant biological, physical, and chemical variables that would obviate the need for a full mechanistic understanding of the processes involved. This approach has led to the construction of algorithms aimed at predicting DMS concentrations from remotely

sensed data such as ocean colour, and well-constrained, or easily measurable environmental parameters [i.e. *Anderson et al.*, 2001; *Simo and Dachs*, 2002; *Belviso et al.*, 2004a]. The algorithm of *Simo and Dachs* [2002] (hereafter referred to as *S&D2002*) is particularly appealing as it has shown success at simulating oceanic DMS based solely on the ratio between SeaWiFS surface chlorophyll and a climatological mixed layer depth. There are currently no comparable algorithms for use in coastal waters as most are either based on open-ocean climatologies [*Anderson et al.*, 2001; *Simo and Dachs*, 2002], and/or have difficulty simulating DMS levels in diatom-dominated coastal waters [*Belviso et al.*, 2004a].

Ultimately, more information is needed on the spatial and seasonal distributions of oceanic gases in conjunction with process studies aimed at elucidating the factors driving the observed distributions. This goal has been hampered by limitations of current analytical methods which often lack the sampling resolution to capture fine-scale variability and measure individual gases in isolation. Insufficient sampling resolution is particularly problematic for DMS which is at best measured a few times an hour with purge-and-trap gas chromatography. As emphasized by *Simo and Dachs* [2002], “it is not enough to quantify the annual DMS emission flux from the global ocean; rather it is necessary to resolve its spatial and temporal variability... which exceeds our capability for sampling and measuring in the field.”

Recent work has demonstrated that membrane inlet mass spectrometry (MIMS) provides the capability to resolve spatial variability in DMS and other gases [*Tortell*, 2005a, 2005b]. This method is ideally suited for underway surveys since a suite of both major and trace gases can be measured simultaneously at a rate of twice per minute, providing a dramatic increase in spatial resolution over current methods, particularly for DMS. Herein, we present the first dedicated application of this method to dynamic, productive coastal waters off British Columbia, Canada.

The emphasis of the present study was to examine the covariance of the gas and hydrographic data to relate observed DMS levels to other environmental variables and to test the applicability of the predictive *S&D2002* DMS algorithm for use in coastal regions. Our findings suggest that DMS concentrations in highly productive areas can be related to the CHL/MLD ratio suggested by these authors, although by a different scaling factor. Our results also emphasize the utility of multi-gas measurements and the need to sample gases at appropriate spatial scales, which are especially short in coastal waters.

3.2 Materials and Methods

Study Area and Sampling- Dissolved gas, temperature, salinity and chlorophyll *a* measurements were made underway along several transects off the west coast of British Columbia, Canada between Aug. 11-19, 2004 onboard the *CCGS John P. Tully* (see Fig. 3.1 for transect locations). The cruise track crossed many dynamic oceanographic features including nearshore straits influenced by strong tidal mixing (e.g. T1a, T8, Fig. 3.1), as well as open shelf areas that are sites of upwelling and the formation of both cyclonic and anticyclonic eddies. The northern shelf transects (T1b-5, Fig. 3.1) were made in Queen Charlotte (QC) Sound, an area that serves as the source region for anticyclonic (downwelling) eddies that carry coastal waters rich in iron offshore to the Gulf of Alaska [*Johnson et al.*, 2005]. During summer, this region is thought to experience relaxation from strong winter downwelling, with very little actual upwelling. Transect 5 crosses from this relaxation region into an area where sporadic summer upwelling is expected off Vancouver Island. Near the southern end of Vancouver Island, transects 6-7 enter the Juan de Fuca eddy, a persistent, localized summertime feature. This cyclonic (upwelling) eddy supports a highly productive, diatom-dominated community [*Marchetti et al.*, 2004].

Gas Measurements- Membrane inlet mass spectrometry (MIMS) was used to measure dissolved gases underway (DMS, O₂, Ar, and CO₂) as recently described in detail in *Tortell [2005a]*. Briefly, seawater from the ship's underway intake system (4.5 m depth) was pumped through polypropylene tubing into a sampling cuvette connected to the mass spectrometer. Flow rates through the cuvette were controlled with a gear pump and were kept constant at ~200 ml min⁻¹. A gas permeable dimethylsilicone membrane inside the cuvette acted as the interface between the water sample and the vacuum of the mass spectrometer. After diffusion through the membrane, gases were measured in the vacuum chamber by single ion monitoring (SIM) of the signal intensities at the relevant m/z (mass to charge) ratios (32, 40, 44 and 62 for O₂, Ar, CO₂, and DMS, respectively). We use a Hiden Analytical HAL20 triple filter quadrupole mass spectrometer with an electron impact ion source set at a 500 μA emission current. All gases were measured at a frequency of twice per minute, or approximately every 160 m at the typical vessel cruising speed of ~10 knots.

The DMS signal output from the MIMS was calibrated using standards prepared by hydrolysis of sterile DMSP stock solutions (Research Plus Inc.) in 1 N NaOH. Aliquots of the liquid DMS standard were added to 500 ml volumes of DMS-free seawater (>1000m depth) and were always diluted 10⁵-10⁶-fold to keep the pH of the final DMS standard constant, and prevent matrix effects on the membrane. Standards were analyzed on the MIMS by recirculating the liquid through the sampling cuvette using a gear pump connected to a manual sampling valve. The detection limit based on a 3:1 signal-to-noise ratio of the blanks was 1 nM. On the last day of sampling we experienced a power failure which caused the instrument to shut down. This resulted in a malfunction in the secondary electron multiplier (SEM), the detector used to measure DMS. Thus, DMS data were not available along T8 (Fig. 3.2f).

Gas standards were not available for CO₂, O₂ or Ar. However, independent measurements of *p*CO₂ obtained from an underway IR *p*CO₂ equilibrator (LI-COR LI-6262) were used to calibrate the MIMS CO₂ signal. Each day of sampling was calibrated separately to compensate for shifts in the *m/z* 44 baseline of the mass spectrometer. Coefficients of determination for the *p*CO₂ calibration were as follows: $r^2 = 0.98$ for T1, $r^2 = 0.60$ for T2, T3, and T4, $r^2 = 0.87$ for T5, $r^2 = 0.96$ for T6, and $r^2 = 0.93$ for T7 and T8. The poor correlation between the MIMS CO₂ signal and the equilibrator data for T2-4 is expected because the range of *p*CO₂ values encountered along these transects (304-335 ppm) was small, such that any noise in the MIMS CO₂ signal and any offsets in the time stamps of the two instruments were amplified. However, despite the poor calibration curve for these transects, the average absolute difference between corresponding measurements from the two instruments was ~5 ppm (data not shown). The oxygen and argon data were not calibrated; however the O₂ signal was normalized to Ar to yield a biologically relevant parameter representing the balance between photosynthesis and respiration. This is possible because oxygen and argon have similar solubilities in seawater and argon concentrations are unaffected by biological processes [Craig and Hayward, 1987]. Thus, the O₂/Ar ratio is a strict measure of biological oxygen with physical processes that affect gas concentrations, such as bubble injections and temperature and salinity changes, removed.

DMSP measurements- Periodically during the underway gas analysis, discrete samples were collected for particulate DMSP (DMSPp) and dissolved DMSP (DMSPd) analysis from the underway intake line. These consisted of 250 ml aliquots of seawater which were immediately gravity filtered onto 47 mm GF/F filters to separate the particulate and dissolved DMSP fractions. The filters containing DMSPp were placed in 5 ml cryovials to which 3 ml of methanol

were added. These samples were stored at $-20\text{ }^{\circ}\text{C}$ until analyzed by MIMS in the laboratory several months later (see below). DMSP stored in methanol is known to be stable for extended periods of time (J. Dacey, pers. comm.).

The filtrates containing DMSPd were transferred to 250 ml ground-glass stoppered bottles, acidified with 500 μl of 12N HCl to prevent microbial degradation of DMSPd, and bubbled with air for 30 minutes to remove DMS. A 5 ml aliquot of 10N NaOH was then added to the samples to hydrolyze the DMSP to DMS. The bottles were stoppered and left to react overnight under minimal headspace. Prior to analysis on the following day, 3.6 ml of 12N HCl were added to the samples to lower the pH to 9.5, the tolerable range for the sampling membrane. Samples were then pumped into the cuvette via the manual sampling valve and analyzed on the MIMS by single ion monitoring of the m/z 62 signal with dwell and settle times of 300 ms. Calibration standards were made by adding aliquots of sterile DMSP to 250 ml volumes of DMS/DMSP-free deep seawater and were treated the same as the samples.

In the laboratory, DMSPp samples were analyzed on the MIMS using a membrane inlet probe specifically designed for small volume, discrete samples. This probe consists of a 1/16" stainless steel capillary with small holes at one end fitted with a 0.005" thick dimethylsilicone sleeve. Prior to analysis, 2 ml aliquots of the DMSP extract in methanol were placed into 14ml serum vials to which 12 ml of 1 N NaOH was added, completely filling the vials. The vials were immediately sealed with gas-tight aluminum crimp seals with Teflon-faced butyl rubber liners and left to react overnight to ensure complete conversion of DMSP to DMS. DMSP concentrations were measured as DMS in the liquid phase by MIMS by inserting the membrane inlet probe directly into the vials. Standards were prepared by adding aliquots of sterile DMSP to 2 ml of methanol and hydrolyzing overnight with 12 ml of 1 N NaOH as above.

We are aware that our DMSP data may be subject to recently identified filtration artefacts [Kiene and Slezak, 2006]. Although we used gravity filtration, our dissolved DMSP numbers may be overestimated and our particulate DMSP underestimated as a result of the relatively large volumes of seawater filtered [Kiene and Slezak, 2006]. However, since the two fractions came from the same water sample, total DMSP concentrations (DMSPd + DMSPp) should be accurate. For the purpose of this study we are more interested in the covariance of the DMSP and DMS data, rather than absolute DMSP values, and we use DMSP as an ancillary parameter to investigate differences in DMS levels between sites. The magnitude of the filtration artefacts is likely dependent on the health and species composition of phytoplankton communities, and may be smaller in coastal upwelling systems than in some of the environments studied by Kiene and Slezak [2006].

Hydrographic Measurements- Surface temperature, salinity and chlorophyll *a* fluorescence data were collected in conjunction with the dissolved gas measurements using a SeaBird SBE-25 CTD continuously sampling from the same seawater intake system as the MIMS. During parts of transects 1 and 3, the SBE-25 was not logging data due to loss of battery power, thus gaps exist in the salinity and chlorophyll data along these transects (Fig. 3.2b-c). Fortunately, the temperature data were available for these areas from the underway *p*CO₂ equilibrator. The fluorescence signal was calibrated with discrete chlorophyll *a* measurements ($r^2 = 0.97$, $n = 18$) determined fluorometrically following filtration of seawater onto GF/F filters and extraction in 90% acetone for 24 hours [Parsons *et al.*, 1984]. At a number of locations along the cruise track, CTD profiles were also obtained using a SeaBird SBE 911+ CTD attached to a rosette sampler.

Data Binning Procedures- In order to test the *S&D2002* algorithm, we binned all the underway DMS and chlorophyll *a* data onto $\frac{1}{4} \times \frac{1}{4}$ degree surface grids and calculated an average value for each parameter for each square. Following the binning procedure, the data were reduced ~100-fold to 29 individual squares each consisting of a single CHL and DMS value. A corresponding mixed layer depth (MLD) was assigned to each data pair. In most cases, MLDs were determined from CTD density profiles and were defined as a $0.125 \sigma_t$ change from the surface value in accordance with the criteria of the algorithm. In QC Sound (T1b-5; Fig. 3.1) where we had good CTD coverage, linear interpolation was used to assign an MLD value to each grid based on neighbouring CTD profiles. Due to the narrow range of MLDs in this region (6-12 m), any error introduced by this interpolation was small.

CTD data were not available during our cruise in the vicinity of T1a in QC Strait, or for T6 and T7 off Barkley Sound. Strong tidal forcing and turbulent flows, rather than wind or buoyancy fluxes control MLDs at the head of QC Strait (T1a), such that the upper mixed layer is consistently deep (40-80 m, P. Cummins, pers. comm.). We used horizontal gradients in surface temperature and $p\text{CO}_2$ to identify these tidally mixed regions, assuming that higher $p\text{CO}_2$ and colder temperatures were indicative of deeper mixing. This estimate yielded a horizontal gradient in MLDs decreasing from 80 m at the head of QC Strait to 50 m towards the mouth. For T6 and T7 off Barkley Sound, MLDs were estimated based on 26 CTD profiles taken in the same area three weeks later (D. Mackas, unpublished data). Mixed layer depths during the latter survey ranged from 8-24 m, and fell within the 95% C.I. of average summertime MLDs determined from several decades worth of CTD data collected in that area [Thomson and Fine, 2003]. Given that winds were weak to moderate prior to, and following our occupation, MLDs estimated for T6 and T7 from the latter survey are likely accurate. Once a mixed layer depth was assigned to

each $\frac{1}{4} \times \frac{1}{4}$ degree square, we calculated the expected DMS concentration using the CHL/MLD ratio and the appropriate equation from *S&D2002* (see results).

Spatial and Statistical Analysis- We examined the spatial variability of the gas and hydrographic data using two different statistical approaches. Lagged autocorrelation functions were computed to estimate decorrelation length scales (DLS) for the various parameters as described by *Murphy et al.* [2001]. These functions compute the correlation of point measurements at steadily increasing sampling intervals, or lags. As the sampling interval increases, the probability that two points separated by that interval are related approaches zero. The DLS thus gives an indication of the spatial length scale at which measurements become independent of each other. To estimate the errors that could result from undersampling highly variable surface data, we calculated interpolation errors following *Hales and Takahashi* [2004]. Essentially, this approach calculates the average error obtained by resampling high resolution data sets with increasingly lower resolution. Principle components analysis (PCA) was also used to examine the covariance of the gas distributions and the hydrographic measurements [*Shaw*, 2003].

3.3 Results

Surface Gas and Hydrographic Distributions- The surface distributions of temperature, salinity and chlorophyll *a* are shown alongside $p\text{CO}_2$, O_2/Ar and DMS data from the MIMS in Figures 3.2a-f, respectively. All parameters exhibited large ranges highlighting the dynamic nature of the study region. Surface temperatures ranged from 10.0-18.6 °C (avg. 16.2 °C; Fig. 3.2a), salinity ranged from 24.2- 32.3 psu (avg. 31.4; Fig. 3.2b), while chlorophyll *a* concentrations ranged from <0.1-33.2 $\mu\text{g L}^{-1}$ (avg. 2.6 $\mu\text{g L}^{-1}$; Fig. 3.2c).

Gas distributions over the study region were also highly variable. The partial pressure of CO₂ during this survey ranged from undersaturated values as low as 201 ppm to highly supersaturated at 747 ppm with an average of 362 ppm. The surface maps show spatial associations between the distribution of *p*CO₂ and that of several physical and biological variables (Fig. 3.2a-d). Although CO₂ concentrations were below atmospheric equilibrium values over most of the study region, they were strongly undersaturated in areas that had high chlorophyll concentrations, indicative of high phytoplankton biomass, and presumably a strong biological CO₂ sink (Fig. 3.2c-d). These low *p*CO₂ areas are evident in Fig. 3.2d along T1a-b in QC Strait, and along T6 and T7 in what is likely the JdF eddy. In contrast, regions of high *p*CO₂ occurred in JdF Strait (T8) and at the head of QC Strait (T1a), areas influenced by strong tidal mixing which brings deep waters enriched in respired CO₂ to the surface. Along T1a in QC Strait we observed a dramatic transition from supersaturated to undersaturated conditions characterized by an almost 500 ppm drop in *p*CO₂ levels (747 ppm to 255 ppm) in the span of 26 minutes or a distance of 8 km (Fig. 3.2d). Smaller regions of CO₂ supersaturation also occurred to a lesser extent when the cruise track crossed the shelf break in areas of localized upwelling (e.g. T5, T7; Fig. 3.2d). The physically induced changes in *p*CO₂ are corroborated by the corresponding low temperatures in these regions which reflect deep waters mixing to the surface (Fig. 3.2a). The average value of *p*CO₂ (362 ppm) indicates that the survey area on the whole was near, or slightly below equilibrium with respect to the atmosphere, but with local areas of large disequilibria.

O₂/Ar ratios expressed as a ratio of the m/z 32/40 ion currents from the MIMS ranged from 7.9-23.5 with an average of 15.1 (Fig. 3.2e). These data are uncalibrated and thus strictly qualitative; however, they do provide an indication of the degree of biological oxygen saturation

[Craig and Hayward, 1987]. Previous laboratory and field studies [i.e. Tortell, 2005b] using air-equilibrated water samples have shown that O_2/Ar ratios of 12-15 represent an oxygen saturation of 100% over a large range of temperature and salinity conditions. The range in the measured saturation ratio represents changes in ion source performance over multiple cruises and varying operating conditions, as opposed to temperature and salinity effects on the ratio *per se*. Thus, although we cannot pinpoint an exact value for 100 % O_2 saturation, O_2/Ar values greater than 15 characterize supersaturated waters, while values less than 12 represent undersaturation. High O_2/Ar ratios in our survey region (>16) coincided with areas of elevated chlorophyll concentrations and low pCO_2 indicating apparent biologically induced oxygen supersaturation (T1, T5, T7; Fig. 3.2c-e). A large area of oxygen undersaturation occurred in JdF Strait (T8) concurrent with the elevated pCO_2 levels of this tidally mixed zone (Fig. 3.2d-e).

Dimethylsulfide concentrations ranged from undetectable (<1 nM) to 28.7 nM with an average of 5.8 nM (Fig. 3.2f). Areas of high DMS levels were confined to QC Sound and corresponded to regions of moderate chlorophyll *a* levels (Figs. 3.2c, 3.2f). In contrast to the other gases, DMS concentrations could not be related in a general sense to the physical or biological environment. Concentrations of this gas were low in regions of both very high and low chlorophyll biomass and in both warm and cold waters. Dissolved, particulate and total DMSP levels were unrelated to the observed DMS concentrations with coefficients of determination (r^2) for all parameters <0.02 (data not shown). DMSPp concentrations ranged from 8.7-167 nM (mean 45 nM) with the highest levels occurring in areas of high biomass off Barkley Sound (T7) and in QC Strait (T1a), where DMS levels were relatively low (<10 nM; Fig. 3.2f). In contrast, the region of high DMS in QC Sound coincided with relatively low DMSPp concentrations (30-

40 nM). Dissolved DMSP concentrations ranged from 5.4-135 nM (mean 27 nM) with most values falling toward the lower end of the spectrum.

Although the maps of near-surface gas distributions shown in Fig. 3.2 provide a general overview of the biological and hydrographic properties of the sampling area, they obscure much of the fine-scale structure revealed by the high resolution MIMS data. Figures 3.3 and 3.4 show expanded views of two transects off the west coast of Vancouver Island (T5 and T7) that highlight the covariance of the gas and hydrographic data in greater detail. Figure 3.3 shows an 8 hour transect (T5) where the highest DMS concentrations were encountered. Interesting physical features are apparent in this high-resolution view, including a region that appears to be influenced by localized upwelling just south of 50.8 °N. This area is illustrated by a large and sudden drop in temperature, a slight increase in salinity, a dramatic spike in $p\text{CO}_2$ and an associated decrease in the O_2/Ar ratio. An anomalously high level of DMSPd (135 nM) was also associated with this strong temperature front (Fig 3.3a, 3.3c). Moving northward from this upwelling zone, both DMS concentrations and chlorophyll levels increased (in conjunction with increasing temperatures) until the two variables became uncoupled at 51.0 °N (Fig. 3.3a). From this point, DMS concentrations continued to increase despite a drop in chlorophyll levels and relatively constant DMSPp concentrations. Another sharp temperature front was encountered at the northernmost section of the transect, where a sudden increase in temperature was associated with a rapid, large drop in DMS concentrations. This greater than 20 nM decline in DMS levels occurred in under 20 minutes, over a short distance (~5.5 km), but was represented by ~40 individual data points (Fig. 3.3a). This type of resolution could not have been achieved with other sampling techniques. The high-resolution data reinforce the observation that DMS seems to vary independently of the other parameters, but changes dramatically at frontal regions where

two water masses converge. In contrast, $p\text{CO}_2$ and O_2/Ar showed a striking anti-correlation along the sampling transect, reflecting the coupling of these gases through photosynthesis and respiration ($r^2 = 0.89$, $p < 0.0001$, Fig 3.3b).

Figure 3.4 shows a second, 3 hour cross-shelf transect (T7) which captured the peak in chlorophyll levels encountered during our survey. In contrast to T5 (Fig. 3.3), the high levels of chlorophyll along T7 were associated with relatively low and constant DMS concentrations despite the presence of a large gradient in DMSPp levels (45-167 nM, Fig. 3.4a). Similar to the observations of T5, however, was the poor correlation between DMS and other measured biological and physical variables. The most striking feature of this transect is the strong correlation between chlorophyll concentrations and the O_2/Ar ratio ($r^2 = 0.86$, $p < 0.001$, Fig. 3.4a-b). This is particularly remarkable considering that the measurements came from independent instruments measuring different parameters: chlorophyll a , a measure of phytoplankton biomass, and the O_2/Ar ratio, a proxy for net community productivity [Kaiser *et al.*, 2005]. The O_2/Ar and $p\text{CO}_2$ distributions were once again anti-correlated, although not as strongly as along transect 5 ($r^2 = 0.64$, $p < 0.0001$, Fig. 3.4b).

Covariance of Gas and Hydrographic Data- Figure 3.5 illustrates the correlation between pairs of variables for the entire dataset. The strong anti-correlation between $p\text{CO}_2$ and O_2/Ar that was obvious for T5 and T7 (Figs. 3.3b, 3.4b) is also apparent for the pooled dataset ($r^2 = 0.90$, $p < 0.0001$; Fig. 3.5a). Overlaid on this scatterplot is the chlorophyll concentration. The highest chlorophyll is associated with the highest O_2/Ar values and the lowest $p\text{CO}_2$ values, while low chlorophyll occurs over a larger range of O_2/Ar and $p\text{CO}_2$ values (Fig. 3.5a). A trend is also evident between O_2/Ar and chlorophyll although there is considerably more scatter around this

relationship ($r^2 = 0.19$, $p < 0.0001$; Fig. 3.5b). From the temperature data overlaid on this plot it is clear that the main deviations from linearity occur at cold surface temperatures that represent water masses from the tidally mixed Juan de Fuca and QC Straits. These upwelled waters bring with them the low O_2/Ar signatures of deep water that has been subject to oxygen loss due to respiration. Data from these areas thus appear as a negative anomaly on the O_2/Ar vs. chlorophyll plot (Fig. 3.5b). Exclusion of all the data at temperatures below $13.0\text{ }^\circ\text{C}$ yields a much tighter positive relationship between O_2/Ar and chlorophyll levels in these “aged” surface waters ($r^2 = 0.73$, $p < 0.0001$; see discussion). DMS is plotted against chlorophyll concentration in Figure 3.6. As illustrated in Figures 3.2-3.4 and evident from this plot, DMS concentrations were not correlated to chlorophyll levels ($r^2 = 0.06$; Fig. 3.6), nor to any other single variable. Although the data in Fig. 3.6 appear to fall into clusters, these clusters did not coincide with geographical location, nor were they related to temperature, salinity, pCO_2 or O_2/Ar levels.

We used principal components analysis (PCA) to examine the underlying associations between the variables in our multidimensional data set. This method is particularly useful when many variables are inter-correlated with each other as is the case for our gas and hydrographic measurements. Use of this technique yielded two predictive factors (linear combinations of the original variables) which explained 74% of the total variance represented by the six underlying parameters. The results of the analysis revealed several clear patterns in the covariance of the data set. The most evident of these was the distinct separation of pCO_2 and O_2/Ar in two-dimensional space, indicative of the strong anti-correlation between these variables along all sampling transects (Fig. 3.7). The second noticeable feature of the PCA was the separation between biological variables (i.e. chlorophyll) and physical ones (temperature and salinity). The location of pCO_2 and O_2/Ar on the plot suggests that these parameters were influenced almost

equally by physical and biological driving forces. In contrast, DMS clustered most tightly with chlorophyll indicative of its biological origin.

A Test of a Predictive DMS Algorithm- Not surprisingly, none of the correlative analyses we applied were capable of explaining the distribution of DMS in our survey. Of all the variables, chlorophyll clustered most tightly with DMS in the PCA (Fig. 3.7), and co-varied with DMS along parts of some transects (Fig. 3.3a), but was a poor predictor of DMS in general (Fig. 3.6). We also observed areas where DMS changed sharply with temperature and salinity across fronts (Fig. 3.3a, 3.3c), suggesting a direct, or indirect, physical influence such as mixed layer depth, on DMS concentrations. Variability in the MLD leads to variable nutrient and light levels, which influence both phytoplankton and bacterial growth rates and species compositions, and thereby DMSP production and its subsequent breakdown [*Simo and Pedros-Alio, 1999*]. Furthermore, surface DMS levels may be related to the thickness of the mixed layer by a simple dilution model, such that DMS levels are high where MLDs are shallow and vice versa [*Aranami and Tsunogai, 2004*]. *Simo and Dachs [2002]* had successfully used the CHL/MLD ratio as a combined biological/physical predictor variable for DMS in their algorithm. Capitalizing on our abundant underway measurements of both chlorophyll and DMS, we were able to test the applicability of this predictive algorithm in the coastal waters of our survey.

Following the binning procedure (see methods), we applied the appropriate equations to calculate the predicted DMS concentration based on the magnitude of the CHL/MLD ratio. In all cases, this ratio was greater than 0.02 and we thus used equation 2 of *S&D2002* that linearly relates DMS to the CHL/MLD ratio according to:

$$\text{DMS} = 55.8 * (\text{CHL}/\text{MLD}) + 0.6. \quad (1)$$

In all but two cases, the *S&D2002* equation overestimated the DMS concentration by a factor of at least 2, resulting in a poor fit to the data (Fig. 3.8, dashed line). However, when the actual DMS concentrations were plotted against their corresponding CHL/MLD ratios, we observed a good linear fit between the two variables ($r^2 = 0.83$, $n = 27$, $p < 0.0001$; Fig. 3.8), after excluding two significant outliers from the regression. There was still no correlation between binned DMS and chlorophyll levels, indicating that the linear trend was not the result of the binning and averaging process itself. The relationship between DMS and CHL/MLD exists despite the fact that many of the chlorophyll values exceeded the $15 \mu\text{g L}^{-1}$ cutoff of the original *S&D2002* algorithm, and mixed layer depths for some of the points were estimated using data from other cruises (open symbols in Fig. 3.8; see methods). When only data from QC Sound were used (where MLDs were measured explicitly), the coefficient of determination for the linear relationship improved to $r^2 = 0.96$ without much effect on the slope (closed symbols in Fig. 3.8). The resultant fit to our data is:

$$\text{DMS} = 21.0 * (\text{CHL}/\text{MLD}) - 0.1. \quad (2)$$

This slope is less than half that of the original *S&D2002* formulation. Our results suggest that the CHL/MLD ratio may be a useful proxy for simulating DMS concentrations even in productive coastal areas, although with a significantly different slope.

Spatial Analyses- In addition to examining the covariance of our measured parameters, we capitalized on the high resolution nature of the dataset to quantify the length scales of variability of the gas and hydrographic data. We computed lagged autocorrelation functions (ACF) along individual transects from which the decorrelation length scales (DLS) were defined as the first zero crossing of the function. A diagram of the ACF for the six measured variables along T5 is shown in Figure 3.9a. Along this transect, DMS had the shortest DLS of 10.5 km indicating that its distribution varied over the shortest distance. In contrast, the physical parameters, temperature and salinity showed longer length scales of variability with DLS of 23-28 km. The striking feature of this figure is the strong similarity between the functions of chlorophyll *a*, $p\text{CO}_2$ and O_2/Ar . All three had roughly the same shape and a DLS of ~ 17 km, falling between that of DMS and the physical parameters. This trend illustrates the tight coupling between these three parameters with changes in phytoplankton biomass likely driving the variability in the $p\text{CO}_2$ and O_2/Ar distributions. The DLS along the six major transects analyzed (T1 and T3 were excluded due to gaps in the hydrographic data, see methods) ranged from 2.5-32.2 km with mean values for the six measured parameters ranging from 7-14 km (Fig. 3.9b). Although the gases appeared to vary on shorter spatial scales than the hydrographic data, the differences were not statistically significant (see discussion).

An additional analysis was used to estimate the errors that could result from lower frequency sampling. Following the work of *Hales and Takahashi* [2004], we resampled our high frequency data at ever coarser resolution, and calculated the average error resulting from linear interpolations between the coarsely sampled data. As the sampling frequency decreases, the interpolation error increases to an asymptotic value. Beyond this point, coarser sampling has

little to no effect on the magnitude of the interpolation error [see *Hales and Takahashi, 2004, Fig. 19*].

Table 3.1 summarizes the asymptotic interpolation errors calculated for each of the six parameters along the six major transects surveyed. Frontal regions evidently had significant effects on the magnitude of the asymptotic interpolation error for all parameters. T5 crossed a local upwelling zone and was characterized by two sharp temperature fronts (Fig. 3.2a, Fig. 3.3c). Consequently, along this transect the interpolation errors for most parameters were large, particularly for DMS which changed dramatically at frontal zones (Fig. 3.3a). The asymptotic interpolation error for DMS in this case was almost 100 % of the 8.6 nM mean concentration along this transect (Table 3.1). In contrast, T7 and T8 were characterized by large, sharp gradients in chlorophyll concentrations (Figs. 3.2c, 3.4a). These large changes in phytoplankton biomass drove high variability in the $p\text{CO}_2$ and O_2/Ar levels which coupled with the mixing of deep waters to the surface along other parts of these transects resulted in large ranges in the $p\text{CO}_2$ (~450 ppm along T8), and O_2/Ar measurements. As a result, the absolute errors for chlorophyll, $p\text{CO}_2$ and O_2/Ar were largest along transects 7 and 8 (Table 3.1).

3.4 Discussion

Spatial Scales of Variability- Biogeochemical variability in this coastal zone was observed both in the large range of values measured and in the short distances over which gas and surface water hydrography varied. Both the autocorrelation functions and the interpolation error analyses showed that, on average, the majority of the variability in the gas, temperature, salinity and chlorophyll distributions occurred on spatial scales of less than 20 km (Fig. 3.9b, Table 3.1), consistent with the expected Rossby radius (the correlation length for physical properties) in this

region. Although the mean DLS seemed to be shorter for the gases (<10 km), than for the hydrographic parameters (12-14 km), the differences were not statistically significant (Fig. 3.9b) owing to large variability in the DLS. However, much of this variability appears to result from an apparent artefact of the analysis in which the DLS for any given parameter increases with increasing transect length. Thus, part of the variability in the mean DLS for each parameter is due to variability in the transect length, making comparison of DLS for a given parameter difficult between transects and even between studies [i.e. *Murphy et al.*, 2001; *Hales and Takahashi*, 2004; *Tortell*, 2005b]. Nonetheless, differences in DLS between parameters along any single transect are meaningful (Fig. 3.9a), and the overall mean values are probably representative of inherent differences between these parameters (Fig. 3.9b). Thus it appears that the gases do vary on shorter length scales than temperature, salinity and chlorophyll, with DMS possibly exhibiting the shortest DLS as suggested by previous data [*Tortell*, 2005b]. More robust statistical approaches may be needed to quantify the relevant spatial scales of variability of our dataset, but the results clearly indicate that gases exhibit variability over distances that are not sufficiently resolved in many field studies.

Asymptotic interpolation errors were calculated to quantify the magnitude of the errors resulting from low resolution sampling. Our calculations show that for DMS and chlorophyll in particular, insufficient sampling resolution can introduce errors approaching 100 % of the mean concentration. Large errors (~20 %) are also associated with $p\text{CO}_2$ and O_2/Ar measurements (Table 3.1). Although the relative error for $p\text{CO}_2$ and O_2/Ar is smaller than that for DMS or chlorophyll a , a 46 ppm average absolute error in the mean $p\text{CO}_2$ concentration would be highly significant if accurate estimates of regional air-sea fluxes were required, and could even change the direction of the flux. The same is true in the case of O_2/Ar , where a unit change in the ratio

can represent a 5-10 % change in the saturation state of O₂. This would have large implications for estimates of net community productivity from O₂/Ar ratios [as in *Kaiser et al.*, 2005].

While the asymptotic interpolation errors represent maximum uncertainty associated with low resolution sampling, e.g. hydrostations with separations of 20-60 km, significant errors can also occur during underway sampling at insufficient resolution. A more meaningful application of the analysis is to calculate actual sampling errors for underway measurements with a given sampling frequency. We calculated interpolation errors for our high-resolution pCO₂ and DMS measurements resampled at the frequency of our pCO₂ equilibrator (5 min.), and a typical underway DMS sampling frequency of 30 minutes. For the pCO₂ equilibrator, the interpolation errors along individual transects ranged from 1.4-8.3 ppm, equivalent to a maximum error of 1.5 % relative to the mean. This relatively small error would not be particularly significant for most biogeochemical studies, and it thus appears that the sampling resolution of the pCO₂ equilibrator is sufficient to capture nearly all of the underlying variability. In contrast, a 30 minute sampling regime for DMS introduced errors of between 0.7-2.8 nM, or as high as 41 % of the mean along a given transect. This error in the mean DMS concentration translates to an equivalent error in the DMS flux, an estimate already prone to large errors due to the uncertainty in the gas transfer coefficient [*Nightingale et al.*, 2000].

pCO₂ and O₂/Ar Distributions- The distributions of pCO₂ and O₂/Ar during this survey exhibited considerable patchiness with regions of strong undersaturation and supersaturation in close proximity to each other (e.g. 500 ppm change in pCO₂ over 8 km, T1a, Fig. 3.2d). The range of pCO₂ concentrations encountered (201-747 ppm) was similar to other summertime values reported for the southwest coast of Vancouver Island [*Ianson et al.*, 2003], and the Oregon

coastal upwelling system [Hales *et al.*, 2005]. In all three surveys, regions of intense CO₂ supersaturation were confined to narrow nearshore strips with the majority of the outer shelf areas undersaturated as a result of biological drawdown. The large regions of CO₂ undersaturation found along the shelf (T6, T7) and in QC Sound (T1b-5) likely compensated for the locally intense CO₂ sources identified in the straits (T1a, T8). We suggest that this region is still an overall CO₂ sink during the time of the survey, although significantly smaller due to the consistent tidal sources. It is important to recognize that these tidally-influenced regions of persistently high CO₂ must have a large impact on net annual carbon budgets, whereas localized upwelling along the shelf leads to transiently high CO₂ concentrations that are usually quickly drawn down by biological production. Although there is still considerable debate as to whether coastal upwelling zones are net sources or sinks of CO₂ over an annual cycle [Ianson and Allen, 2002; Hales *et al.*, 2005], Hales *et al.* [2005] suggest that CO₂ uptake in the upwelling margins along the west coast of North America is equivalent to 50% of the entire summertime, oceanic North Pacific CO₂ sink. These findings clearly demonstrate the disproportionately large influence of coastal margins in the oceanic carbon cycle and the need to incorporate these areas into global CO₂ climatologies.

There is much current interest in identifying the relative importance of biological processes versus physical ones in driving the distribution (and hence air-sea flux) of CO₂ [Sarmiento *et al.*, 2000]. Our results demonstrate that variability in surface $p\text{CO}_2$ was largely influenced by the opposing biological processes of photosynthesis and respiration in this productive, coastal margin. This is evident from the tight anti-correlation between $p\text{CO}_2$ and O₂/Ar (a strictly biological parameter) along all sampling transects even in the finest resolution (Figs. 3.3b, 3.4b, and 3.5a), and the occurrence of low $p\text{CO}_2$ levels in regions of high biomass

along certain transects (e.g. T1b, T7, Fig. 3.2c-d). However, it was the physics of this region (upwelling, tidal mixing) that drove the large-scale $p\text{CO}_2$ distributions and accounted for the large range of $p\text{CO}_2$ levels by providing a mechanism for deep waters enriched in remineralized CO_2 to reach the surface.

Atmospheric exchange also affects the distribution of $p\text{CO}_2$ in surface waters although its effects are not as pronounced as those of mixing and biological drawdown. This is due in part to the slow rate of CO_2 exchange which occurs on timescales of days to weeks and is about 10 times slower than the rate of O_2 exchange [Broecker and Peng, 1982]. These differential gas exchange rates may explain the divergent slopes of the $p\text{CO}_2$ vs. O_2/Ar relationship on the left side of the plot in Fig. 3.5a. Here, $p\text{CO}_2$ concentrations of ~ 200 ppm are associated with two very different levels of chlorophyll and O_2/Ar ratios. At the top of the plot, the highest chlorophyll levels (red area, Fig. 3.5a) correspond to the highest O_2/Ar ratios and lowest $p\text{CO}_2$ values measured, yet lower down on the y-axis, the same $p\text{CO}_2$ levels are associated with much lower chlorophyll and O_2/Ar levels (Fig. 3.5a). Thus it appears that the O_2 concentrations in these latter waters were able to re-equilibrate to the surrounding biomass much faster than CO_2 levels. Due to the longer “history” of the $p\text{CO}_2$ signature, a strong anti-correlation between $p\text{CO}_2$ levels and chlorophyll concentrations was only evident in areas where biomass was high, presumably where productivity rates were at their peak (Fig. 3.4a-b).

The O_2/Ar ratio has been used as a proxy for the net community production of a water mass integrated over a time scale that depends on the gas transfer velocity and the depth of the mixed layer [Kaiser *et al.*, 2005]. We observed a strong linear relationship between O_2/Ar and chlorophyll levels in surface waters indicating increasing primary productivity with increasing phytoplankton biomass (Fig. 3.5b). However, several factors complicate the relationship between

chlorophyll and O_2/Ar . On the one hand, deep mixing brings up cold subsurface waters which carry the low O_2/Ar values characteristic of oxygen loss due to respiration. This creates an initial oxygen deficit in surface waters which persists despite the growth of phytoplankton and the addition of photosynthetically derived oxygen. This scenario may explain the negative anomaly in the O_2/Ar vs. chlorophyll relationship (blue regions in Fig. 3.5b), and highlights the difficulty of estimating net community productivity from O_2/Ar ratios in regions with significant upwelling or vertical mixing [Kaiser *et al.*, 2005]. On the other hand, high O_2/Ar ratios may persist in the mixed layer despite the presence of low surface chlorophyll levels (red regions in Fig. 3.5b). These waters may have warmed and stratified to the extent of cutting off the supply of nutrients from below the mixed layer, thus either creating a subsurface chlorophyll maximum, or causing the phytoplankton to be removed from the surface before the O_2/Ar productivity signature could be reset by atmospheric exchange. Thus, knowledge of the relevant timescales of both gas exchange and phytoplankton turnover rates is critical when inferring production rates from gas distributions.

Factors Driving DMS Distributions- The range of DMS concentrations encountered during our survey was large and variable, from undetectable (<1 nM) to almost 30 nM. The upper end of this range is at least an order of magnitude higher than current estimates of the global mean DMS concentration [Belviso *et al.*, 2004b], and comparable to data obtained in various other coastal regions [Leck *et al.*, 1990; Townsend and Keller, 1996; Locarnini *et al.*, 1998; Tortell, 2005b]. However, our measurements provide much higher spatial resolution than previous surveys and thus offer new insight into the small-scale patchiness of DMS distributions in coastal waters (Fig. 3.2f).

We compared our DMS data to measurements taken in the same general area (coastal British Columbia between 48-55° N), during the same week, the previous year by automated purge-and-trap gas chromatography sampling at a frequency of once every 30 minutes (J.E. Johnson, unpublished data available at <http://saga.pmel.noaa.gov/dms/>). The range of DMS concentrations encountered in 2003 (0.7-17.6 nM) was smaller than that observed during our 2004 survey (<1- 28.7 nM), but the mean DMS concentrations were remarkably similar (5.3 nM vs. our value of 5.8 nM). It is possible that the range of concentrations during 2003 was lower because Johnson's survey may have been unable to resolve the true variability of the DMS distributions (as indicated by our 30 min. interpolation error analysis). As observed previously [Hales and Takahashi, 2004; Tortell, 2005b], we note that the measured range of a given parameter is much more prone to sampling errors than the regional mean. It is thus not surprising that the overall mean of Johnson's survey was similar to that of the present survey, despite a much smaller range of reported DMS concentrations. However, many environmental factors could account for the interannual variability in DMS concentrations. Variations in wind velocity could be responsible for the difference in maximum DMS levels between the two years. Winds were very light during our entire cruise (rarely exceeding 5 m s⁻¹), compared to those reported in 2003 (max 13 m s⁻¹, mean 5.1 m s⁻¹). As a result, a larger gas transfer velocity in 2003 could have created a larger DMS loss term in surface waters, acting against the accumulation of high DMS concentrations in the mixed layer. It should be noted, however, that ventilation to the atmosphere is only one sink for DMS and often only a minor one [Kiene and Bates, 1990]. Photolysis [Kieber et al., 1996; Toole et al., 2004] and bacterial consumption [Kiene and Bates, 1990] can be much larger sinks for DMS, and these along with underlying differences in phytoplankton species composition and biomass, zooplankton grazing rates, nutrient supply and

light intensity could all account for interannual variability in DMS concentrations. Despite these potential differences, we observed a striking similarity in the spatial distribution of DMS between the two years. Both the 2003 survey and our 2004 survey reported peak DMS levels in the region north of Vancouver Island between 51-52 °N. The area of summer relaxation over the broad shelf in QC Sound may thus be a region of persistently high DMS during August.

The high DMS concentrations (>10 nM) observed in QC Sound during our survey were associated with moderate levels of chlorophyll (T1b, T4, T5; Figs. 3.2c, 3.2f). In contrast, DMS concentrations were low in areas where chlorophyll levels exceeded 15 $\mu\text{g L}^{-1}$ (T1a, T7; Figs. 3.2c, 3.2f). Since DMSP production by phytoplankton is known to be highly species-specific [Keller *et al.*, 1989], variability in phytoplankton community composition may account for differences in DMS levels between regions. This taxonomic effect is potentially confounded, however, by differing environmental conditions across our sampling region. Since DMSP and its byproducts are powerful antioxidants, cells increase their DMSP (and DMS) production when exposed to oxidative stressors such as low nutrients and high UV light [Sunda *et al.*, 2002]. These conditions generally occur in later stage blooms when surface waters have stratified, cutting off the supply of nutrients from below the thermocline and exposing cells to higher levels of UV light. Stratified waters tend to favour flagellate groups such as prymnesiophytes that have adapted to living under low nutrient, high light conditions [Margalef, 1978] and are perhaps non-coincidentally the same groups that are prominent DMSP-producers [Keller *et al.*, 1989]. Furthermore, nutrient limitation can induce DMSP production in groups such as diatoms [Sunda *et al.*, 2002; Bucciarelli and Sunda, 2003], that have traditionally been considered low DMSP-producers [Keller *et al.*, 1989]. The high DMS concentrations in QC Sound occurred where mixed layer depths were less than 12 m and surface nitrate was depleted, suggesting an oxidative

stress effect on DMSP/DMS production. In contrast, the waters in QC Strait and in the JdF eddy (T1a, T7) were receiving a steady nutrient supply through localized upwelling or deep mixing resulting in high (or measurable) surface nitrate and high phytoplankton biomass, with little DMS production. The occurrence of low DMS levels in recently upwelled waters has been observed previously [Belviso *et al.*, 2003]. However, since changes in phytoplankton species composition generally occur in conjunction with changing environmental conditions, it is difficult to distinguish between species composition effects and nutrient/light effects in determining DMS levels.

As in previous studies [Locarnini *et al.*, 1998; Tortell, 2005b], DMS concentrations during this survey changed dramatically at fronts, regions where abrupt gradients in nutrient concentrations, light regimes, productivity and plankton community composition are common. This trend reflects the complex interplay of physics and biology that characterizes the oceanic DMS cycle [see Simo, 2004]. The anomalously high level of DMSPd (135 nM) measured off the northwest coast of Vancouver Island (Fig. 3.3a) also occurred at a sharp temperature front. The exceptionally high abundance of zooplankton encountered at this site (R. El-Sabaawi, unpublished data) may have been responsible for massive grazer-mediated release of DMSP [Dacey and Wakeham, 1986].

Towards Global DMS Prediction- Intense efforts have been aimed at understanding the factors controlling DMS production in the oceans, and quantifying its atmospheric flux in order to evaluate the feasibility of the hypothesized biologically-mediated homeostasis (CLAW hypothesis) [Charlson *et al.*, 1987]. It has proved difficult to project future oceanic DMS emissions in a changing climate due to an incomplete mechanistic understanding of the DMS

cycle and uncertainties in the global and seasonal distributions of this gas. These uncertainties coupled with uncertainties in the gas transfer coefficient [Nightingale *et al.*, 2000] hamper the ability of atmospheric sulfur models to evaluate the modulating effect of this gas on global climate.

Two complementary approaches are needed to better constrain the global distribution of DMS. Accurate, spatially resolved global DMS measurements with good seasonal coverage are the first step, and MIMS can greatly facilitate this endeavour. Even with an automated MIMS system, it would still be unfeasible to map the entire ocean at sufficient temporal resolution. Hence, the second approach involves developing predictive algorithms that simulate DMS levels based on well constrained biogeochemical parameters. A recent comparison of several such algorithms has shown that they have various strengths and weaknesses and differ in their ability to accurately replicate DMS levels both seasonally and regionally [Belviso *et al.*, 2004b].

We chose to evaluate the algorithm of *Simo and Dachs* [2002] with our coastal dataset because it is one of the few without a modeled term that relies on two commonly measured parameters (chlorophyll and MLD). As noted above, the mixed layer depth encompasses a number of factors such as nutrient availability, light availability and phytoplankton succession, (which appeared to explain many of the regional differences in observed DMS levels), into a single variable. Although the original *Simo and Dachs* [2002] algorithm failed to re-create the DMS levels found during our survey, with a different slope the CHL/MLD ratio was a good predictor of surface DMS concentrations ($r^2 = 0.83$; Fig. 3.8). This is particularly impressive considering the complete lack of a relationship between DMS and chlorophyll alone ($r^2 = 0.06$; Fig. 3.6).

Our slope (21.0) is less than half that of the original algorithm (55.8) which may result from the higher relative proportion of diatoms (with lower DMSP content per unit chlorophyll) [Keller *et al.*, 1989] in coastal regions compared to oceanic waters. Our coastal data encompassed a much larger range of CHL/MLD ratios (0.03-2.26) than originally used to formulate the algorithm (<0.20), and we observed a good fit to the DMS data up to a CHL/MLD ratio of 1.0. The two prominent outliers that were excluded from the regression had CHL/MLD ratios greater than 1.0 and came from the region of high biomass off Barkley Sound. Although we did not explicitly measure MLDs outside the area of QC Sound, we chose to incorporate the whole survey region into the algorithm to expand the ranges of MLD, DMS, and chlorophyll concentrations used. Thus we relied on previous knowledge of the area, and data from other cruises to estimate MLDs outside of QC Sound (open symbols, Fig. 3.8). As a result, there is potential error in the MLDs for the two outliers from Barkley Sound. However, based on the measured DMS and chlorophyll concentrations, MLDs for the two outliers would have had to have been unreasonably deep (75-100 m) in order to fit the curve. It is possible that the linear relationship simply does not hold beyond CHL/MLD ratios greater than 1.0 which would characterize rare regions of very high biomass and relatively shallow mixed layers. The area off Barkley Sound where these high CHL/MLD ratios were observed was likely part of the Juan de Fuca eddy, where exceedingly high phytoplankton biomass is sustained throughout the summer through the constant injection of nutrients into the eddy core [Marchetti *et al.*, 2004]. The *S&D2002* algorithm uses both a linear and a negative logarithmic equation to model DMS concentrations based on the magnitude of the CHL/MLD ratio. Our results indicate a linear equation works in the CHL/MLD range of 0.02-1.0 but not beyond. Either no relationship exists between DMS and CHL/MLD beyond CHL/MLD >1 or a different equation applies. More data

in productive regions where these high CHL/MLD ratios are likely to be found is needed to test this possibility.

3.5 Conclusions

Our findings extend the utility of the CHL/MLD ratio as a predictor of DMS levels into highly productive coastal waters. Application of similar analyses in various coastal waters is needed to test the general applicability of our derived algorithm. This would aid in determining whether the relationship is specific to this particular region, or season, or more broadly applicable to distinct coastal systems (i.e. temperate). Our results also emphasize the utility of membrane inlet mass spectrometry for resolving spatial variability in gas distributions, and the need for high-frequency sampling in coastal waters if the aim is to accurately quantify fluxes of both major and trace gases in these important regions. The application of MIMS (or other comparable analytical tools) is thus likely to significantly increase our understanding of oceanic gas distributions over the coming decade. As more information becomes available on the concentration and variability of gases in dynamic coastal regions, new insight may be gained into the biological and physical controls on gas distributions. In the case of the DMS cycle, a better mechanistic understanding is required of the underlying production and consumption processes, and this may be obtained by coupling focused process studies with real-time underway surveys. Ultimately, this information will aid in the development of better predictive algorithms which are needed to understand the potential impact of DMS emissions on future climate, and conversely, the impact of climate change on the oceanic cycle of DMS.

Table 3.1: Absolute and relative asymptotic interpolation errors along the 6 major transects

Transect	Temp. (°C)		Sal. (psu)		Chl <i>a</i> (µg L ⁻¹)		O ₂ /Ar (torr ratio)		<i>p</i> CO ₂ (ppm)		DMS (nM)	
	*abs. error	†rel. error (%)	abs. error	rel. error (%)	abs. error	rel. error (%)	abs. error	rel. error (%)	abs. error	rel. error (%)	abs. error	rel. error (%)
2	0.45	2.7	0.06	0.19	0.15	22	0.15	1.0	12	3.7	1.25	48
4	0.28	1.6	0.17	0.54	0.80	65	0.28	1.8	8	2.5	6.0	90
5	2.25	15	0.23	0.71	3.50	97	1.30	8.2	45	13.9	8.0	93
6	0.18	1.1	0.15	0.47	0.80	97	0.70	4.3	30	9.9	1.5	52
7	0.90	6.1	0.15	0.47	7.50	62	2.00	11.5	55	18.0	1.0	24
8	0.35	3.1	0.10	0.32	2.75	55	1.75	14.7	125	23.4	--	--
mean	0.74	5.0	0.14	0.45	2.6	66	1.0	6.9	46	12	3.6	61

* absolute asymptotic interpolation error represents the maximum error in the mean (in the respective units of each parameter), obtained when the actual data along each transect is re-sampled at ever coarser resolution. The asymptotic error was reached at an average sampling distance of 34 km. The characteristic error length scale (analogous to the DLS) is computed as 2/3 the distance to the asymptote (~20 km) [Hales and Takahashi, 2004]. † relative asymptotic interpolation error is the percentage of the mean value along each transect that the absolute error represents

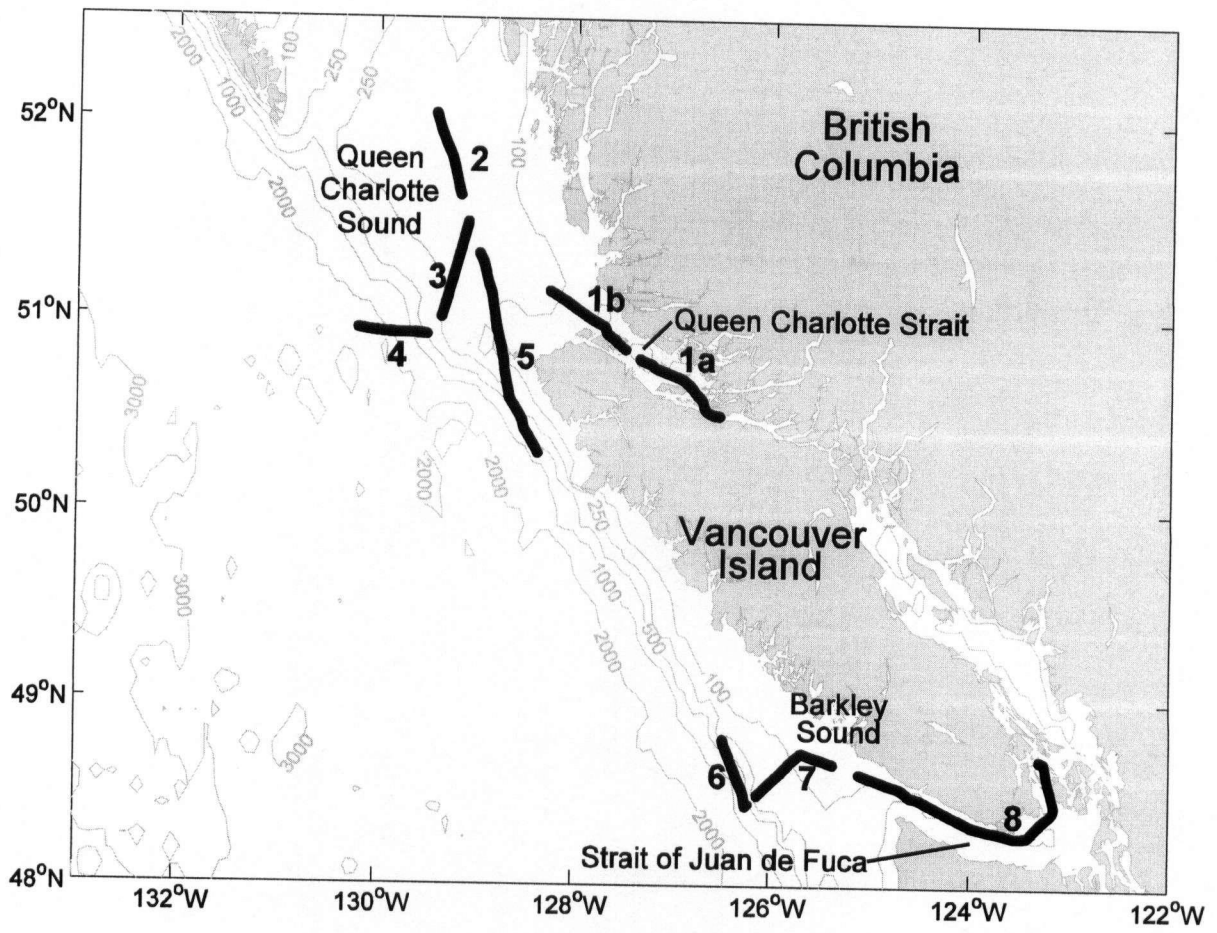


Figure 3.1: Map of southwestern British Columbia, Canada showing the location of underway transects.

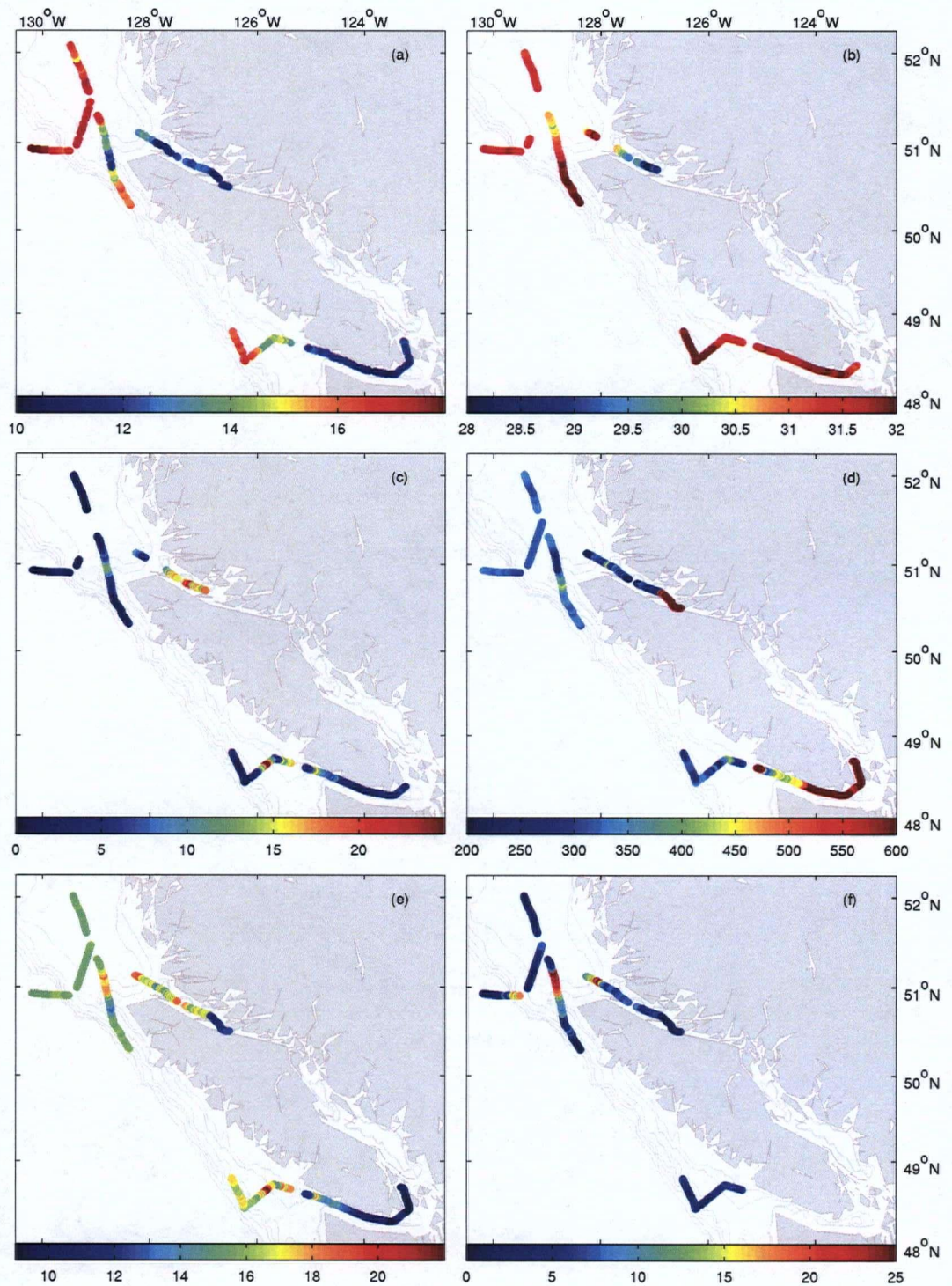


Figure 3.2: Surface plots of (a) temperature ($^{\circ}\text{C}$), (b) salinity (psu), (c) chlorophyll *a* ($\mu\text{g L}^{-1}$), (d) $p\text{CO}_2$ (ppm), (e) O_2/Ar (torr ratio), and (f) DMS (nM). See Fig. 3.1 for transect labels. See methods for explanation of gaps in salinity, chlorophyll and DMS plots.

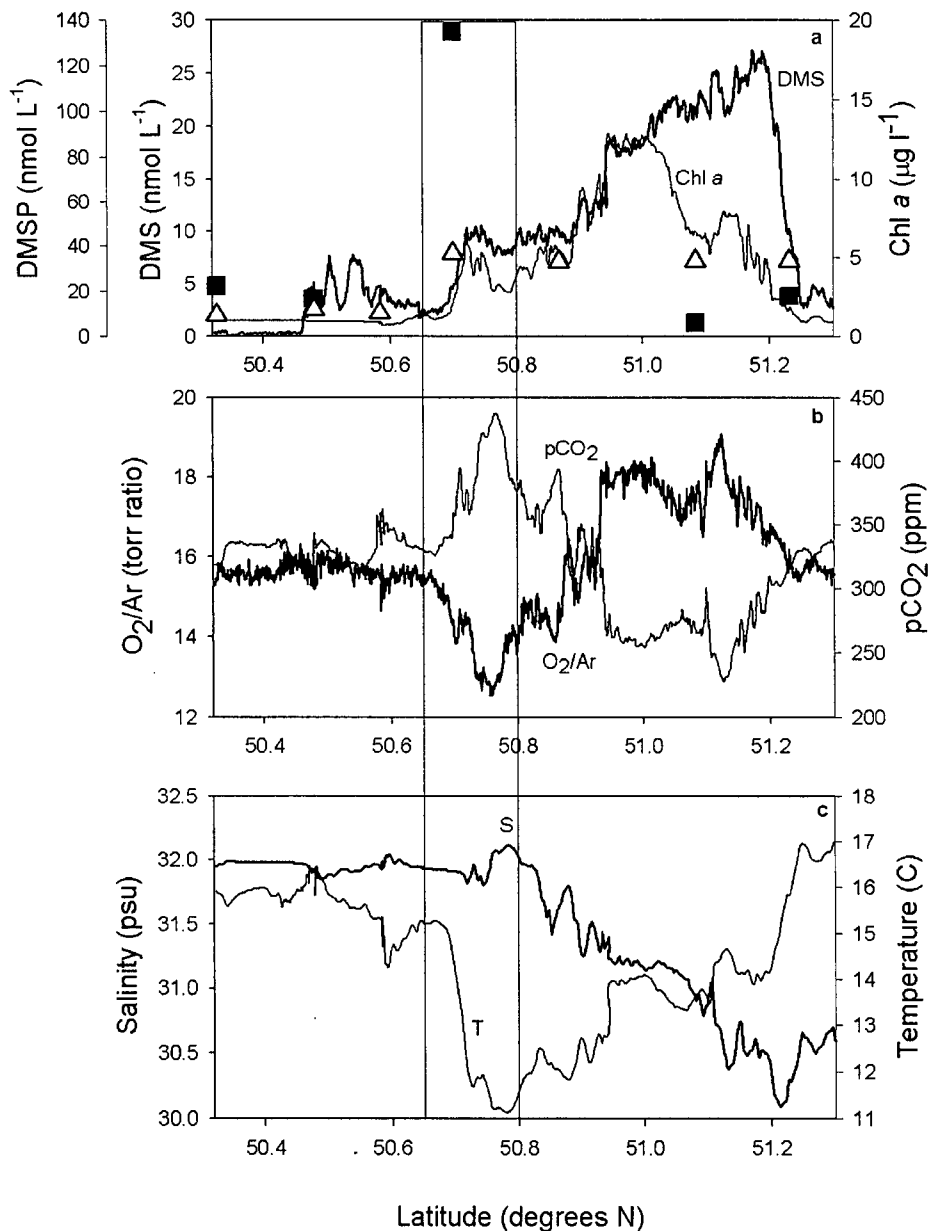


Figure 3.3: Detailed south-north view of all variables measured along T5 (see Fig. 3.1 for location); (a) DMS (—), chl *a* (---), DMSPd (■), DMSPp (△); (b) O₂/Ar (—), pCO₂ (---); (c) salinity (—), and temperature (---). Note the high DMSPd that coincides with the sharp temperature front south of 50.8 °N. Localized upwelling is evident just south of 50.8 °N.

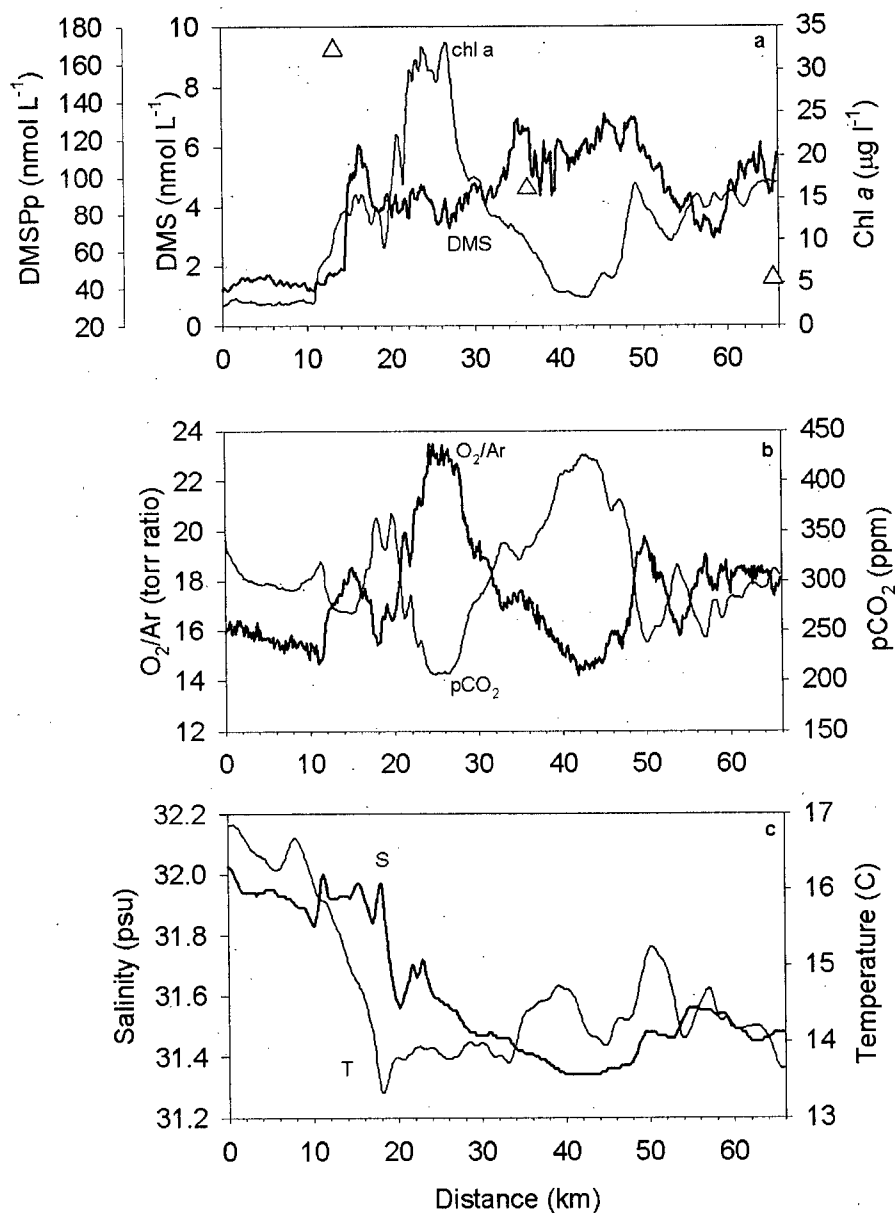


Figure 3.4: Detailed view of all variables measured along T7 (see Fig. 3.1 for location); (a) DMS (—), chl *a* (---), DMSPP (△); (b) O₂/Ar (—), pCO₂ (---); (c) salinity (—), and temperature (---). Note the strong correspondence of the chl *a* and O₂/Ar traces and the mirror images of the pCO₂ and O₂/Ar data. DMSPP data were not available for this transect due to the malfunction of the SEM detector near the end of the cruise.

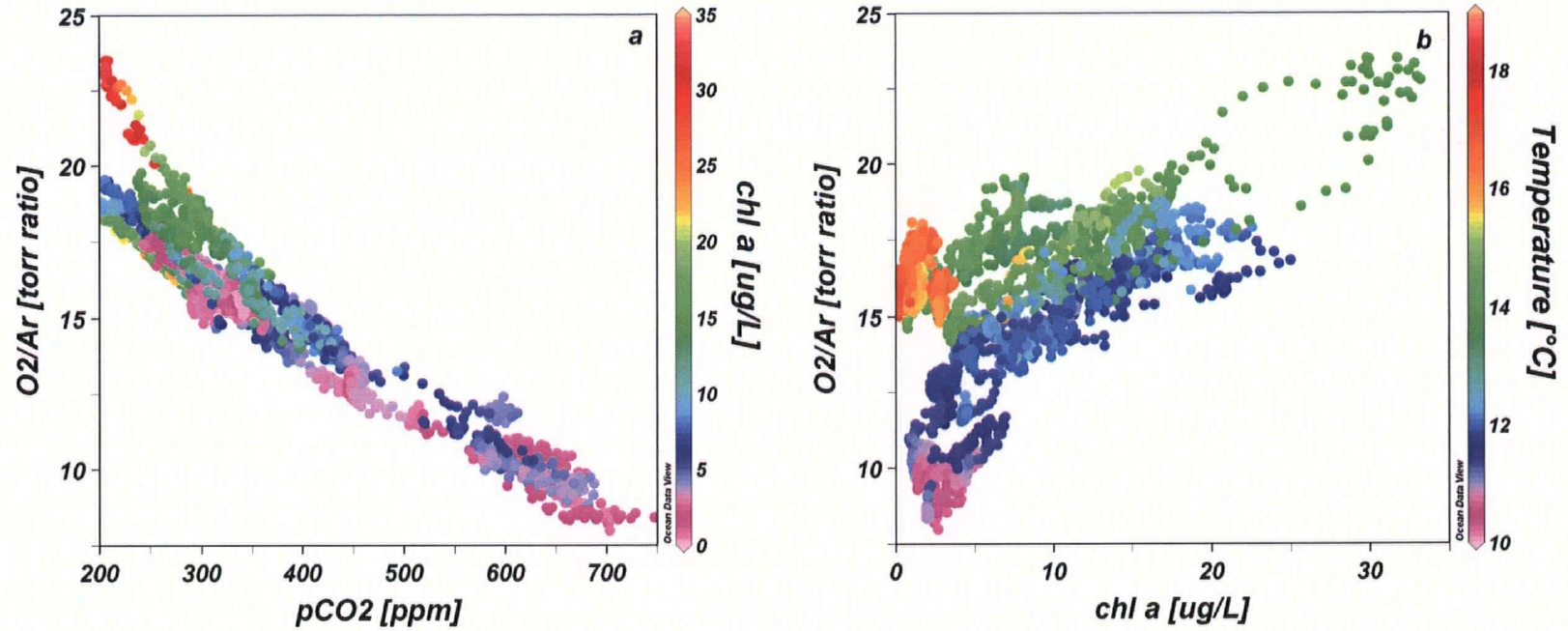


Figure 3.5: The correlation across all transects between (a) $p\text{CO}_2$ and O_2/Ar ($r^2 = 0.90$) with corresponding chl *a* concentrations overlaid (colourbar), and (b) chl *a* and O_2/Ar ($r^2 = 0.19$) with corresponding temperature overlaid (colourbar). Deviations from linearity in (b) mainly occur at cold surface temperature representing deep-mixed water masses, exclusion of these data from the regression improves the correlation to $r^2 = 0.73$.

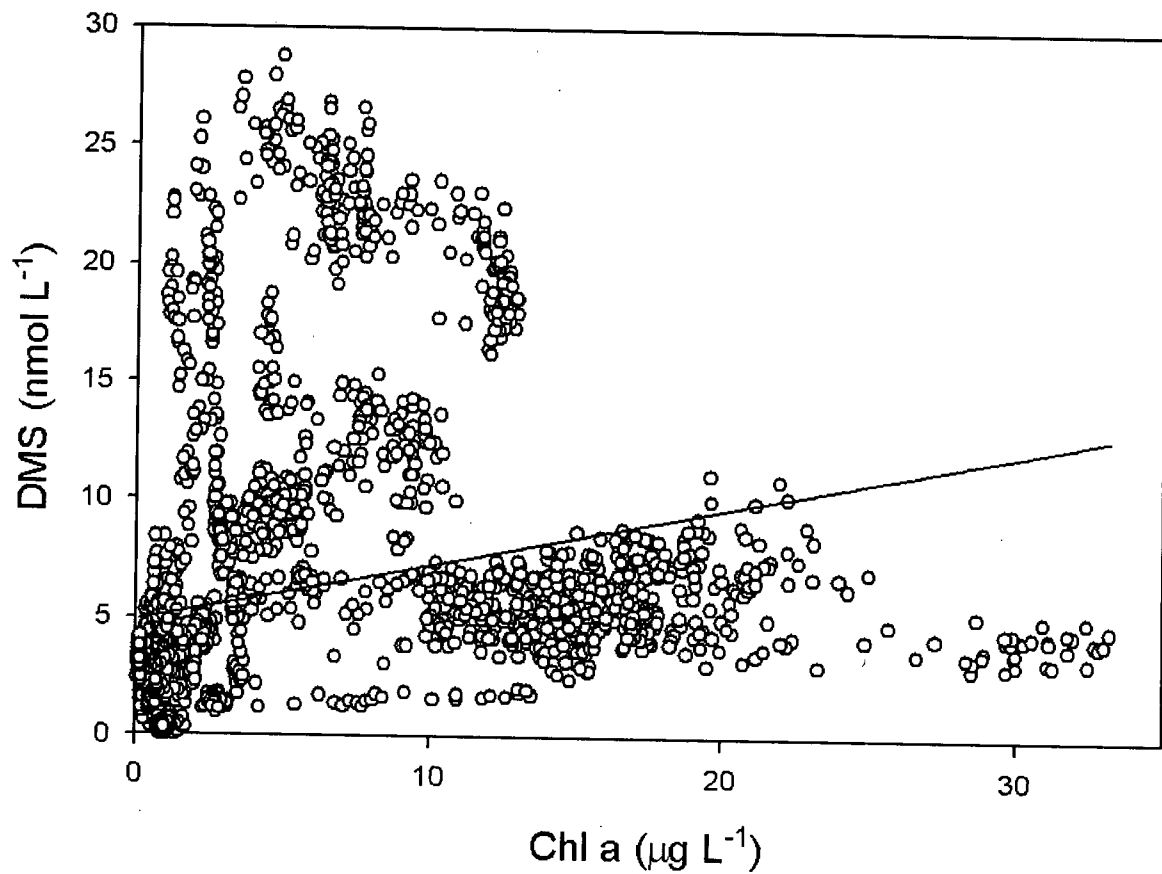


Figure 3.6: The correlation across all transects between chl *a* and DMS ($r^2 = 0.06$). Note that high DMS was generally associated with low to moderate chl *a* levels ($<10 \mu\text{g L}^{-1}$) while regions with high chl *a* had relatively low DMS concentrations.

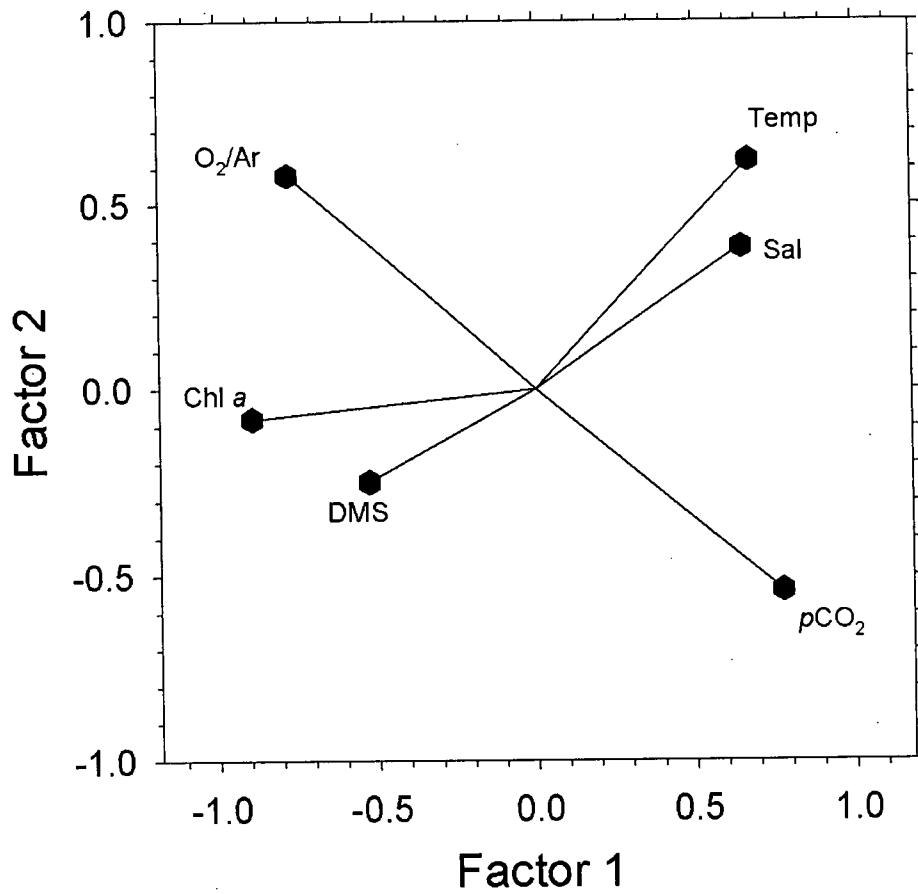
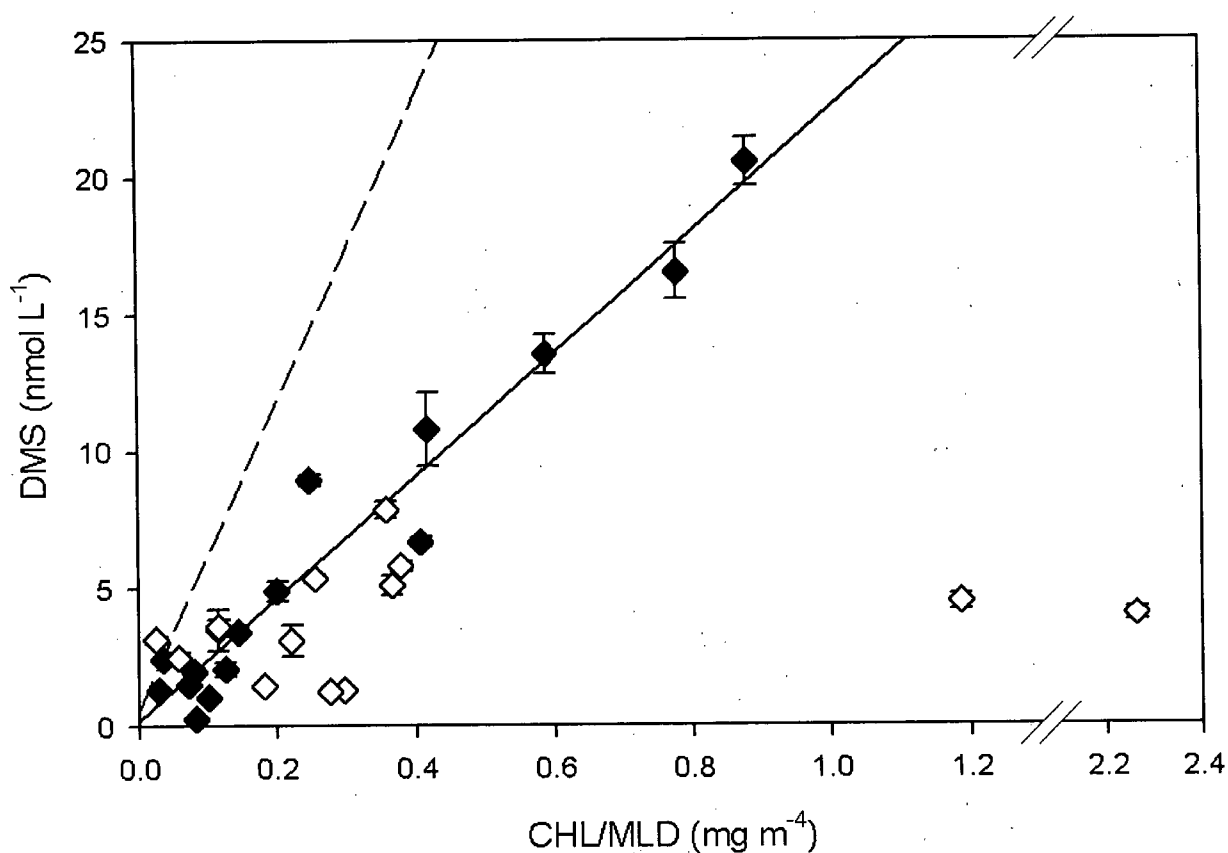


Figure 3.7: Results of the PCA showing the strong separation between $p\text{CO}_2$ and O_2/Ar in two-dimensional space and the clear partitioning between physical (T, S) and biological (chl *a*) variables.



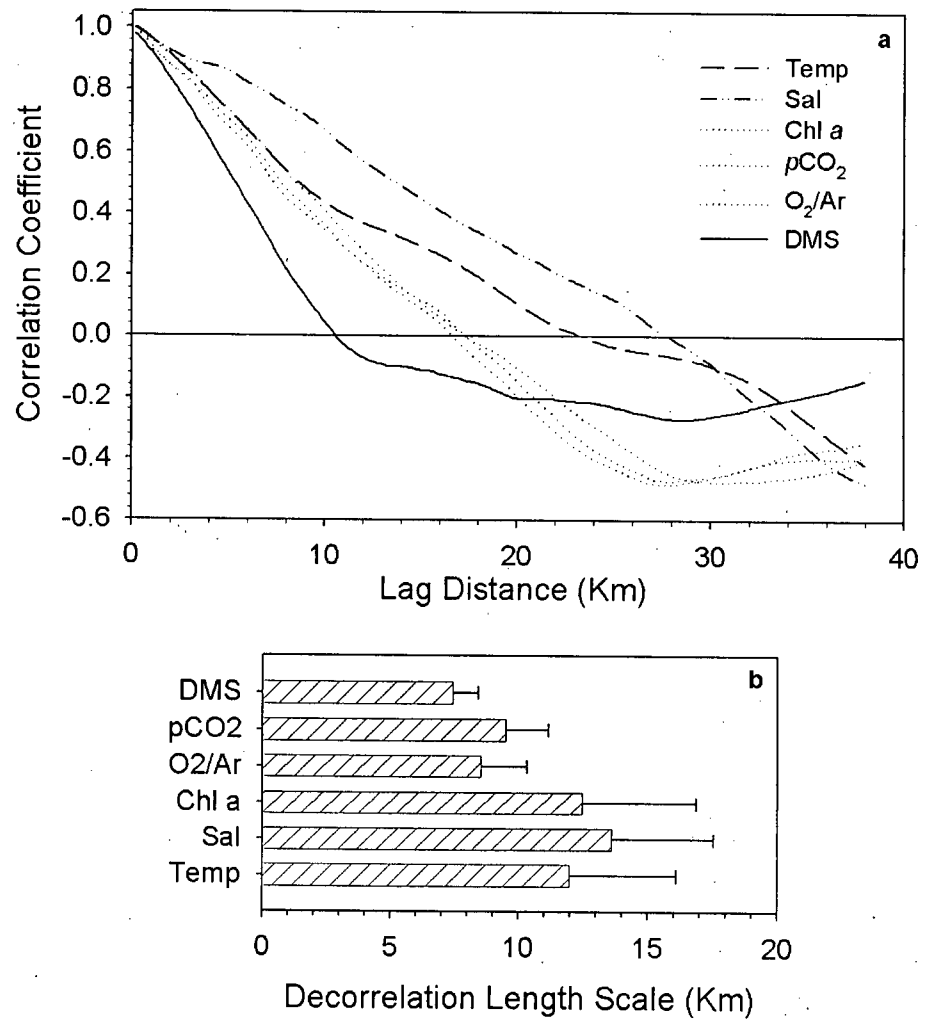


Figure 3.9: Autocorrelation functions for all parameters measured along transect 5 (a); the DLS is the first zero crossing of the function; average DLS for all parameters for the entire survey (b). Note that DMS appears to have the shortest length scale of variability, although the results are not statistically significant (see discussion).

3.6 References:

- Anderson, T.R., S.A. Spall, A. Yool, P. Cipollini, P.G. Challenor, and M.J.R. Fasham (2001), Global fields of sea surface dimethylsulfide predicted from chlorophyll, nutrients and light, *J. Mar. Syst.*, 30, 1-20.
- Aranami, K., and S. Tsunogai (2004), Seasonal and regional comparison of oceanic and atmospheric dimethylsulfide in the northern North Pacific: Dilution effects on its concentration during winter, *J. Geophys. Res.*, 109, D12303, doi:10.1029/2003JD004288.
- Belviso, S., A. Sciandra, C. Copin-Montegut (2003), Mesoscale features of surface water DMSP and DMS concentrations in the Atlantic Ocean off Morocco and in the Mediterranean Sea, *Deep-Sea Res. I*, 50, 543-555.
- Belviso, S., C. Moulin, L. Bopp, and J. Stefels (2004a), Assessment of a global climatology of oceanic dimethylsulfide (DMS) concentrations based on SeaWiFS imagery (1998-2001), *Can. J. Fish. Aquat. Sci.*, 61, 804-816.
- Belviso, S., L. Bopp, C. Moulin, J. C. Orr, T. R. Anderson, O. Aumont, S. Chu, S. Elliott, M. E. Maltrud, and R. Simo (2004b), Comparison of global climatological maps of sea surface dimethyl sulfide, *Global Biogeochem. Cycles*, 18, GB3013, doi:10.1029/2003GB002193.
- Broecker, W.S., and T.H. Peng (1982), *Tracers in the Sea*, Lamont Doherty Geol. Observ. Press, Palisades, N.Y.
- Bucciarelli, E., and W.G. Sunda (2003), Influence of CO₂, nitrate, phosphate, and silicate limitation on intracellular dimethylsulfoniopropionate in batch cultures of the coastal diatom *Thalassiosira pseudonana*, *Limnol. Oceanogr.* 48, 2256-2265.
- Charlson, R.J., J.E. Lovelock, M.O. Andreae, and S.G. Warren (1987), Oceanic phytoplankton, atmospheric sulfur, cloud albedo and climate, *Nature*, 326, 655-661.
- Chin, M., and D.J. Jacob, (1996) Anthropogenic and natural contributions to tropospheric sulphate: a global model analysis, *J. Geophys. Res.*, 101, 18,691-18,699.
- Craig, H., and T. Hayward (1987), Oxygen supersaturation in the ocean: biological versus physical contributions, *Science*, 235, 199-202.
- Dacey, J.W.H., and S.G. Wakeham (1986), Oceanic dimethylsulfide: Production during zooplankton grazing on phytoplankton, *Science*, 233(4770), 1314-1316.
- Denman, K., E. Hofmann, and H. Marchant (1996), Marine biotic responses to environmental change and feedbacks to climate, in *Climate Change 1995 IPCC*, pp. 487-516, Cambridge Univ. Press, New York.

- Hales, B., and T. Takahashi (2004), High-resolution biogeochemical investigation of the Ross Sea, Antarctica, during the AESOPS (U.S. JGOFS) program, *Global Biogeochem. Cycles*, 18, GB3006, doi: 10.1029/2003GB002165.
- Hales, B., T. Takahashi, and L. Bandstra (2005), Atmospheric CO₂ uptake by a coastal upwelling system, *Global Biogeochem. Cycles*, 19, GB1009, doi:10.1029/2004GB002295.
- Ianson, D., and S.E. Allen (2002), A two-dimensional nitrogen and carbon flux model in a coastal upwelling region, *Global Biogeochem. Cycles*, 16(1), 1011, doi:10.1029/2001GB001451.
- Ianson, D., S.E. Allen, S.L. Harris, K.J. Orians, D.E. Varela, and C.S. Wong (2003), The inorganic carbon system in the coastal upwelling region west of Vancouver Island, Canada, *Deep-Sea Res. I*, 50, 1023-1042.
- Johnson, W.K., L.A. Miller, N.E. Sutherland, and C.S. Wong (2005), Iron transport by mesoscale Haida eddies in the Gulf of Alaska, *Deep-Sea Res. II*, 52 (7-8), 933-953.
- Jones, A., D.L. Roberts, M.J. Woodage, and C.E. Johnson, (2001) Indirect sulphate aerosol forcing in a climate model with interactive sulphur cycle, *J. Geophys. Res.*, 106, 20,293-20,310.
- Kaiser, J., M.K. Reuer, B. Barnett, and M.L. Bender (2005), Marine productivity estimates from continuous O₂/Ar ratio measurements by membrane inlet mass spectrometry, *Geophys. Res. Lett.*, 32, L19605, doi:10.1029/2005GL023459.
- Keller, M.D., W.K. Bellows, and R.R.L. Guillard (1989), Dimethyl sulfide production in marine phytoplankton, in *Biogenic sulfur in the environment*, edited by E.S. Saltzman and W.J. Cooper, p. 167-180, American Chemical Society, Washington, D.C.
- Kettle, A.J., M.O. et al. (1999), A global database of sea surface dimethylsulfide (DMS) measurements and a procedure to predict sea surface DMS as a function of latitude, longitude and month, *Global Biogeochem. Cycles*, 13, 399-444.
- Kieber, D.J., J. Jiao, R.P. Kiene, and T.S. Bates (1996), Impact of dimethylsulfide photochemistry on methyl sulfur cycling in the equatorial Pacific Ocean, *J. Geophys. Res.*, 101(C2), 3715-3722.
- Kiene, R.P., and T.S. Bates (1990), Biological removal of dimethyl sulfide from sea water, *Nature*, 345, 702-705.
- Kiene, R.P., and D. Slezak (2006), Low dissolved DMSP concentrations in seawater revealed by small-volume gravity filtration and dialysis sampling, *Limnol. Oceanogr.: Methods*, 4, 80-95.

- Leck, C., U. Larsson, L.E. Bagander, S. Johansson, and S. Hajdu (1990), Dimethyl sulfide in the Baltic Sea: annual variability in relation to biological activity, *J. Geophys. Res.*, *95*, 3353-3363.
- Locarnini, S.J.P., S.M. Turner, and P.S. Liss (1998), The distribution of dimethylsulfide, DMS, and dimethylsulfoniopropionate, DMSP in waters off the Western Coast of Ireland, *Cont. Shelf Res.*, *18*, 1455-1473.
- Marchetti, A., V.L. Trainer, and P.J. Harrison (2004), Environmental conditions and phytoplankton dynamics associated with *Pseudo-nitzschia* abundance and domoic acid in the Juan de Fuca eddy, *Mar. Ecol. Prog. Ser.*, *281*, 1-12.
- Margalef, R. (1978), Life-forms of phytoplankton as survival alternatives in an unstable environment, *Oceanol. Acta.*, *1*, 493-509.
- Murata, A., and T. Takizawa (2003), Summertime CO₂ sinks in shelf and slope waters of the western Arctic Ocean, *Cont. Shelf Res.*, *23*, 753-776.
- Murphy, P.P., Y. Nojiri, D.E. Harrison, and N.K. Larkin (2001), Scales of spatial variability for surface ocean pCO₂ in the Gulf of Alaska and Bering Sea: Towards a sampling strategy, *Geophys. Res. Lett.*, *28*, 1047-1050
- Nightingale, P.D., P.S. Liss, and P. Schlosser (2000), Measurements of air-sea gas transfer during an open ocean algal bloom, *Geophys. Res. Lett.* *27*, (14), 2117-2120.
- Parsons, T. R., Y. Maita, and C.M. Lalli (1984), *A manual of chemical and biological methods for seawater analysis*, Pergamon Press, New York, N.Y.
- Sarmiento, J.L., P. Monfray, E. Maier-Reimer, O. Aumont, R.J. Murnane, and J.C. Orr (2000), Sea-air CO₂ fluxes and carbon transport: A comparison of three ocean general circulation models, *Global Biogeochem. Cycles*, *14*(4), 1267-1281.
- Shaw, P.J.A (2003), *Multivariate statistics for the environmental sciences*, Oxford Univ. Press, New York, N.Y.
- Simo, R. (2001), Production of atmospheric sulphur by oceanic plankton: biogeochemical, ecological and evolutionary links, *Trends in Ecol. & Evol.*, *16*(6), 287-294.
- Simo, R. (2004), From cells to globe: approaching the dynamics of DMS(P) in the ocean at multiple scales, *Can. J. Fish. Aquat. Sci.*, *61*, 673-684.
- Simo, R., and C. Pedros-Alio (1999), Role of vertical mixing in controlling the oceanic production of dimethyl sulphide, *Nature*, *402*, 396-399.

- Simo, R. and J. Dachs (2002), Global ocean emission of dimethylsulfide predicted from biogeophysical data, *Global Biogeochem. Cycles*, 16(4), 1078, doi: 10.1029/2001GB001829.
- Sunda, W., D.J. Kieber, R.P. Kiene, and S. Huntsman (2002), An antioxidant function for DMSP and DMS in marine algae, *Nature*, 418, 317-320.
- Takahashi, T., S.C. Sutherland, C. Sweeney, A. Poisson, N. Metzl, B. Tilbrook, N. Bates, R. Wanninkhof, R.A. Felly, C. Sabine, J. Olafsson, and Y. Nojiri (2002), Global sea-air CO₂ flux based on climatological surface ocean pCO₂, and seasonal biological and temperature effects, *Deep-Sea Res. II*, 49(9-10), 1601-1622.
- Thomson, R.E., and I.V. Fine (2003), Estimating mixed layer depth from oceanic profile data, *J. Atmos. Oceanic Technol.*, 20(2), 319-329.
- Toole, D.A., D.J. Kieber, R.P. Kiene, E.M. White, J. Bisgrove, D.A. del Valle, and D. Slezak (2004), High dimethylsulfide photolysis rates in nitrate-rich Antarctic waters, *Geophys. Res. Lett.*, 31, L11307, doi:10.1029/2004GL019863.
- Tortell, P.D. (2005a), Dissolved gas measurements in oceanic waters made by membrane inlet mass spectrometry, *Limnol. Oceanogr. Methods*, 3, 24-37.
- Tortell, P.D. (2005b), Small-scale heterogeneity of dissolved gas concentrations in marine continental shelf waters, *Geochem. Geophys. Geosyst.*, 6, Q11M04, doi:10.1029/2005GC000953.
- Townsend, D.W., and M.D. Keller (1996), Dimethylsulfide (DMS) and dimethylsulfoniopropionate (DMSP) in relation to phytoplankton in the Gulf of Maine, *Mar. Ecol. Prog. Ser.*, 137, 229-241.
- Volk, T., and M.I. Hoffert, (1985) Ocean carbon pumps: analysis of relative strengths and efficiencies in ocean-driven atmospheric pCO₂ changes, in *The carbon cycle and atmospheric CO₂: Natural variations, archean to present*, *Geophys. Monogr. Ser.*, edited by E.D. Sundquist and W.S. Broecker, pp. 99-110, AGU, Washington, D.C.

Chapter 4: Conclusions

4.1 Thesis Overview

The importance of constraining global DMS fluxes and unravelling the complex oceanic sulfur cycle is becoming increasingly clear as we face a changing global climate. Biogenic sulfur emissions from the world's oceans have a large impact on the Earth's climate and may help to counteract the effects of increasing greenhouse gas emissions [Watson and Liss, 1998; Gunson *et al.*, 2006]. However, to evaluate the magnitude of this impact we need (1) a better mechanistic understanding of the DMS cycle, and (2) more advanced methodology to facilitate measurement of DMS in the oceans.

The preceding two chapters that formed the body of this work tackled these two goals. Each focused on a different application of membrane inlet mass spectrometry to the study of biogenic sulfur compounds in the oceans. These chapters introduced new methodology for measuring both dissolved and particulate DMSP concentrations as well as volatile DMS, and provided new insights into the distributions of these important compounds. The focus of Chapter 2 was on discrete, vertical measurements of springtime DMSPp in oceanic waters along Line P over a three year time period. This survey attempted to relate DMSPp concentrations to the composition of the phytoplankton community and offered insight into the vertical variability of this compound on an interannual timescale in an ocean basin where such measurements did not previously exist. In contrast, Chapter 3 focused on continuous, real-time, surface measurements of DMS in coastal surface waters around Queen Charlotte Sound over a week-long period in summer. This study examined the high-resolution co-variance of multiple parameters in relation to DMS distributions in a highly dynamic and productive region.

4.2 Evaluation of MIMS for DMSP/DMS Measurements

Initially, our results from the Line P and Queen Charlotte Sound surveys indicated that MIMS was a promising new technique for measuring oceanic DMSPp (and DMSPd) concentrations. Measurement precision was good, calibration curves were linear over a large range and analysis times were short (see Section 2.3). However, some recently published data as well as some of our own findings indicate that there are potential problems with this method. Firstly, we discovered that prolonged exposure of the dimethylsilicone membrane to strong base (such as that used to hydrolyze DMSP samples) leads to a breakdown of the membrane and subsequent silicone contamination of the mass spectrometer ion source. This results in a drastic loss of sensitivity which can only be rectified by costly replacements of the entire ion source. This problem does not affect the quality of the data, but leads to frequent, impractical and expensive repairs.

Dissolved DMSP samples are also typically measured at high pH. We attempted to circumvent the above problem for DMSPd analysis during our Queen Charlotte Sound survey by lowering the pH of the seawater sample to 9.5 following the 24 hour hydrolysis period (see Section 3.2). This reduced pH prolonged the life of the membrane without affecting the DMS in the sample. However, this method did not produce reliable results when tested with extracted DMSPp samples which lacked the buffering capacity of seawater. Even when exact additions of acid and base were made, slight variability in the pH between samples affected the permeability of the membrane which in turn led to variability in the DMS signals for a given concentration. Thus, DMSPp samples had to be measured at high pH using the small-area probe with the risk of damaging the system.

The second recently identified problem that makes MIMS not ideal for dissolved and particulate DMSP analysis is the relatively large sample volumes required. In the case of DMSP_p, we filtered 250 ml of seawater to compensate for the reduced sensitivity of the small-area membrane inlet probe used. In hindsight, this volume could have been reduced to 50 ml if a 3 ml vial had been used during analysis without affecting the ~1 nM detection limit of *in situ* DMSP_p (see Section 2.3). However, low ambient DMSP_d concentrations need to be measured on the more sensitive large-area membrane cuvette that requires a relatively large volume of recirculating sample (>200 ml). It has only recently come to light that filtering large volumes of water for DMSP_d analysis (even by gravity) leads to elevated DMSP_d levels due to ruptured phytoplankton cells [Kiene and Slezak, 2006]. These filtration artifacts can be quite significant and increase with the volume of water filtered [Kiene and Slezak, 2006]. It is now recommended that only the first 3.5 ml of filtrate collected by gravity filtration be used to determine DMSP_d concentrations, while DMSP_p concentrations are best calculated from total DMSP (DMSP_t = DMSP_d + DMSP_p) determined from whole seawater samples [Kiene and Slezak, 2006]. Although the sensitivity of the MIMS is sufficient to measure ambient DMSP_t concentrations in most regions of the world's oceans, an unconcentrated 3.5 ml DMSP_d sample could not be measured with either the small or large-area membrane inlets with the current MIMS configuration given that the global average DMSP_d concentration is estimated at < 3 nM [Kiene and Slezak, 2006].

4.3 Successes and Pitfalls

During the Line P surveys we were able to achieve our original goal of adapting MIMS for oceanic DMSP_p measurements, but the data may have underestimated the true DMSP_p

concentrations in this region because of the filtration method used. However, the filtration-induced artifact is likely not as severe for DMSPp, which is present at 10-100-fold higher concentrations than DMSPd [Kiene and Slezak, 2006]. Furthermore, the majority of investigators have collected DMSPp samples in much the same way in the past, with many using more damaging vacuum filtration [i.e. *Ledyard and Dacey, 1996; Matrai and Vernet, 1997*] and others filtering up to 1 L volumes of seawater [*Dacey et al., 1998*]. Therefore, although the true DMSPp concentrations in the NE Pacific may indeed be slightly higher than we measured, our data are still useful for comparison with other studies in other regions of the world's oceans. In 2003, we used low vacuum filtration, whereas in subsequent years we switched to the more gentle method of gravity filtration. We would thus expect that 2003 DMSPp concentrations were potentially more underestimated than in later years. This implies that the true decline in DMSPp levels along Line P between 2003 and 2004 may be even larger than our results suggest (see Section 2.3).

Perhaps the biggest limitation of the Line P DMSPp survey lies in the phytoplankton data. The microscopic method used to count individual cells appeared to underestimate the true autotrophic biomass as evident from the resultant low C:chl ratios and the high estimates of cellular DMSP quotas (see Section 2.4). This likely hampered attempts to relate DMSPp levels to the biomass of specific phytoplankton groups in 2003. The biggest shortfall of the 3-year dataset however, is the lack of supporting phytoplankton data for 2004 and 2005. As a result, we were unable to distinguish between the roles of phytoplankton taxonomy and physiology in driving cross-station or interannual DMSPp variability. Nonetheless, our study provided the first DMSPp measurements made in this important and well-studied HNLC region that provide a reference point for future measurements in this area.

The Queen Charlotte Sound survey on the other hand was a resounding success and we were able to meet or exceed all of our research goals. We were able to show that DMS levels exhibited rapid, large fluctuations over spatial scales that could not be resolved with traditional GC methods. More importantly, we were able to convincingly relate surface DMS levels to the ratio of chlorophyll/mixed layer depth, something that had previously not been achieved in high productivity, coastal regions. Furthermore, we obtained interesting results on the strong co-variance of chlorophyll concentrations, O₂/Ar levels and pCO₂ levels. These data highlighted the power of MIMS for measuring multiple gases at high-resolution simultaneously, and thereby providing valuable ancillary information useful for interpreting DMS distributions. This dataset could, however, have been improved by calibrating the O₂/Ar signal to give more meaningful % O₂ saturation values. This was not possible during this cruise due to time and man-power constraints. In the future, more frequent sampling of total DMSP would be useful to examine its co-variance with DMS. Sampling for total DMSP would require less effort than separating the dissolved and particulate fractions, and would bypass some of the issues associated with these measurements as mentioned above.

4.4 Future Directions

We have shown that MIMS has capabilities that far exceed many of those of PTGC for the measurement of oceanic DMS concentrations, and have thus moved closer to accomplishing the second goal outlined above: the development of advanced methodologies that simplify oceanic DMS measurements. The one area where MIMS currently falls short is in sensitivity. Due to a lack of a concentrating step for DMS, the current detection limit of ~ 1 nM is not sufficient to accurately measure this gas in many oceanic regions, particularly during the winter

months. Sensitivity can be improved in the future by increasing the surface area of the membrane; however, this would likely necessitate the employment of a water trap to counteract the negative impact of an increase in water vapour in the vacuum of the mass spectrometer. As noted above, the MIMS system in its present configuration is not useful for dissolved DMSP measurements, and thus will not replace PTGC for small volume, high sensitivity applications.

In order to predict the impact of DMS emissions on future climate and the impact of a changing climate on the sulfur cycle, we need to achieve the primary goal as stated above: a mechanistic understanding of the underlying processes that drive the production and consumption of DMSP, DMS and related compounds. Recent progress in this area has been steady, with ^{35}S tracer studies mapping the fate of DMSP assimilation and destruction pathways [Kiene and Linn, 2000; Vila *et al.*, 2004] and providing estimates of sulfur cycling rates [Toole *et al.*, 2004]. Future applications of MIMS should aim to couple its continuous sampling capabilities with detailed process studies. For example, rates of microbial DMS/DMSP decay could be monitored in real-time without the need for radioisotopes or destructive, interval sampling. Furthermore, capitalizing on the real-time nature of the MIMS output in the field would allow for immediate, targeted sampling of ancillary parameters at DMS “fronts” such as those observed during the Queen Charlotte Sound survey (see Section 3.3). Such studies will further enhance our understanding of the intricacies of the marine sulfur cycle and lead us closer to proving or refuting the CLAW hypothesis.

4.5 References

- Dacey, J.W.H., F.A. Howse, A.F. Michaels, and S.G. Wakeham (1998), Temporal variability of dimethylsulfide and dimethylsulfoniopropionate in the Sargasso Sea, *Deep-Sea Res. I* 45, 2085-2104.
- Gunson, J.R., S.A. Spall, T.R. Anderson, A. Jones, I.J. Totterdell, and M.J. Woodage (2006), Climate sensitivity to ocean dimethylsulphide emissions, *Geophys. Res. Lett.*, 33, L07701, doi:10.1029/2005GL024982.
- Kiene, R.P., and L.J. Linn (2000), Distribution and turnover of dissolved DMSP and its relationship with bacterial production in the Gulf of Mexico, *Limnol. Oceanogr.*, 45, 849-861.
- Kiene, R.P. and D. Slezak (2006), Low dissolved DMSP concentrations in seawater revealed by small-volume gravity filtration and dialysis sampling, *Limnol. Oceanogr.: Methods*, 4, 80-95.
- Ledyard, K.M. and J.W.H. Dacey (1996), Microbial cycling of DMSP and DMS in coastal and oligotrophic seawater, *Limnol. Oceanogr.*, 41, 33-40.
- Matrai, P.A. and M. Vernet (1997), Dynamics of the vernal bloom in the marginal ice zone of the Barents Sea: dimethylsulfide and dimethylsulfoniopropionate budgets, *J. Geophys. Res.*, 102, 22965-22979.
- Toole, D.A., D.J. Kieber, R.P. Kiene, E.M. White, J. Bisgrove, D.A. del Valle, and D. Slezak (2004), High dimethylsulfide photolysis rates in nitrate-rich Antarctic waters, *Geophys. Res. Lett.*, 31, L11307, doi:10.1029/2004GL019863.
- Vila, M., R. Simo, R.P. Kiene, J. Pinhassi, J.A. Gonzalez, M.A. Moran, and C. Pedros-Alio (2004), Use of microautoradiography combined with fluorescence in situ hybridization to determine dimethylsulfoniopropionate incorporation by marine bacterioplankton taxa, *Appl. Environ. Microbiol.*, 70 (8), 4648-4657.
- Watson, A.J. and P.S. Liss (1998), Marine biological controls on climate via the carbon and sulfur geochemical cycles, *Phil. Trans. Roy. Soc. Lon. Ser. B-Biol. Sci* 353, (1365), 41-51.